A Covariant Natural Ultraviolet Cutoff in Inflationary Cosmology

by

Aidan Chatwin-Davies

A thesis
presented to the University of Waterloo
in fulfillment of the
thesis requirement for the degree of
Master of Mathematics
in
Applied Mathematics

Waterloo, Ontario, Canada, 2013

I hereby declare that I am the sole author of this thesis. This is a true copy of the thesis, including any required final revisions, as accepted by my examiners.

I understand that my thesis may be made electronically available to the public.

Abstract

In the field of quantum gravity, it is widely expected that some form of a minimum length scale, or ultraviolet cutoff, exists in nature. Recently, a new natural ultraviolet cutoff that is fully covariant was proposed. In the literature, most studies of ultraviolet cutoffs are concerned with Lorentz-violating ultraviolet cutoffs. The difficulty in making a minimum length cutoff covariant is rooted in the fact that any given length scale can be further Lorentz contracted. It was shown that this problem is avoided by the proposed covariant cutoff by allowing field modes with arbitrarily small wavelengths to still exist, albeit with exceedingly small, covariantly-determined bandwidths. In other words, the degrees of freedom of sub-Planckian modes in time are highly suppressed.

The effects of this covariant ultraviolet cutoff on the kinematics of a scalar quantum field are well understood. There is much to learn, however, about the effects on a field's dynamics. These effects are of great interest, as their presence may have direct observational consequences in cosmology. As such, this covariant ultraviolet cutoff offers the tantalizing prospect of experimental access to physics at the Planck scale.

In cosmology, the energy scales that are probed by measurements of cosmic microwave background (CMB) statistics are the closest that we can get to the Planck scale. In particular, the statistics of the CMB encodes information about the quantum fluctuations of the scalar inflaton field. A measure of the strength of a field's quantum fluctuations is in turn given by the magnitude of the field's Feynman propagator. To this end, in this thesis I study how this covariant ultraviolet cutoff modifies the Feynman propagator of a scalar quantum field.

In this work, I first calculate the cutoff Feynman propagator for a scalar field in flat spacetime, and then I address the cutoff Feynman propagator of a scalar field in curved spacetime. My studies culminate with an explicit calculation for the case of a power-law Friedmann-Lemaître-Robertson-Walker (FLRW) spacetime. This last calculation is cosmologically significant, as power-law FLRW spacetime is a prototypical and realistic model for early-universe inflation.

In preparation for studying the covariant cutoff on curved spacetime, I will review the necessary background material as well as the kinematic influence of the covariant cutoff. I will also discuss several side results that I have obtained on scalar quantum field theories in spacetimes which possess a finite start time.

Acknowledgements

First and foremost, I would like to thank my supervisor and close collaborator, Professor Achim Kempf. Professor Kempf has consistently made the greatest of efforts to offer advice, support, and perspective in all aspects of my Master's studies – even when we literally stood at opposite ends of the Earth! I am particularly grateful for what he taught me about formulating and expressing my ideas, and for giving me opportunities to present our collaborative work.

I would also like to acknowledge my other collaborator, Dr. Robert Martin, with whom I often worked closely. The bulk of this thesis came out of my work in the three-way collaboration between Prof. Kempf, Dr. Martin, and myself.

Next, I would like to thank the students and postdocs with whom I shared an office: Dr. William Donnelly, Dr. Eduardo Martín-Martínez, Robert Jonsson, Mikhail Panine, and Eric Webster. I would especially like to thank Dr. Donnelly for the countless conversations that we had and the wealth of feedback that he gave me.

I would like to thank the engineer Michael Smart for teaching me about Nelder-Mead optimization and for being a great housemate. In a similar vein, I owe much of the balance in my daily life to my close friend Stephen Favron. Finally, I would like to thank Fan Jiang, a very special significant other who brought much joy to my life during these last two years.

Table of Contents

List of Tables

List of Figures

List of Symbols

For convenience, several symbols and conventions that are observed in this thesis are listed here.

- Natural units with $c = 1$ (speed of light) and $\hbar = 1$ (reduced Planck's constant) are used throughout this thesis.
- The Einstein summation convention is used throughout this thesis.
- Greek tensor indices denote full spacetime indices, while latin tensor indices only denote spatial indices.
- A comma preceding an index μ denotes differentiation with respect to the μ^{th} coordinate. A semicolon preceding an index μ denotes covariant differentiation with respect to the μ^{th} coordinate.
- A prime $'$ denotes differentiation with respect to the independent variable of a one-dimensional function. A dot $\dot{}$ denotes differentiation with respect to t.
- A circumflex $\hat{}$ over a symbol denotes an operator-valued quantity.
- The bra-ket $\langle \cdot | \cdot \rangle$ denotes the standard inner product on a Hilbert space.

Chapter 1

Introduction

In the field of quantum gravity, it is widely expected that some form of a minimum length scale, or natural ultraviolet (UV) cutoff, exists in nature at the order of the Planck scale [1]. Consider, for instance, the following heuristic argument. Suppose one wishes to resolve some very fine physical feature or to make a very precise distance measurement. Doing so, Heisenberg's Uncertainty Principle implies that there will be a large uncertainty in the momentum of the object that is being measured. From Einstein's equations, we know that momentum curves spacetime. As such, the momentum uncertainty induces uncertainty in the curvature of the local spacetime. One must know how spacetime curves, however, in order to measure distance. Therefore, the uncertainty in curvature causes uncertainty in the original distance measurement. One thus concludes that there should be a smallest length scale, presumably at the order of a Planck length, beyond which smaller distances cannot be resolved. Any attempts to resolve finer lengths are undone by curvature uncertainties.

In the literature, most studies of natural UV cutoffs have been concerned with cutoffs that break local Lorentz symmetry. The difficulty in making a minimum length cutoff covariant is rooted in the fact that any given length scale can be further Lorentz contracted. Put simply, length is not a covariant quantity. Nevertheless, it is possible to overcome this difficulty. That the notion of a minimum length may be consistent with Lorentz contractions was first demonstrated in [2]. Other studies of covariant minimum lengths may be found in [3, 4, 5, 6, 7, 8].

Recently, a new notion of a fully covariant UV cutoff was proposed in [9, 10]. The proposed cutoff is a kind of bandlimit, or maximum frequency for fields in nature, where the bandlimit itself is covariant. It was shown that this cutoff can coexist with Lorentz contractions by allowing field modes with arbitrarily small wavelengths to still exist, albeit with exceedingly small, covariantly-determined bandwidths. In other words, the degrees of freedom in time of sub-Planckian modes are highly suppressed. As such, this cutoff has a natural information theoretic interpretation, namely as a cutoff on the density of a field's degrees of freedom.

This kinematic effect on the degrees of freedom of a quantized scalar field is well understood. There is much to learn, however, about this covariant cutoff's effects on the dynamics of a scalar field. These effects are of great interest, as their presence may have direct observational consequences in cosmology. As such, this covariant UV cutoff offers the tantalizing prospect of experimental access to physics at the Planck scale.

In cosmology, the energy scales that are probed by measurements of cosmic microwave background (CMB) statistics are the closest that we can get to the Planck scale. In particular, the statistics of the CMB's temperature and polarization fluctuations are of great interest. In the standard model of cosmic inflation, these fluctuations are thought to have been seeded by the fluctuations of a primordial scalar inflaton field at the end of inflation. In most models of inflation, the Planck length and the Hubble length – the two relevant characteristic length scales of this epoch – are thought to have been separated by only five to six orders of magnitude [11, 12]. Therefore, it may be that Planck scale effects could be observed in the CMB at only five to six orders of magnitude below the baseline.

Such precision may be within the reach of conceivable experiments assuming that the cosmic foreground can be subtracted with sufficient accuracy. Past and ongoing CMB experiments, such as the Wilkinson Microwave Anisotropy Probe (WMAP), the Acatama Cosmology Telescope (ACT), and the South Pole Telescope (SPT) have been able to constrain cosmological parameters to within a few percent [13]. At the present forefront of experimental cosmology, the Planck satellite achieves about 1 % resolution on the CMB temperature fluctuations themselves over a large part of its measurement range [14, 15]. Furthermore, this resolution may improve following the second data release in 2014, which will also see the release of Planck's B-mode polarization fluctuation data. The SPT has already published preliminary polarization data [16]. While the present data are only on foreground polarization fluctuations, it is hopefully only a matter of time before primordial B-polarization data become available.

As such, to be able to look for evidence of the proposed covariant UV cutoff in the CMB, one should understand the effect that this covariant cutoff has on the temperature and polarization fluctuations of the CMB. Or, equivalently, one should understand the effect that this covariant cutoff has on the fluctuations of the inflaton field. A measure of the strength of a field's quantum fluctuations is given by the magnitude of the field's Feynman propagator. To this end, the main goal of this thesis is to study how the proposed covariant UV cutoff modifies the Feynman propagator of a scalar quantum field.

This thesis begins with a review of preliminary materials in Chapter 2. In particular, a brief review of cosmology and of inflation is given. The review culminates with an explanation of how the fluctuations of the inflaton field are quantified using the Feynman propagator. Chapter 3 discusses in great detail how one calculates the Feynman propagator of a scalar field. The quantum field theoretic groundwork for determining the effect of the covariant cutoff on the Feynman propagator is laid here. A surprising new finding, namely, that canonical quantization is untenable in certain spacetimes, is also discussed. A short review of the proposed covariant cutoff is given in Chapter 4. The definition of the cutoff is discussed, and its kinematic effect is also reviewed. Finally, in Chapter 5 it is shown how one imposes this covariant UV cutoff on the Feynman propagator of a scalar field. The calculation is first performed for a scalar field in flat spacetime. A general approach for Friedmann-Lemaître-Robertson-Walker spacetimes is discussed next. This is followed by an explicit calculation for a power-law spacetime and a discussion of the effect of this covariant UV cutoff.

Chapter 2

Review of Preliminaries

In this chapter, we will review the physics and mathematics that are necessary to understand both the nature of the covariant UV cutoff as well as how the covariant cutoff enters cosmological calculations. We will begin with a review of inflationary cosmology in sections 2.1 and 2.2. In section 2.3, we will review the quantization of a scalar field in curved spacetime. Then, in section 2.4, we will see how the quantum fluctuations of a scalar inflaton field are related to the fluctuations of the CMB. In later chapters, we will see how the covariant cutoff affects scalar field fluctuations. Therefore, by the end of this chapter, we will have seen where in cosmology the observational consequences of the covariant cutoff occur. Finally, we will review some additional mathematics in section 2.5. The techniques outlined in this last section are the techniques that we will use to introduce the covariant cutoff into cosmological fluctuation spectrum calculations.

2.1 Cosmology for Relativists

On cosmic scales much larger than our galaxy and our local cluster, the universe appears to be remarkably homogeneous and isotropic. Therefore, a simple yet exceptionally useful model for the universe is a spacetime

$$M = \mathcal{I} \times \Sigma, \tag{2.1}$$

where $\mathcal{I} \subseteq \mathbb{R}$ and where $(\Sigma, \bar{g})$ is a homogeneous and isotropic Riemannian manifold [17, Chapter 5.3]. Such a spacetime is called a *Friedmann-Lemaître-Robertson-Walker* (FLRW) *spacetime*. Concretely, we may write the line element of M as

$$ds^2 = -dt^2 + a^2(t)\bar{g}_{ij}dx^i dx^j, \tag{2.2}$$

where $\bar{g}$ is a spatial metric with constant curvature that is independent of the cosmic time t. The quantity $a(t)$ is called the scale factor, and we assume that $a(t) > 0$ for all $t \in \mathcal{I}$.

For a Riemannian manifold $(\Sigma, \bar{g})$ with constant curvature, the Riemann tensor, Ricci tensor, and Ricci scalar are given by

$$\bar{R}_{ijkl} = K(\bar{g}_{ik}\bar{g}_{jl} - \bar{g}_{il}\bar{g}_{jk}), \qquad \bar{R}_{jl} = 2K\bar{g}_{jl}, \qquad \text{and} \qquad \bar{R} = 6K \tag{2.3}$$

respectively [17, Chapter 5.2]. The constant K determines the curvature of $(\Sigma, \bar{g})$; when $K > 0$, $(\Sigma, \bar{g})$ is a positively curved spherical manifold, when $K = 0$, $(\Sigma, \bar{g})$ is flat, and when $K < 0$, $(\Sigma, \bar{g})$ is a negatively curved hyperbolic manifold.

The FLRW metric (2.2) and the form of the Riemann tensor given in line (2.3) are enough to show that the elements of the Einstein tensor are given by

$$G_{00} = -g_{00}\left[3\left(\frac{\dot{a}}{a}\right)^2 + \frac{3K}{a^2}\right], \tag{2.4}$$

$$G_{ij} = -g_{ij}\left[2\frac{\ddot{a}}{a} + \left(\frac{\dot{a}}{a}\right)^2 + \frac{K}{a^2}\right], \tag{2.5}$$

and $G_{0i} = G_{i0} = 0$. Therefore, if $\{\bar{\theta}^j\}$ is an orthonormal triad for Σ, $\theta^0 := dt$ and $\theta^j := a(t)\bar{\theta}^j$ together constitute an orthonormal tetrad for M. Using this tetrad basis, one has that $g_{\mu\nu} = \eta_{\mu\nu}$ so that the Einstein tensor reduces to

$$G_{00} = 3\left(\frac{\dot{a}}{a}\right)^2 + \frac{3K}{a^2}, \tag{2.6}$$

$$G_{ii} = -2\frac{\ddot{a}}{a} - \left(\frac{\dot{a}}{a}\right)^2 - \frac{K}{a^2}, \tag{2.7}$$

and all other components are zero.

The Einstein equation $G_{\mu\nu} = 8\pi G\, T_{\mu\nu}$ implies that the stress-energy tensor must also be diagonal and must have the form $T_{00} = \rho$, $T_{ii} = P$. This is the stress-energy tensor of a perfect fluid with energy density ρ and pressure P. Therefore, the equations of motion that govern a FLRW spacetime and its energy content are

$$\left(\frac{\dot{a}}{a}\right)^2 + \frac{K}{a^2} = \frac{8\pi G}{3}\rho\,, \tag{2.8}$$

$$2\frac{\ddot{a}}{a} + \left(\frac{\dot{a}}{a}\right)^2 + \frac{K}{a^2} = -8\pi G\, P. \tag{2.9}$$

For historical reasons, the first equation is often referred to as the *Friedmann equation*.

To "solve" this spacetime amounts to writing down a set of functions $a(t)$, $\rho(t)$, and $P(t)$ which satisfy equations (2.8–2.9), subject to a complete set of boundary conditions. Of course, the two equations (2.8–2.9) alone do not determine the three unknown functions $a(t)$, $\rho(t)$, and $P(t)$. Typically, one introduces an equation of state that relates $\rho(t)$ and $P(t)$ via an equation of state parameter $w(t)$:

$$P(t) = w(t)\rho(t) \tag{2.10}$$

The strategy is then to express ρ as a function of a and to use this expression to solve the Friedmann equation for $a(t)$.

From the continuity condition $T^{\mu\nu}{}_{;\nu} = 0$, for $\mu = 0$ one finds that $\dot{\rho} = -3(\dot{a}/a)(\rho + P)$ [18]. Using the equation of state (2.10) and writing $\frac{d}{dt} = \dot{a}\frac{d}{da}$, it follows that $\frac{d}{da}\ln\rho = (-3/a)(1 + w)$. This has the solution

$$\rho(a) = \rho_0 \exp\left\{-3\int_1^a \frac{1}{a'}(1 + w(a'))\, da'\right\}, \tag{2.11}$$

where $\rho(a=1)=\rho_0$.[1] Then, given a specific w, one could in principle use this expression for $\rho(a)$ to solve the Friedmann equation for $a(t)$.

In practice, what is usually done is to solve the Friedmann equation for constant w. Any period of cosmic time during which the equation of state parameter w is approximately constant is called a *cosmic epoch*. This solution strategy for the Friedmann equation is motivated by the fact that the history of the universe is very naturally partitioned into cosmic epochs.

Consider figure 2.1, which shows a sketch of the post-Big Bang universe. After the Big Bang, the universe was first in a radiation-dominated epoch, for which $w=1/3$. As the universe expanded and cooled, the universe became dominated by pressureless dust, for which $w=0$. This last epoch has lasted until our present era. Now, there is a growing amount of evidence which suggests that we are entering a new epoch in which $w\approx -1$.

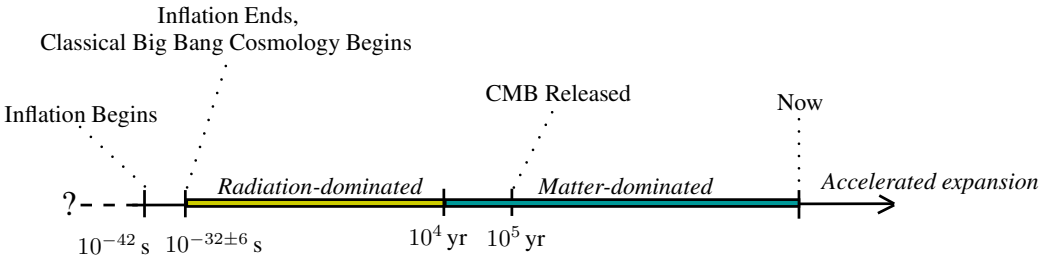

Figure 2.1: A brief sketch of the history of the universe. Events and times are taken from [19, Table 2.1].

When w is a constant, equation (2.11) simplifies to $\rho(a)=\rho_0 a^{-3(1+w)}$. Observationally, it seems that the universe is flat, or $K\approx 0$ to a very good approximation [19, Chapter 3.1]. Thus, setting $K=0$ and using this simplified expression for $\rho(a)$, one finds that the solution of the Friedmann equation is given by

$$a(t)=\begin{cases}\left(\pm\dfrac{t}{t_0}\right)^{2/(3(1+w))} & w\neq -1\\ a_0 e^{\pm Ht} & w=-1,\quad H:=\sqrt{\frac{8\pi G\rho_0}{3}}\end{cases}. \tag{2.12}$$

Note that since only $\dot{a}^2$ appears in the Friedmann equation, there are always both an expanding and a contracting solution for $a(t)$. Unless otherwise noted, we will only consider the expanding solution from now on.

As an illustration, for a dust-dominated universe with $w=0$, one finds that $a(t)\sim t^{2/3}$ and that $\rho(a)\sim a^{-3}$. In other words, the energy density of dust scales inversely with the volume of the universe. For a radiation-dominated universe with $w=1/3$, one finds that $a(t)\sim t^{1/2}$ and that $\rho(a)\sim a^{-4}$. Like for dust, the volume of space contributes to the scaling of the energy density of radiation. An extra factor of a^{-1} comes from the fact that the wavelength of a given mode of radiation is also stretched out as the universe expands.

When $K=0$ and when working in the tetrad basis, the line element (2.2) simply reads $ds^2=-dt^2+a^2(t)d\mathbf{x}^2$. The coordinates $(t,\mathbf{x})$ are called *comoving coordinates*. They describe a coordinate system

[1] A typical convention in cosmology is to normalize the current value of the universe's scale factor to $a(t_0)=1$.

which grows along with the expansion of the universe. In other words, if two observers each maintain a constant comoving separation Δr, then the proper distance between them is increasing, according to $\Delta R(t) = a(t)\Delta r$. To see this, consider null separations $ds^2 = 0$, for which $dt = a(t)dr$. If t is cosmic, or *proper* time, then it is clear that the infinitesimal proper distance travelled by a light ray during an infinitesimal proper time interval dt is $a(t)dr$.

At this point, we seem to have a suitable model for the large-scale structure of the spacetime of the universe.[2] Nevertheless, upon closer examination, we will see soon enough that the FLRW universe constructed thus far suffers two inconveniences: the flatness problem and the horizon problem. We will also see that a resolution of these problems is offered by postulating that a short period of *inflation* preceded the standard Big Bang cosmology. Let us close this short review of FLRW cosmology by stating the following definition:

Definition 2.1.1 *An* inflationary era *is any period of cosmic time during which* $\ddot{a} > 0$.

From equations (2.8–2.9) and (2.10), one finds that $\ddot{a} = -(4\pi G/3)a\rho(1 + 3w)$. Therefore, any cosmic epoch during which $w < -1/3$ is an inflationary epoch.

2.2 Inflation

Two important general relativistic motivations for inflation are the flatness problem and the horizon problem [19, 20, 21].

2.2.1 The Flatness Problem

Consider again the Friedmann equation (2.8) and suggestively rewrite it as follows:

$$K = \frac{8\pi G}{3}a^2(t)\rho(t) - \dot{a}^2(t) \tag{2.13}$$

If $K = 0$ at some given time, then the energy density must be equal to the critical energy density $\rho_{crit}(t) := 3\dot{a}^2(t)/(8\pi G a^2(t))$ at that time t. Define $\Omega(t) := \rho(t)/\rho_{crit}(t)$. Equation (2.13) then reads

$$\Omega(t) - 1 = \frac{K}{\dot{a}^2(t)}. \tag{2.14}$$

The quantity $\Omega(t)$ tells one how close the universe is to being spatially flat at any given cosmic time t.

One can also use the equation above to compare the flatness of the universe now at $t = t_0$ to any other earlier time t_e independently of K by taking a ratio:

$$\frac{\Omega(t_0) - 1}{\Omega(t_e) - 1} = \left(\frac{\dot{a}(t_e)}{\dot{a}(t_0)}\right)^2 \tag{2.15}$$

[2] We have said very little about the energy content of the universe and about localized inhomogeneities. We in our galaxy are in fact one such inhomogeneity! This was never a goal of the FLRW model, however, as it is founded upon the postulates of universal homogeneity and isotropy. We will nonetheless return to this issue in section 2.4.

For example, during a dust-dominated epoch with $w = 0$, using equation (2.12) one has that

$$\frac{\Omega(t_0) - 1}{\Omega(t_e) - 1} = \left(\frac{t_0}{t_e}\right)^{2/3}. \tag{2.16}$$

Notice that for very small values of t_e, the ratio $(\Omega(t_0) - 1)/(\Omega(t_e) - 1)$ becomes increasingly large. In other words, the universe must have been flatter at earlier times than it is now. This phenomenon is also present in radiation-dominated epochs. If one also recalls that observationally, the universe is very nearly flat now, one concludes that the early universe must have been *incredibly* flat shortly after the Big Bang.

This is the *flatness problem*. It is a problem of generality. Of course, one could simply conclude that the universe was extremely flat in its infancy and leave it at that; however, one has no way to explain *why* it would have been so. Out of all the possible ways that the universe could curve, why would it start out so close to flatness?

A period of inflation at the beginning of the universe provides a mechanism to explain why the universe was so flat to begin with. Recall that an inflationary period is any period of cosmic time during which $\ddot{a}(t) > 0$. So, if during this period the magnitude of $\dot{a}(t)$ is increasing, one sees from equation (2.14) that $\Omega(t)$ must be approaching 1. In other words, inflation drives the universe toward flatness. Furthermore, only a very short period of rapid inflation is necessary to produce the initial flatness that is required to explain the degree of flatness that is seen in the universe today [19, Chapter 3].

2.2.2 The Horizon Problem

In order to understand the horizon problem, we must first revisit the history of the universe (figure 2.1). Recall that in classical Big Bang cosmology, the entire energy content of the universe is created by some unspecified mechanism at the Big Bang. The universe was extremely energetic (hot) during its first few moments, but it began to cool as expansion took place. Eventually, once the energy density of radiation had decreased to the point that the universe was in a matter-dominated epoch, there came a time when the universe had cooled to the point where neutral atomic matter could form.

Before this time, the universe was opaque to electromagnetic radiation, as photons would continually scatter off of the charged matter that filled the universe. Once charged subatomic components could coalesce into neutral atoms, however, the universe essentially became transparent to electromagnetic radiation. Therefore, even now the universe is filled with a bath of photons that were emitted when neutral matter formed. These photos have been freely propagating in the universe ever since. Of course, expansion has continued since the formation of neutral matter. These photons have thus continued to cool, and their mean frequency is now in the microwave band. As such, this bath of primordial photons is called the Cosmic Microwave Background (CMB). Much of the experimental data that we have on the early universe come from measurements of the CMB.

The CMB is extraordinarily homogeneous in all directions [22, 23, 14]. While this is a great validation of the FLRW model for cosmology, it also presents us with a problem. Given the best estimates of the age of the universe, CMB photons that come to us from directions separated by more than about one degree could never have been in causal contact. In other words, it would seem that there was not enough time for distant regions of the visible universe to communicate with each other and to thermalize between

the Big Bang and the emission of the CMB. There is no reason *why* the CMB should be so thermally homogeneous[3].

This problem is known as the *horizon problem*, so named because of the existence of causal particle horizons in any FLRW spacetime that possesses an initial singularity. For example, figure 2.2a shows a conformal diagram for a FLRW spacetime filled with matter ($w = 0$), in which it is quite clear that distant points on the CMB are acausal.

Intuitively, a period of inflation solves the horizon problem by inflating a small patch of spacetime into what is the visible universe now. It is then unsurprising that this small patch would be in thermal equilibrium. Inflation formally solves the horizon problem because a period of intense inflation which lasts a very short amount of cosmic time corresponds to a very large period of *conformal time*, which constitutes the vertical axis of a conformal diagram such as figure 2.2. A sufficient increase in the amount of conformal time between the Big Bang and the release of the CMB allows all points on the CMB to be in causal contact with each other, as shown in figure 2.2b.

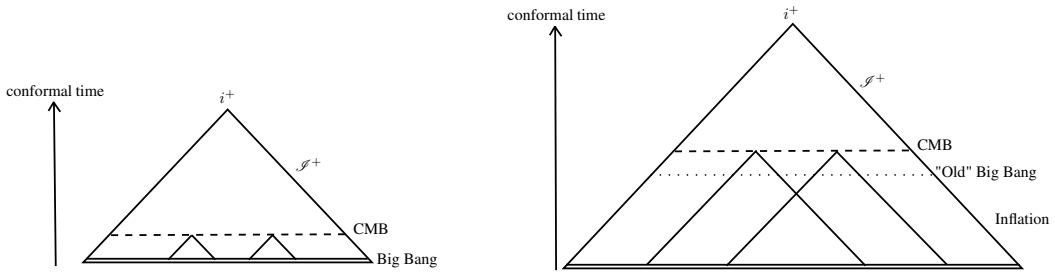

(a) FLRW (b) FLRW with inflationary epoch

Figure 2.2: Penrose diagrams for (a) matter-dominated FLRW spacetime, and (b) matter-dominated FLRW spacetime with an initial inflationary epoch. Diagrams are adapted from [17, Figure 21].

For a concrete illustration, consider a flat FLRW spacetime with the following scale factor:

$$a(t) = \begin{cases} t^2 & 0 < t < t_\star \\ t_\star^{4/3} t^{2/3} & t \geq t_\star \end{cases} \tag{2.17}$$

This corresponds to a spacetime that undergoes inflation for $0 < t < t_\star$ and then transitions to regular expansion for $t \geq t_\star$. We define the conformal time as

$$\eta(t) := \int_{t_\star}^{t} a^{-1}(t')dt' = \begin{cases} \dfrac{1}{t_\star} - \dfrac{1}{t} & 0 < t < t_\star \\ 3t_\star^{4/3}(t^{1/3} - t_\star^{1/3}) & t \geq t_\star \end{cases} . \tag{2.18}$$

With this definition, the metric in comoving coordinates becomes conformally flat and reads $ds^2 = a^2(\eta)[-d\eta^2 + d\mathbf{x}^2]$.

Let us now compare $\Delta\eta := \eta(t_2) - \eta(t_1)$, the amount of conformal time that elapses between two points in cosmic time, for $0 < t_1, t_2 < t_\star$ and $t_1, t_2 \geq t_\star$. Holding $\Delta t := t_2 - t_1$ fixed, we can plot $\Delta\eta$ as a function

[3]For a more thorough review of the history of the universe and of the CMB, the reader is invited to consult a comprehensive text such as [19] or [24].

of t_1 (figure 2.3). This plot illustrates that more conformal time elapses per unit of cosmic time during inflation than during regular universal expansion.

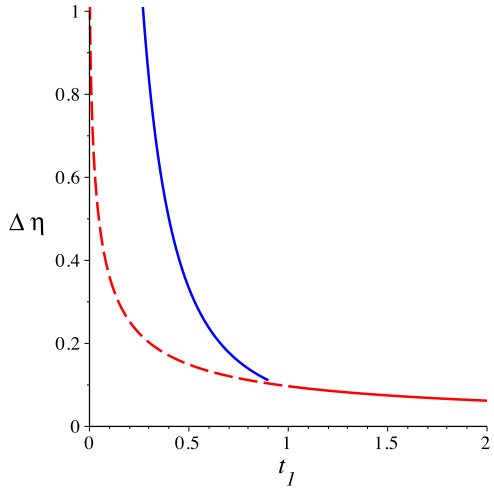

Figure 2.3: Plot of the amount of conformal time that elapses per cosmic time $\Delta t = 0.1$ for the scale factor (2.17), with $t_\star = 1$. The inflationary phase is plotted in solid blue and the non-inflationary phase is plotted in solid red. The dashed red line is an extension of the non-inflationary phase down to $t_1 = 0$. The dashed line is well below the blue line, so more conformal time elapses per unit of cosmic time during the inflationary phase.

2.3 The Quantized Scalar Field in Curved Spacetime

Next, we will address quantum aspects of inflation. We begin with a short review of the quantization of a scalar field in curved space time. The foundational concepts we stress largely parallel those put forward in a series of lectures by Kempf [20]. A more detailed treatment of more or less the same material may be found in [25, 26, 27].

Consider first the classical theory. The classical action for a free scalar field ϕ in a curved spacetime is

$$S_{KG}[\phi] = \int \left(-\tfrac{1}{2}\, g^{\mu\nu}\phi_{,\mu}\phi_{,\nu} - V(\phi)\right) \sqrt{|g|}\, d^4x, \tag{2.19}$$

where $V(\phi)$ is the potential of the scalar field. For simplicity, let us consider $V(\phi) = \frac{1}{2}m^2\phi^2$, which is among the simplest potentials that one could write down for a free scalar field with mass m. Setting the variation of the action with respect to ϕ to zero yields the Klein-Gordon equation, *i.e.*, the field's equation of motion:

$$(\Box - m^2)\phi(x) = 0 \tag{2.20}$$

The symbol $\Box$ denotes the D'Alembertian, which in curved spacetime is given by

$$\Box := \frac{1}{\sqrt{|g|}} \frac{\partial}{\partial x^\mu} \left(g^{\mu\nu} \sqrt{|g|} \frac{\partial}{\partial x^\nu} \right). \tag{2.21}$$

Let us also suppose that the spacetime is globally hyperbolic and that it possesses a coordinatization $(x^0, \mathbf{x})$, where x^0 is a timelike coordinate. This lets one define the canonical conjugate field π via

$$\pi(x^0, \mathbf{x}) \equiv \frac{\delta L_{KG}[\phi]}{\delta \phi_{,0}(x^0, \mathbf{x})}, \tag{2.22}$$

where the Lagrangian $L_{KG}[\phi]$ is defined through the relation

$$S_{KG}[\phi] = \int L_{KG}[\phi]\, dx^0. \tag{2.23}$$

From the action (2.19) for a scalar field, one has that

$$\pi(x^0, \mathbf{x}) = -g^{0\nu}\sqrt{|g|}\,\phi_{,\nu}(x^0, \mathbf{x}). \tag{2.24}$$

In the quantized theory, we assume that the action remains unchanged. The field $\phi(x)$, however, is replaced with an operator-valued distribution $\hat{\phi}(x)$. "Solving" the quantum field theory amounts to writing down an expression for $\hat{\phi}(x)$ which obeys the Klein-Gordon equation and which also satisfies the canonical commutation relations. For simplicity, let us assume that the field has no charge. Classically, this means that the field $\phi(x)$ is real. Correspondingly, in the quantum theory, the field $\hat{\phi}(x)$ is Hermitian. We may compactly summarize the problem of quantizing an uncharged free scalar field as follows:

Definition 2.3.1 *Consider an uncharged free scalar field. The quantized field $\hat{\phi}(x)$, together with its canonical conjugate $\hat{\pi}(x)$, are operator-valued distributions that satisfy*

1. $\hat{\phi}(x) = \hat{\phi}^\dagger(x)$ (H)

2. $$\begin{aligned}\left[\hat{\phi}(x^0, \mathbf{x}), \hat{\phi}(x^0, \mathbf{x}')\right] &= \left[\hat{\pi}(x^0, \mathbf{x}), \hat{\pi}(x^0, \mathbf{x}')\right] = 0 \\ \left[\hat{\phi}(x^0, \mathbf{x}), \hat{\pi}(x^0, \mathbf{x}')\right] &= i\delta^3(\mathbf{x} - \mathbf{x}')\end{aligned}$$ (CCR)

3. $(\Box - m^2)\hat{\phi}(x) = 0$ (EOM)

These three conditions are Hermiticity (H), the Canonical Commutation Relations (CCR), and an Equation of Motion (EOM).

The canonical quantization of the field decomposes $\hat{\phi}(x)$ into an integral over spatial modes. We adopt the following ansatz:

$$\hat{\phi}(x^0, \mathbf{x}) = \frac{1}{(2\pi)^{3/2}} \int d^3k \left(u_{\mathbf{k}}(x^0, \mathbf{x}) a_{\mathbf{k}} + u_k^*(x^0, \mathbf{x}) a_{\mathbf{k}}^\dagger\right) \tag{2.25}$$

Each pair of $a_{\mathbf{k}}$ and $a_{\mathbf{k}}^\dagger$ are raising and lowering operators which satisfy $[a_{\mathbf{k}}, a_{\mathbf{k}'}] = [a_{\mathbf{k}}^\dagger, a_{\mathbf{k}'}^\dagger] = 0$ and $[a_{\mathbf{k}}, a_{\mathbf{k}'}^\dagger] = \delta^3(\mathbf{k} - \mathbf{k}')$. The functions $u_{\mathbf{k}}(x^0, \mathbf{x})$ are the *mode functions* of the field $\hat{\phi}$.

By construction, the ansatz (2.25) satisfies the Hermiticity condition (H). It is also clear that the field will satisfy its equation of motion provided the mode functions satisfy the equation of motion (EOM).

The canonical commutation relations (CCR) place a constraint on the mode functions. In particular, considering the equal time commutation relation between $\hat{\phi}$ and $\hat{\pi}$, one obtains the following:

$$\begin{aligned}[\hat{\phi}(x^0,\mathbf{x}),\hat{\pi}(x^0,\mathbf{x}')] &= \frac{1}{(2\pi)^3}\iint d^3k\, d^3k' \Big[u_{\mathbf{k}}(x^0,\mathbf{x})a_{\mathbf{k}} + u^*_{\mathbf{k}}(x^0,\mathbf{x})a^\dagger_{\mathbf{k}}, \\ &\qquad - g^{0\nu}\sqrt{|g|}\,\frac{\partial}{\partial x'^\nu}u_{\mathbf{k}'}(x'^0,\mathbf{x}')a_{\mathbf{k}'} - g^{0\nu}\sqrt{|g|}\frac{\partial}{\partial x'^\nu}u^*_{\mathbf{k}'}(x'^0,\mathbf{x}')a^\dagger_{\mathbf{k}'}\Big]_{x'^0=x^0} \\ &= g^{0\nu}\sqrt{|g|}\int\frac{d^3k}{(2\pi)^3}\left(u^*_{\mathbf{k}}(x^0,\mathbf{x})\frac{\partial}{\partial x'^\nu}u_{\mathbf{k}}(x'^0,\mathbf{x}') - u_{\mathbf{k}}(x^0,\mathbf{x})\frac{\partial}{\partial x'^\nu}u^*_{\mathbf{k}}(x'^0,\mathbf{x}')\right)_{x'^0=x^0} \end{aligned} \tag{2.26}$$

Therefore, one must have

$$g^{0\nu}\sqrt{|g|}\int\frac{d^3k}{(2\pi)^3}\left(u^*_{\mathbf{k}}(x^0,\mathbf{x})\frac{\partial}{\partial x'^\nu}u_{\mathbf{k}}(x'^0,\mathbf{x}') - u_{\mathbf{k}}(x^0,\mathbf{x})\frac{\partial}{\partial x'^\nu}u^*_{\mathbf{k}}(x'^0,\mathbf{x}')\right)_{x'^0=x^0} = i\delta^3(\mathbf{x}-\mathbf{x}'). \tag{2.27}$$

This is known as the *generalized Wronskian condition*, which we abbreviate by (W). In a globally hyperbolic spacetime, solutions of the Klein-Gordon equation which satisfy (W) are always guaranteed to exist [20, 27].

Example 2.3.2 *Flat Spacetime*

Consider flat spacetime with the metric $ds^2 = -dt^2 + d\mathbf{x}^2$. Here, the D'Alembertian is simply

$$\Box = -\frac{\partial^2}{\partial t^2} + \triangle, \tag{2.28}$$

where $\triangle \equiv \sum_{j=1}^3 \frac{\partial^2}{\partial x^{j\,2}}$ is the spatial Laplacian. The canonical conjugate field $\hat{\pi}$ is just the time derivative of $\hat{\phi}$, *i.e.*, $\hat{\pi}(t,\mathbf{x}) = \partial_t\hat{\phi}(t,\mathbf{x})$. Let us write the mode functions as

$$u_{\mathbf{k}}(t,\mathbf{x}) = \frac{1}{\sqrt{2}}\,v^*_k(t)e^{i\mathbf{k}\cdot\mathbf{x}}, \tag{2.29}$$

where $k \equiv |\mathbf{k}|$. Despite the potential ambiguity that it introduces, we will also refer to the $v_k(t)$ as mode functions. It should be clear from the context when the term "mode functions" refers to the v_k or to the $u_{\mathbf{k}}$. In any case where it is not clear, we will explicitly indicate which type of mode function is being referred to.

Consequently, the field $\hat{\phi}$ takes the form

$$\hat{\phi}(t,\mathbf{x}) = \frac{1}{(2\pi)^{3/2}}\int d^3k\,\frac{1}{\sqrt{2}}\left(v^*_k(t)e^{i\mathbf{k}\cdot\mathbf{x}}a_{\mathbf{k}} + v_k(t)e^{-i\mathbf{k}\cdot\mathbf{x}}a^\dagger_{\mathbf{k}}\right). \tag{2.30}$$

Taking the spatial Fourier transform of the $u_k(t,\mathbf{x})$'s equation of motion gives a simplified equation of motion for the $v_k(t)$:

$$\left(\Box_k - m^2\right)v_k(t) = \left(-\frac{\partial^2}{\partial t^2} - |\mathbf{k}|^2 - m^2\right)v_k(t) = 0. \tag{2.31}$$

The general solution is

$$v_k(t) = A_k e^{i\omega_k t} + B_k e^{-i\omega_k t}, \tag{2.32}$$

where $\omega_k := \sqrt{|\mathbf{k}|^2 + m^2}$ and where $A_k, B_k \in \mathbb{C}$. The equal-time commutator between $\hat{\phi}$ and $\hat{\pi}$ now reads

$$\left[\hat{\phi}(t,\mathbf{x}), \hat{\pi}(t,\mathbf{x}')\right] = \int \frac{d^3k}{(2\pi)^3}\frac{1}{2}\left(\dot{v}_k(t)v_k^*(t) - v_k(t)\dot{v}_k^*(t)\right)e^{-i\mathbf{k}\cdot(\mathbf{x}-\mathbf{x}')} \stackrel{?}{=} i\delta^3(\mathbf{x}-\mathbf{x}'), \tag{2.33}$$

so (W) simplifies to give the usual *Wronskian condition* from quantum field theory in flat spacetime:

$$\dot{v}_k(t)v_k^*(t) - v_k(t)\dot{v}_k^*(t) = 2i \tag{2.34}$$

Applied to the solution (2.32), the Wronskian condition requires that

$$|A_k|^2 - |B_k|^2 = \frac{1}{\omega_k}. \tag{2.35}$$

The standard choice of A_k and B_k is $A_k = 1/\sqrt{\omega_k}$ and $B_k = 0$. In this case, the final field operator reads

$$\hat{\phi}(t,\mathbf{x}) = \frac{1}{(2\pi)^{3/2}}\int d^3k\, \frac{1}{\sqrt{2\omega_k}}\left(e^{-i\omega_k t + i\mathbf{k}\cdot\mathbf{x}}a_{\mathbf{k}} + e^{i\omega_k t - i\mathbf{k}\cdot\mathbf{x}}a_{\mathbf{k}}^\dagger\right). \tag{2.36}$$

In principle, we could make another choice of A_k and B_k, which would define a different set of mode functions. Suppose we have two sets of mode functions, $\{v_k\}$ and $\{\tilde{v}_k\}$. How does one choice of mode functions physically differ from another? The answer is that a particular choice of mode functions corresponds to a choice of the vacuum state. (Recall that the vacuum state $|0\rangle$ is defined as that state which is mapped to zero by all of the annihilation operators $a_{\mathbf{k}}$, *i.e.*, $a_{\mathbf{k}}|0\rangle = 0\ \forall\ \mathbf{k} \in \mathbb{R}^3$.) Let us demonstrate this.

Since the k-D'Alembertians ($\Box_k - m^2$) are second-order differential operators, both $\{v_k, v_k^*\}$ and $\{\tilde{v}_k, \tilde{v}_k^*\}$ span the two-dimensional solution space for a fixed k. Therefore, there exist $\alpha_k, \beta_k \in \mathbb{C}$ such that

$$\begin{aligned} v_k(t) &= \alpha_k\tilde{v}_k(t) + \beta_k\tilde{v}_k^*(t) \\ v_k^*(t) &= \alpha_k^*\tilde{v}_k^*(t) + \beta_k^*\tilde{v}_k(t) \end{aligned}. \tag{2.37}$$

This lets us rewrite equation (2.30) as

$$\begin{aligned} \hat{\phi}(t,\mathbf{x}) &= \frac{1}{(2\pi)^{3/2}}\int d^3k\,\frac{1}{\sqrt{2}}\left[(\alpha_k^*\tilde{v}_k^*(t) + \beta_k^*\tilde{v}_k(t))e^{i\mathbf{k}\cdot\mathbf{x}}a_{\mathbf{k}} + (\alpha_k\tilde{v}_k(t) + \beta_k\tilde{v}_k^*(t))e^{-i\mathbf{k}\cdot\mathbf{x}}a_{\mathbf{k}}^\dagger\right] \\ &= \frac{1}{(2\pi)^{3/2}}\int d^3k\,\frac{1}{\sqrt{2}}\left[\tilde{v}_k^*(t)e^{i\mathbf{k}\cdot\mathbf{x}}\underbrace{(\alpha_k^*a_{\mathbf{k}} + \beta_k a_{-\mathbf{k}}^\dagger)}_{\tilde{a}_{\mathbf{k}}} + \tilde{v}_k(t)e^{-i\mathbf{k}\cdot\mathbf{x}}\underbrace{(\beta_k^*a_{-\mathbf{k}} + \alpha_k a_{\mathbf{k}}^\dagger)}_{\tilde{a}_{\mathbf{k}}^\dagger}\right] \end{aligned} \tag{2.38}$$

Equation (2.38) defines new creation and annihilation operators $\tilde{a}_{\mathbf{k}}$ and $\tilde{a}_{\mathbf{k}}^\dagger$, and hence defines a new vacuum state $|\tilde{0}\rangle$. This is because the new annihilation operators $\tilde{a}_{\mathbf{k}}$ always contain a certain amount of the old creation operators $a_{\mathbf{k}}^\dagger$, and so they do not map the old vacuum state to zero.

In flat spacetime, a single vacuum state (given by the choice of A_k and B_k above) is very naturally singled out. This is the state that, for instance, minimizes the expectation value of the Hamiltonian and that respects all of the symmetries of flat spacetime. In curved spacetimes, however, there is no longer necessarily a privileged vacuum vacuum state. The choice of vacuum is often a very delicate matter [27]. ▷

Example 2.3.3 *FLRW Spacetime*

Consider a flat FLRW spacetime with the metric $ds^2 = -dt^2 + a^2(t)d\mathbf{x}^2$. From now on, we will only study FLRW spacetimes with zero spatial curvature, so whenever we refer to a FLRW spacetime, we will be referring to a flat FLRW spacetime.

Here as well, we suppose that the general form of the field is given by equation (2.30). The mode functions $v_k(t)$ obey a different equation of motion, however, since the d'Alembertian is different. For the metric given above, the d'Alembertian reads

$$\Box = a^{-3}(t)\left(-\partial_t a^3(t)\partial_t + a(t)\triangle\right), \tag{2.39}$$

where $\triangle$ again denotes the flat spatial Laplacian. Under a Fourier transform with respect to $\mathbf{x}$, the d'Alembertian becomes

$$\Box_k = -a^{-3}(t)\left(\partial_t a^3(t)\partial_t + k^2 a(t)\right), \tag{2.40}$$

where $k \equiv |\mathbf{k}|$. Therefore, the mode functions in a FLRW spacetime must obey the following equation of motion:

$$\ddot{v}_k(t) + 3\frac{\dot{a}(t)}{a(t)}\dot{v}_k(t) + \left(\frac{k^2}{a^2(t)} + m^2\right)v_k(t) = 0 \tag{2.41}$$

Also note that the generalized Wronskian condition (W) assumes the simplified form

$$\dot{v}_k(t)v_k^*(t) - v_k(t)\dot{v}_k^*(t) = \frac{2i}{a^3(t)}. \tag{2.42}$$

When we work with FLRW spacetimes, it will sometimes be convenient to work in conformal time η, where

$$\eta(t) := \int^t a^{-1}(t')\,dt'. \tag{2.43}$$

Under this change of time variable, the metric becomes conformally flat and reads $ds^2 = a^2(\eta)\left[-d\eta^2 + d\mathbf{x}^2\right]$. Likewise, the k-d'Alembertians read

$$\Box_k = -a^{-4}(\eta)\left(\partial_\eta a^2(\eta)\partial_\eta + k^2 a^2(\eta)\right). \tag{2.44}$$

It is also customary in the literature to rescale the mode functions by defining $\chi_k(\eta) := a(\eta)v_k(\eta)$. Doing so, one obtains the following equation of motion for the $\chi_k(\eta)$:

$$\chi_k''(\eta) + \left[k^2 + m^2a^2(\eta) - \frac{a''(\eta)}{a(\eta)}\right]\chi_k(\eta) = 0 \tag{2.45}$$

Note that $'$ denotes differentiation with respect to η. As is manifest in the equation above, this rescaling conveniently yields an equation of motion for a simple harmonic oscillator with a time-dependent frequency. Using the chain rule, one also deduces from equation (2.42) that the Wronskian condition reads

$$\chi_k'(\eta)\chi_k^*(\eta) - \chi_k(\eta)\chi_k^{*\prime}(\eta) = 2i. \tag{2.46}$$

Later, we will also want to work with an equation of motion for a simple harmonic oscillator with a time-dependent frequency, but in cosmic time t. As such, one may define rescaled mode functions $w_k(t) := a^{3/2}(t)v_k(t)$ whose equation of motion is

$$\ddot{w}_k(t) + \left[\frac{k^2}{a^2(t)} + m^2 - \frac{3}{2}\left(\frac{\dot{a}^2(t)}{2a^2(t)} + \frac{\ddot{a}(t)}{a(t)}\right)\right]w_k(t) = 0. \tag{2.47}$$

Similarly, the Wronskian condition reads

$$\dot{w}_k(t)w_k^*(t) - w_k(t)\dot{w}_k^*(t) = 2i. \tag{2.48}$$

▷

2.4 Quantum Fields in Inflationary Cosmology

We have now collected all of the machinery that is necessary to put in place the last piece of the inflationary model. With the collected tools, one can propose a mechanism which both produces inflation and accounts for the energy content of the universe.

2.4.1 The Inflaton Field

In this subsection, we will see how a scalar field can give rise to inflation. This field is called the *inflaton field*.

Consider again the action (2.19) for a scalar field in curved spacetime with some potential $V(\phi)$. Varying the action with respect to the metric, one finds that

$$\frac{\delta S_{KG}[\phi]}{\delta g_{\mu\nu}} = \frac{1}{2}\sqrt{|g|}\left(g^{\mu\alpha}g^{\nu\beta}\phi_{,\alpha}\phi_{,\beta} - \frac{1}{2}g^{\mu\nu}\left[g^{\alpha\beta}\phi_{,\alpha}\phi_{,\beta} + V(\phi)\right]\right). \tag{2.49}$$

Recall that the stress-energy tensor is defined as

$$T^{\mu\nu} := \frac{2}{\sqrt{|g|}}\frac{\delta S_{KG}[\phi]}{\delta g_{\mu\nu}}. \tag{2.50}$$

With covariant indices, the stress-energy tensor for a scalar field thus reads

$$T_{\mu\nu} = \phi_{,\mu}\phi_{,\nu} - \frac{1}{2}g_{\mu\nu}\left[g^{\alpha\beta}\phi_{,\alpha}\phi_{,\beta} + V(\phi)\right]. \tag{2.51}$$

Suppose now that we are working in a FLRW spacetime. Making use of the tetrad basis described in section 2.1, one finds that the energy density and pressure of the field are

$$\rho(t) = T_{00} = \frac{1}{2}\dot{\phi}^2(t) + V(\phi), \tag{2.52}$$

$$P(t) = T_{ii} = \frac{1}{2}\dot{\phi}^2(t) - V(\phi). \tag{2.53}$$

The equation of state parameter is therefore

$$w(t) = \frac{\frac{1}{2}\dot{\phi}^2 - V(\phi)}{\frac{1}{2}\dot{\phi}^2 + V(\phi)}. \tag{2.54}$$

A crucial observation is that if $\dot{\phi}^2 \ll V(\phi)$ for some period of time, then $w \approx -1$. In other words, that period is an inflationary epoch.

This observation, along with experimental indications, motivates the *slow-roll* model for early-universe inflation [19]. In its most basic form, slow-roll inflation maintains that early-universe inflation was driven by a scalar inflaton field having a potential of the kind shown in figure 2.4. In this model, the inflaton field is first excited to a high potential that has a very gradual downward slope (which produces a small $\dot{\phi}(t)$), thus driving inflation. After a period of slow-roll, the field falls into the potential well and equilibrates about the bottom of the well. During this equilibration, the potential energy of the inflation field is dissipated into the other fields that make up the energy content of the universe. The universe is thus populated with (the progenitors of) the matter and radiation that we see today. This last period is called *reheating*, and its end marks the resumption of standard Big Bang cosmology in the standard theory of the history of the universe.

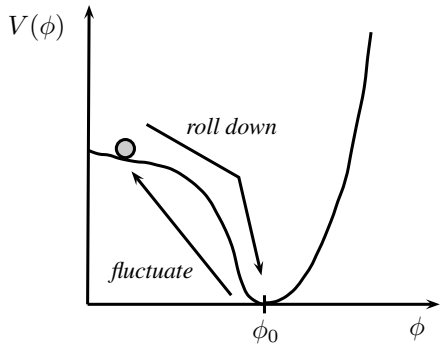

Figure 2.4: Archetypal slow-roll potential

One model for the slowly-rolling part of inflation is *power-law inflation*, where the scale factor takes the form

$$a(t) = ct^{\alpha}\ ; \qquad c > 0, \qquad \alpha \gg 1, \qquad t \in [t_i, t_f]. \tag{2.55}$$

We can roughly motivate this model as follows. During a period of slow-roll inflation, the Friedmann equation (2.8) approximately reads

$$\left(\frac{\dot{a}(t)}{a(t)}\right)^2 \approx \frac{8\pi G}{3} V(\phi(t)). \tag{2.56}$$

Since $V(t) = V(\phi(t))$ is approximately constant during this period, an approximate solution for $a(t)$ is

$$a(t) \approx a_0 \exp\left\{t\sqrt{\frac{8\pi G}{3}V(t)}\right\}. \tag{2.57}$$

If we postulate that $a(t) \sim t^{\alpha}$, then approximately it must be that $\sqrt{V(t)} \sim t^{-1}\ln t$. This $V(t)$ is plotted in figure 2.5. From the plot, we see that $V(t)$ is indeed slowly rolling for suitable $0 < t_i < t_f$. In our studies of the covariant cutoff, we will mainly be concerned with power-law inflation.

To study the full quantum inflaton field in power-law spacetime is somewhat difficult. When one studies a quantized scalar field in curved spacetime, the two equations which govern the dynamics of the spacetime and the field are the Einstein equation and the Klein-Gordon equation respectively. Both of these come

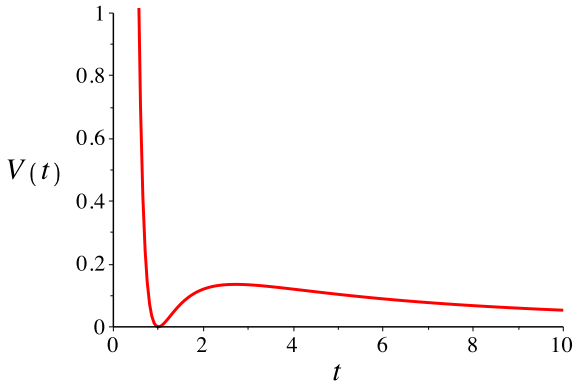

Figure 2.5: Approximate power-law slow-roll potential

from variations of a total action

$$\begin{aligned} S_{tot}[g,\phi] &= S_{EH}[g] + S_{KG}[g,\phi] \\ &= \frac{1}{16\pi G}\int (R-2\Lambda)\,\sqrt{|g|}\,d^4x + \int \left(-\tfrac{1}{2}\,g^{\mu\nu}\phi_{,\mu}\phi_{,\nu} - V(\phi)\right)\sqrt{|g|}\,d^4x\,, \end{aligned} \tag{2.58}$$

where $S_{EH}[g]$ is the Einstein-Hilbert action, and $S_{KG}[\phi]$ is the scalar field action from before. Because of this common origin, the evolution of the field and the evolution of the spacetime are intimately linked. In particular, if one specifies the scale factor $a(t)$, then the potential $V(\phi)$ is fixed.

For a power-law scale factor, one finds that the inflaton potential goes like $V(\phi) \sim \exp\{-(\phi-\phi_i)/\sigma\}$, where $\phi_i \equiv \phi(t_i)$ and where $\sigma = \sqrt{\alpha/(4\pi G)}$ [28]. The Klein-Gordon equation in this case is quite complicated. As such, instead of studying the full inflaton field itself, one splits the field into two parts: a classical homogeneous part $\phi_0(t)$ and a quantum spatially-inhomogeneous part $\hat{\varphi}(t,\mathbf{x})$, *i.e.*,

$$\hat{\phi}(t,\mathbf{x}) = \phi_0(t)\,\hat{\mathbb{1}} + \hat{\varphi}(t,\mathbf{x}). \tag{2.59}$$

One can then show that $\phi_0(t)$ evolves classically along with the spacetime and that $\hat{\varphi}(t,\mathbf{x})$ behaves as a massless quantized field on a curved spacetime background [20, 29]. In other words, the quantized deviations from spatial homogeneity are effectively decoupled from the potential $V(\phi)$ and evolve according to equation (2.20) with $m=0$. Moreover, the quantum fluctuations of $\hat{\phi}(t,\mathbf{x})$ are precisely the quantum fluctuations of $\hat{\varphi}(t,\mathbf{x})$.

As such, in this thesis we will study the dynamics of a scalar field that exists *on* a background power-law spacetime. Unless otherwise indicated, we will denote such a field by $\hat{\phi}$ from this point onward. Explicitly, we will study a scalar field whose equation of motion is given by (2.20), where $\Box$ is the d'Alembertian for power-law spacetime.

Finally, we should note that the picture of the inflaton field from equation (2.59) is still an approximation to a full quantum theory. A full theory would require a fluctuating metric to go along with a fluctuating quantized inflaton field. Of course, this would demand a theory of quantum gravity. Without

quantum gravity, however, one can still consider a better approximation by writing the metric in terms of a classical part $\tilde{g}_{\mu\nu}(t)$ and a small perturbation $\gamma_{\mu\nu}(t, \mathbf{x})$:

$$g_{\mu\nu}(t, \mathbf{x}) = \tilde{g}_{\mu\nu}(t) + \gamma_{\mu\nu}(t, \mathbf{x}) \tag{2.60}$$

One can then quantize the perturbation $\hat{\gamma}_{\mu\nu}(t, \mathbf{x})$ and consider its fluctuations together with the fluctuations of $\hat{\varphi}(t, \mathbf{x})$. The gauge-invariant combination of these two fluctuating quantities yields the variables $v(t, \mathbf{x})$ (the *Mukhanov variable*) and $h_{ij}(t, \mathbf{x})$, which describe fluctuations of purely scalar and purely tensorial natures respectively. Moreover, v and h_{ij} obey equations of motion which are completely analogous to the equation of motion of a scalar field on a curved spacetime background. We refer the interested reader to [29] for a review of the theory of quantized perturbations.

2.4.2 Fluctuations

Recall that when one measures the photons which make up the CMB, one measures a very uniform temperature in all directions. Nevertheless, there are small, local temperature fluctuations on top of this uniform background. There are also fluctuations in the polarization of the CMB. Crucially, the statistics of the temperature and polarization fluctuations of the CMB can be related to the scalar and tensorial fluctuations of the inflaton field (or more precisely, to v and h_{ij}). Precision measurements of these CMB statistics therefore lets one quantitatively test inflationary predictions.

For this thesis, let us return to the scenario of a quantized scalar field on a curved spacetime background. In order to quantify the fluctuations of a scalar field, one introduces the notions of the averaged field and of averaged fluctuations.

Definition 2.4.1 *Let $B \in \mathbb{R}^3$ be a region with volume V. The* averaged field $\hat{\phi}_B(t)$ *is defined as*

$$\hat{\phi}_B(t) := \int_{\mathbb{R}^3} \hat{\phi}(t, \mathbf{x}) W(\mathbf{x})\, d^3x, \tag{2.61}$$

where $W(\mathbf{x})$ is a window function with the following behaviour:

$$W(\mathbf{x}) \approx \begin{cases} 0 & \mathbf{x} \notin B \\ V^{-1} & \mathbf{x} \in B \end{cases} \tag{2.62}$$

The average field is motivated by the fact that in practice one cannot measure a quantum field's amplitude everywhere in space at a given time. At best, one can only witness the average of the field at some observational scale.

Suppose now that we are working with a FLRW spacetime and that B is a region of volume V in comoving coordinates. Let us adopt for our field an ansatz of the form (2.30). Suppose that we make a particular choice of mode functions such that the state $|\Omega\rangle$ is the vacuum at some time t_0. Also suppose that the field is in this state. (Note that we are working in the Heisenberg evolution picture, so this state

remains the same for all time.) One can show that the expectation value of the averaged field vanishes:

$$\begin{aligned}\bar{\phi}_B(t) &= \langle\Omega|\hat{\phi}_B(t)|\Omega\rangle \\ &= \int \langle 0|\hat{\phi}(t,\mathbf{x})|0\rangle W(\mathbf{x})\, d^3x \\ &= \int \frac{1}{(2\pi)^{3/2}} \int d^3k\, \frac{1}{\sqrt{2}} \left(v_k^*(t) e^{i\mathbf{k}\cdot\mathbf{x}} \underbrace{\langle 0|a_{\mathbf{k}}|0\rangle}_{=0} + v_k(t) e^{-i\mathbf{k}\cdot\mathbf{x}} \underbrace{\langle 0|a_{\mathbf{k}}^\dagger|0\rangle}_{\sim\langle 0|1\rangle=0} \right) W(\mathbf{x})\, d^3x \\ &= 0 \end{aligned} \tag{2.63}$$

The variance, or in other words, the *averaged fluctuations* of the field do not vanish:

$$\begin{aligned}\Delta\phi_B^2(t) &= \langle\Omega| \left(\hat{\phi}_B(t) - \bar{\phi}_B(t)\right)^2 |\Omega\rangle \\ &= \langle\Omega|\hat{\phi}_B^2(t)|\Omega\rangle \\ &= \iint \langle 0|\hat{\phi}(t,\mathbf{x})\hat{\phi}(t,\mathbf{y})|0\rangle W(\mathbf{x})W(\mathbf{y})\, d^3x\, d^3y \end{aligned} \tag{2.64}$$

The expectation value in the last line is calculated as follows:

$$\begin{aligned}\langle 0|\hat{\phi}(t,\mathbf{x})\hat{\phi}(t,\mathbf{y})|0\rangle &= \frac{1}{(2\pi)^3} \iint d^3k\, d^3k'\, \frac{1}{2} \langle 0| \left(v_k^*(t) e^{i\mathbf{k}\cdot\mathbf{x}} a_{\mathbf{k}} + v_k(t) e^{-i\mathbf{k}\cdot\mathbf{x}} a_{\mathbf{k}}^\dagger \right) \\ &\qquad \times \left(v_k^*(t) e^{i\mathbf{k}'\cdot\mathbf{y}} a_{\mathbf{k}'} + v_k(t) e^{-i\mathbf{k}'\cdot\mathbf{y}} a_{\mathbf{k}'}^\dagger \right) |0\rangle \qquad (2.65) \\ &= \frac{1}{(2\pi)^3} \frac{1}{2} \int d^3k\, |v_k(t)|^2 e^{i\mathbf{k}(\mathbf{x}-\mathbf{y})} \qquad (2.66) \end{aligned}$$

Therefore, one has that

$$\begin{aligned}\Delta\phi_B^2(t) &= \iint \frac{1}{(2\pi)^3} \frac{1}{2} \int d^3k\, |v_k(t)|^2 e^{i\mathbf{k}(\mathbf{x}-\mathbf{y})} W(\mathbf{x})W(\mathbf{y})\, d^3x\, d^3y \\ &= \frac{1}{2} \int d^3k\, |v_k(t)|^2 \left[\frac{1}{(2\pi)^{3/2}} \int e^{-i\mathbf{k}\cdot\mathbf{x}} W^*(\mathbf{x})\, d^3x \right]^* \left[\frac{1}{(2\pi)^{3/2}} \int e^{-i\mathbf{k}\cdot\mathbf{y}} W(\mathbf{y})\, d^3y \right] \\ &= \frac{1}{2} \int d^3k\, |v_k(t)|^2\, |\tilde{W}(\mathbf{k})|^2\,. \end{aligned} \tag{2.67}$$

$\tilde{W}(\mathbf{k})$ denotes the Fourier transform of the window function.

Let us now compute $\Delta\phi_B^2$ another way. The forthcoming calculation is less direct, but amenable to the imposition of the covariant cutoff. Consider the two-point, time-ordered expectation value

$$\langle 0|T\hat{\phi}(t,\mathbf{x})\hat{\phi}(s,\mathbf{y})|0\rangle := \theta(t-s)\langle 0|\hat{\phi}(t,\mathbf{x})\hat{\phi}(s,\mathbf{y})|0\rangle + \theta(s-t)\langle 0|\hat{\phi}(s,\mathbf{y})\hat{\phi}(t,\mathbf{x})|0\rangle. \tag{2.68}$$

Here, T is the time-ordering operator, and θ is the Heaviside step function:

$$\theta(t) = \begin{cases} 0 & t < 0 \\ \frac{1}{2} & t = 0 \\ 1 & t > 0 \end{cases} \tag{2.69}$$

The non-equal time two point functions $\langle 0|\hat{\phi}(t,\mathbf{x})\hat{\phi}(s,\mathbf{y})|0\rangle$ and $\langle 0|\hat{\phi}(s,\mathbf{y})\hat{\phi}(t,\mathbf{x})|0\rangle$ are computed the same way as in equations (2.65) and (2.66). Therefore, one has that[4]

$$\begin{aligned}\langle 0|T\hat{\phi}(t,\mathbf{x})\hat{\phi}(s,\mathbf{y})|0\rangle &= \theta(t-s)\frac{1}{(2\pi)^3}\frac{1}{2}\int d^3k\, v_k^*(t)v_k(s)e^{i\mathbf{k}(\mathbf{x}-\mathbf{y})} \\ &\quad + \theta(s-t)\frac{1}{(2\pi)^3}\frac{1}{2}\int d^3k\, v_k^*(s)v_k(t)e^{-i\mathbf{k}(\mathbf{x}-\mathbf{y})} \qquad (2.70)\\ &= \frac{1}{(2\pi)^{3/2}}\int \frac{d^3k}{(2\pi)^{3/2}}\frac{1}{2}\left\{\theta(t-s)v_k^*(t)v_k(s)+\theta(s-t)v_k(t)v_k^*(s)\right\}e^{i\mathbf{k}(\mathbf{x}-\mathbf{y})} \qquad (2.71)\end{aligned}$$

Evaluated at equal time, the last line reads

$$\langle 0|T\hat{\phi}(t,\mathbf{x})\hat{\phi}(t,\mathbf{y})|0\rangle = \frac{1}{(2\pi)^3}\frac{1}{2}\int d^3k\,|v_k(t)|^2 e^{i\mathbf{k}(\mathbf{x}-\mathbf{y})} \qquad (2.72)$$

Now let $\mathbf{y}=\mathbf{x}+\mathbf{L}$ and rewrite the last integral in spherical coordinates, with $L\equiv|\mathbf{L}|$:

$$\begin{aligned}\langle 0|T\hat{\phi}(t,\mathbf{x})\hat{\phi}(t,\mathbf{x}+\mathbf{L})|0\rangle &= \frac{1}{(2\pi)^3}\frac{1}{2}\int k^2\sin\theta\, dk\, d\theta\, d\phi\,|v_k(t)|^2\, e^{-ikL\cos\theta} \\ &= \frac{1}{(2\pi)^2}\int_0^\infty |v_k(t)|^2\,\frac{\sin(kL)}{kL}\,k^2\,dk \qquad (2.73)\end{aligned}$$

Observe that the sinc function $\sin(kL)/kL$ is (up to a factor of $(2\pi)^{-1/2}$) the Fourier transform of the unit box of length $2L$ and height $1/2L$. In other words, it is the Fourier transform of the prototypical window function. If we rewrite the expression we obtained for $\Delta\phi_B^2(t)$ in (2.67) as an integral in spherical coordinates (assuming that $|\tilde{W}(\mathbf{k})|$ is spherically-symmetric), we have that

$$\Delta\phi_B^2(t) = \frac{1}{2}\int_0^\infty |v_k(t)|^2\,|\tilde{W}(k)|^2\,4\pi k^2\,dk\,. \qquad (2.74)$$

Roughly speaking, if $\tilde{W}(k)$ is such that it we can approximate $|\tilde{W}(k)|\sim|\tilde{W}(k)|^2$, then equations (2.73) and (2.74) describe the same quantity. This is the case, for instance, for a $\tilde{W}(k)$ which obeys

$$\tilde{W}(k)\approx\begin{cases}1 & k\le k_\star\\ 0 & k>k_\star\end{cases}\,. \qquad (2.75)$$

In our case, we can make the following approximation:

$$\frac{\sin(kL)}{kL}\approx\begin{cases}1 & kL\le 1\\ 0 & kL>1\end{cases} \qquad (2.76)$$

Therefore, we conclude that both $\Delta\phi_B^2(t)$ and $\langle 0|T\hat{\phi}(t,\mathbf{x})\hat{\phi}(t,\mathbf{x}+\mathbf{L})|0\rangle$ describe the same measure of the strength of the fluctuations of $\hat{\phi}$ on comoving length scales of order L.

[4]Note that to go to from (2.70) to (2.71), we have exploited the fact that $k=|\mathbf{k}|=|-\mathbf{k}|$. If we were working in some general globally hyperbolic spacetime such that the mode functions were indexed by a vector $\mathbf{k}$ instead of k, line (2.71) would read

$$\frac{1}{(2\pi)^{3/2}}\int\frac{d^3k}{(2\pi)^{3/2}}\frac{1}{2}\left\{\theta(t-s)v_{\mathbf{k}}^*(t)v_{\mathbf{k}}(s)+\theta(s-t)v_{-\mathbf{k}}(t)v_{-\mathbf{k}}^*(s)\right\}e^{i\mathbf{k}(\mathbf{x}-\mathbf{y})}\,.$$

Finally, let us make use of the aforementioned approximation to estimate the integral (2.73):

$$\int_0^\infty |v_k(t)|^2 \, \frac{\sin(kL)}{kL} \, k^2 \, dk \sim \int_0^{\pi/L} |v_k(t)|^2 \, k^2 \, dk \tag{2.77}$$

The k^2 term in the previous line suppresses small vales of the integrand, so let us further estimate $|v_k(t)|^2$ by its value at $k = \pi/L$, giving

$$\int_0^{\pi/L} |v_k(t)|^2 \, k^2 \, dk \approx |v_{\pi/L}(t)|^2 \int_0^{\pi/L} k^2 \, d^3 \, k \sim k^3 |v_k(t)|^2 \big|_{k=\pi/L} \, . \tag{2.78}$$

This little series of calculations and approximations motivates the following definition [24, Equation 6.52]:

Definition 2.4.2 *The* fluctuation spectrum *of a scalar field $\hat{\phi}$ is defined as*

$$\delta\phi_k(t) := \frac{1}{2\pi} k^{3/2} \, |v_k(t)| \, . \tag{2.79}$$

It is a measure of the strength of the quantum fluctuations of the k^{th} comoving mode of the field $\hat{\phi}$. Equivalently, it is a measure of the strength of the quantum fluctuations of the field $\hat{\phi}$ at comoving distance scales of order k^{-1}.

To summarize, we see that $\Delta\phi_B^2(t) \sim \langle 0|T\hat{\phi}(t,\mathbf{x})\hat{\phi}(t,\mathbf{y})|0\rangle$ for a window function which falls off for comoving scales that are larger than $|\mathbf{x}-\mathbf{y}|$. In particular, this relation demonstrates that the spatial Fourier transform of $\langle 0|T\hat{\phi}(t,\mathbf{x})\hat{\phi}(t,\mathbf{y})|0\rangle$,

$$\frac{1}{(2\pi)^{3/2}} \int d^3k \, e^{-i\mathbf{k}\cdot(\mathbf{x}-\mathbf{y})} \langle 0|T\hat{\phi}(t,\mathbf{x})\hat{\phi}(t,\mathbf{y})|0\rangle = \frac{1}{(2\pi)^{3/2}} \frac{1}{2} |v_k(t)|^2, \tag{2.80}$$

is a momentum density which describes the strength of the quantum fluctuations of the inflation field $\hat{\phi}$ at comoving wavenumbers of order $k \sim |\mathbf{x}-\mathbf{y}|^{-1}$. Multiplying this density by k^3 defines a *bona fide* variance, and the square root of this variance is (up to a multiplicative constant) the fluctuation spectrum of the field. This fluctuation spectrum may be experimentally determined by measuring the fluctuations of the CMB.

In the rest of this thesis, we will extensively study the time-ordered two-point function $\langle 0|T\hat{\phi}(x)\hat{\phi}(y)|0\rangle$, which is otherwise known as the *Feynman propagator* $G_F(x,y)$. It is the avenue that we will use to study the covariant cutoff in cosmology.

Example 2.4.3 *Flat Spacetime*

It would be remiss to close this section without considering any examples of field fluctuations, so let us first consider a scalar field $\hat{\phi}(t,\mathbf{x})$ of mass m in flat spacetime. Recall that the mode functions are given by $v_k(t) = \omega_k^{-1/2} \exp\{i\omega_k t\}$, where $\omega_k := \sqrt{k^2+m^2}$. From equation (2.80), the equal-time spatial Fourier transform of the Feynman propagator is thus

$$G_F(t=t',k) = \frac{1}{(2\pi)^{3/2}} \frac{1}{2\omega_k}, \tag{2.81}$$

and the fluctuation spectrum is

$$\delta\phi_k(t) = \frac{1}{2\pi}\frac{k^{3/2}}{(k^2+m^2)^{1/4}} \sim \begin{cases} k^{3/2}/m^2 & k \ll m^2 \\ k & k \gg m^2 \end{cases} . \tag{2.82}$$

These two functions are plotted in figures 2.6a and 2.6b respectively. Note that small-k fluctuations, or in other words, fluctuations on large comoving length scales, are strongly suppressed in flat spacetime.

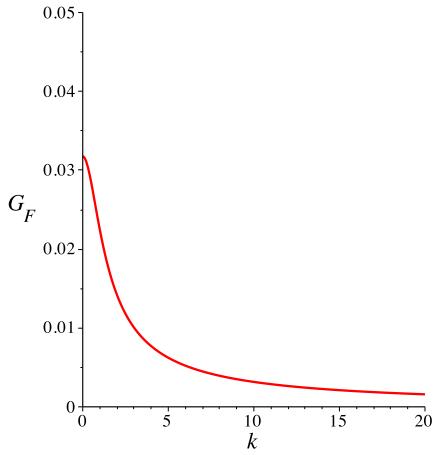

(a) Plot of $G_F(t = t', k)$.

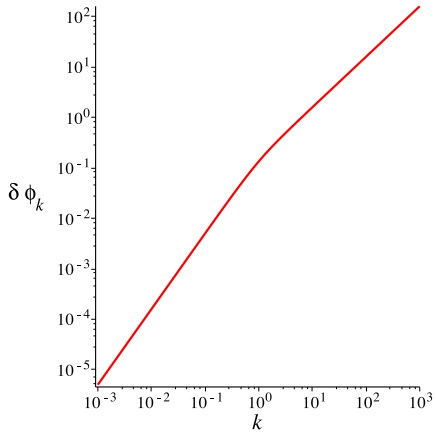

(b) Log-log plot of $\delta\phi_k(t)$.

Figure 2.6: Plots of the equal-time Feynman propagator and of the fluctuation spectrum in flat spacetime. The fluctuation spectrum is time-independent. A value of $m = 1$ was used to generate these plots.

▷

Example 2.4.4 *Power-Law Spacetime*

Consider a scalar field $\hat{\phi}(t, \mathbf{x})$ on power-law spacetime (equation (2.55)). We must first determine what the mode functions are. It is easiest to work in conformal time and to compute the scaled mode functions $\chi_k(\eta) = a(\eta)v_k(\eta)$ defined in example 2.3.3.

Define the conformal time coordinate as

$$\eta(t) := -\int_t^\infty a^{-1}(s)\,ds = -\int_t^\infty \frac{1}{cs^\alpha}\,ds = \frac{1}{c(\alpha-1)t^{\alpha-1}}, \tag{2.83}$$

so that both $t, \eta \in [0, \infty)$. As t runs from 0 up to ∞, η runs from ∞ down to 0. (Recall that $\alpha > 1$ by assumption.) It then follows that the scale factor is

$$a(\eta) = c\left[c(\alpha-1)\eta\right]^{-\alpha/(\alpha-1)}, \tag{2.84}$$

so that the equation of motion (2.45) reads

$$\chi_k''(\eta) + \left[k^2 + m^2\left[\frac{1}{c\left((\alpha-1)\eta\right)^\alpha}\right]^{2/(\alpha-1)} - \frac{\alpha(2\alpha-1)}{(\alpha-1)^2}\frac{1}{\eta^2}\right]\chi_k(\eta) = 0. \tag{2.85}$$

A closed-form solution to this equation can only be written down when $m = 0$. In this case, the general solution is

$$\chi_k(\eta) = \sqrt{\eta}\left(A_k J_n(k\eta) + B_k Y_n(k\eta)\right), \tag{2.86}$$

where J_n and Y_n denote the Bessel J and Y functions of order n, and where $A_k, B_k \in \mathbb{C}$ are arbitrary constants. The constant n is

$$n = \frac{3\alpha - 1}{2(\alpha - 1)}. \tag{2.87}$$

In order to fix a specific linear combination of solutions as the mode function, or in other words, in order to make a choice of vacuum, we appeal to the *Bunch-Davies criterion* [26, Chapter 7.2.1]. The Bunch-Davies criterion states that for early times (and thus late conformal times), the field modes should not feel the curvature of the FLRW spacetime and as such should tend to flat mode functions,[5] *i.e.*,

$$\lim_{\eta\to\infty} \chi_k(\eta) \sim \frac{1}{\sqrt{k}} e^{-ik\eta}\,. \tag{2.88}$$

Recalling the Bessel function asymptotics for large $|z|$,

$$J_p(z) \sim \sqrt{\frac{2}{\pi z}} \cos\left(z - \frac{p\pi}{2} - \frac{\pi}{4}\right) \tag{2.89}$$

$$Y_p(z) \sim \sqrt{\frac{2}{\pi z}} \sin\left(z - \frac{p\pi}{2} - \frac{\pi}{4}\right), \tag{2.90}$$

one sees that the Bunch-Davies criterion indicates that $A_k = \sqrt{\pi/2}$ and $B_k = -i\sqrt{\pi/2}$. Therefore, the scaled mode functions which define the *Bunch-Davies vacuum* are

$$\chi_k(\eta) = \sqrt{\frac{\pi\eta}{2}}(J_n(k\eta) - iY_n(k\eta)) = \sqrt{\frac{\pi\eta}{2}} H_n^{(2)}(k\eta), \tag{2.91}$$

where $H_n^{(2)}$ is the Hankel function of the second kind of order n.

The equal-time spatial Fourier transform of the Feynman propagator is thus

$$G_F(\eta = \eta', k) = \frac{1}{(2\pi)^{3/2}} \frac{1}{2a^2(\eta)} \frac{\pi\eta}{2} \left(J_n^2(k\eta) + Y_n^2(k\eta)\right). \tag{2.92}$$

The fluctuation spectrum is

$$\delta\phi_k(\eta) = \frac{1}{2\pi} k^{3/2} \frac{1}{a(\eta)} \left[\frac{\pi\eta}{2}\left(J_n^2(k\eta) + Y_n^2(k\eta)\right)\right]^{1/2} \sim \begin{cases} k & k \gg \eta^{-1} \\ k^{3/2-n} & k \ll \eta^{-1} \end{cases}. \tag{2.93}$$

The small-k behaviour of $\delta\phi_k(\eta)$ is determined using the Bessel function asymptotics for small $|z|$.

$$J_p(z) \sim \frac{1}{\Gamma(p+1)} \left(\frac{z}{2}\right)^p \tag{2.94}$$

$$Y_p(z) \sim -\frac{\Gamma(p)}{\pi} \left(\frac{2}{z}\right)^p \tag{2.95}$$

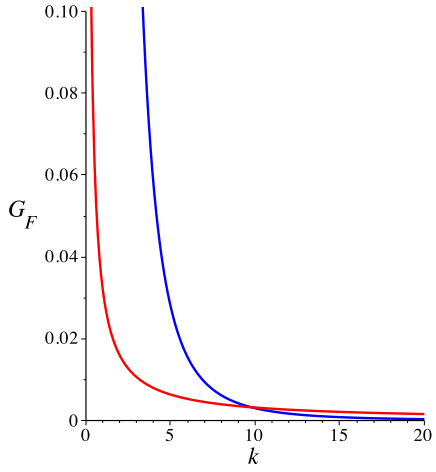

(a) Plots of $G_F(t = t' = 1.3, k)$.

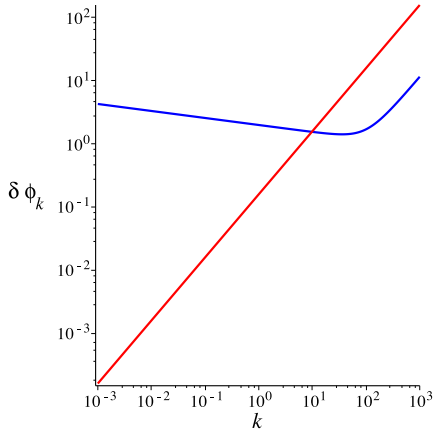

(b) Log-log plots of $\delta\phi_k(t = 1.3)$.

Figure 2.7: Plots of the equal-time Feynman propagator and the fluctuation spectrum for a massless scalar field in flat spacetime (red) and power-law spacetime (blue). In power-law spacetime, the fluctuation spectrum is time-dependent. Values of $t = 1.3$, $c = 1$, and $\alpha = 10$ were used to generate these plots.

The Feynman propagator and the fluctuation spectrum are plotted in figures 2.7a and 2.7b respectively.

In stark contrast to the case of flat spacetime, small-k (or large comoving wavelength) fluctuations remain more or less constant in strength in power-law spacetime. Indeed, as $\alpha \to \infty$, $n \to 3/2$ so that $\delta\phi_k(t) \sim$ *constant* for small k. This is one of the most salient features of inflation and certainly one of the most important to have been verified in the CMB [22, 30, 15]. Furthermore, this freezing of large-scale fluctuations constitutes a mechanism for the seeding of inhomogeneities in the early universe. If indeed the potential of the inflaton field is the primordial source of all matter and energy in the universe, then the field's large-scale fluctuations would have produced a primordial distribution of matter and energy with small inhomogeneities. These inhomogeneities would have given rise to the large-scale structure that we observe today. Further discussion of this topic is beyond the scope of this thesis. A comprehensive study of inflationary cosmology may be found in [19]. ▷

2.5 The Theory of Self-Adjoint Extensions

The last preliminary of which we will make extensive use is the theory of self-adjoint extensions of symmetric operators. We will only review the essentials of the general theory, as well as selected results for Sturm-Liouville differential operators. The reader is invited to consult one of the many texts on the subject of the theory of self-adjoint extensions for a more detailed treatment. Excellent references are [31, Chapter VII] and [32, Chapter 8].

[5]There is one small subtlety here. Recall that the massless flat mode functions are $v_k(t) = k^{-1/2}\exp\{ikt\}$, *i.e.*, the argument of the exponent is positive. For the definition of conformal time which we have adopted, however, in flat spacetime we would have $\eta_{flat}(t) = -\int_0^t ds = -t$. Finally, since $a(t) = 1$ for flat spacetime, we have that $\chi_{k,flat}(\eta) = k^{-1/2}\exp\{-ik\eta\}$.

2.5.1 General Results

Originally due to von Neumann, the theory of self-adjoint extensions answers the questions of when a symmetric operator has self-adjoint extensions and how these extensions are constructed. Let us dissect this last sentence by collecting several definitions. All of the definitions will be drawn from [31, Chapters 4, 8]. In what follows, we will denote a Hilbert space by $\mathcal{H}$ and its inner product by $\langle\cdot|\cdot\rangle$. All operators will be linear and will map from $\mathcal{H}$ into $\mathcal{H}$.

First, let us recall the definition of the adjoint of an operator.

Definition 2.5.1 *Let T be a densely-defined operator on $\mathcal{H}$ with domain* $\mathrm{dom}(T)$*. The domain of the adjoint of T is defined as follows:*

$$\mathrm{dom}(T^*) := \{g \in \mathcal{H} \ : \ \exists\, h_g \in \mathcal{H} \ \text{ such that } \ \langle Tf|g\rangle = \langle f|h_g\rangle \ \ \forall\, f \in \mathrm{dom}(T)\} \tag{2.96}$$

The adjoint operator T^* has as its action $T^*g = h_g$.

Next, we define Hermitian and symmetric operators.

Definition 2.5.2 *An operator T is* Hermitian *if $\langle Tf|g\rangle = \langle f|Tg\rangle$ for all $f, g \in \mathrm{dom}(T)$.*

Definition 2.5.3 *An operator S is* symmetric *if it is Hermitian and densely-defined.*

Finally, we may define self-adjointness.

Definition 2.5.4 *A symmetric operator T is* self-adjoint *if $T = T^*$, i.e.,* $\mathrm{dom}(T) = \mathrm{dom}(T^*)$.

Note that a symmetric operator and its adjoint only differ by their domains, and that $\mathrm{dom}(S) \subseteq \mathrm{dom}(S^*)$. In general, whenever two operators T and T' are such that $\mathrm{dom}(T) \subseteq \mathrm{dom}(T')$ and the restriction $T'|_{\mathrm{dom}(T)}$ is equal to T, we say that T' is an extension of T.

Von Neumann's theorems settle the questions of when a symmetric operator has self-adjoint extensions and how they are constructed. First, let us recall that an operator T is closed if and only if its graph $G(T) := \{(f, Tf) \,|\, f \in \mathrm{dom}(T)\}$ is closed in $\mathcal{H}\times\mathcal{H}$. Von Neumann's first theorem then states the following:

Theorem 2.5.5 (Von Neumann I) *Let S be a closed, symmetric operator on $\mathcal{H}$. The domain of its adjoint is given by*

$$\mathrm{dom}(S^*) = \mathrm{dom}(S) \dotplus N_+ \dotplus N_- \tag{2.97}$$

The symbol $\dotplus$ denotes a direct sum, and $N_\pm$ are the *deficiency spaces* of the operator S. These are the eigenspaces of the adjoint S^* to the eigenvalues $\pm i$. Explicitly, one has that

$$N_\pm := \ker(\pm i - T^*) = \mathrm{ran}(\mp i - T)^\perp \,. \tag{2.98}$$

Von Neumann's first theorem states that the domain of the adjoint S^* only differs from the domain of S by the deficiency spaces $N_\pm$. Therefore, any self-adjoint extension of S can only be constructed by enlarging the domain of S to include vectors from the deficiency spaces. How this enlargement is made and to what the deficiency vectors are mapped is addressed by von Neumann's second theorem.

Theorem 2.5.6 (Von Neumann II) *Let S be a closed, symmetric operator on $\mathcal{H}$.*

(a) *S' is a closed symmetric extension of S if and only if there exist closed subspaces $F_+ \subseteq N_+$, $F_- \subseteq N_-$ and an isometry $V : F_+ \to F_-$ such that*

$$\mathrm{dom}(S') = \mathrm{dom}(S) + \{g + Vg \ : \ g \in F_+\} \tag{2.99}$$

(b) *S' is self-adjoint if and only if $F_+ = N_+$ and $F_- = N_-$.*

Recall that a linear map V is an isometry if $\mathrm{dom}(V)$ is closed and $\langle Vf|Vg\rangle = \langle f|g\rangle$ for all $f, g \in \mathrm{dom}(V)$. Crucially, it therefore follows from von Neumann's second theorem that a symmetric operator S only has self-adjoint extensions if the dimensions of the deficiency spaces are the same. The dimensions of the deficiency spaces are called the *deficiency indices* of S. Writing $\dim(N_\pm) = n_\pm$, we say that S has deficiency indices (n_+, n_-).

Lastly, let us also note the following useful theorem [31, Theorem 8.1].

Theorem 2.5.7 *For a Hermitian operator T, one has that* $\dim\ker(z - T^*)$ *is constant on the complex upper half-plane $\mathbb{C}^+ \setminus \mathbb{R}$ and on the complex lower half-plane $\mathbb{C}^- \setminus \mathbb{R}$.*

In particular, this theorem implies that n_+ (resp. n_-) is equal to the dimension of the eigenspace of T^* to any eigenvalue in the complex upper (resp. lower) half-plane. We may thus choose eigenvalues other than $\pm i$ to compute $n_\pm$ should it simplify the calculations.

2.5.2 Sturm-Liouville Differential Operators

Of particular interest for this thesis are Sturm-Liouville differential operators and their self-adjoint extensions. All of the definitions and theorems in this section are drawn from [33]. To begin, consider the following definition:

Definition 2.5.8 *A* Sturm-Liouville differential expression *is a formal differential expression τ where*

$$\tau f(x) = \frac{1}{r(x)}\left[-(pf')'(x) + q(x)f(x)\right] \quad \text{for} \quad x \in (a,b),\ -\infty \le a < b \le \infty \tag{2.100}$$

The functions p, q, and r are subject to the following basic assumptions:

1. *p, q, r are real-valued and measurable in (a, b)*
2. *$p, r > 0$ almost everywhere in (a, b)*
3. *p^{-1}, q, and r are locally integrable in (a, b)*

One can form differential operators by having τ act on function in domains contained in the Hilbert space $\mathcal{H} = L^2((a,b),\, r(x)\,dx)$. These operators are clearly symmetric in the standard inner product of $\mathcal{H}$:

$$\begin{aligned}\langle \tau f | g\rangle &= \int_a^b \frac{1}{r(x)}\left[-(pf^{*\prime})'(x) + q(x)f^*(x)\right] g(x) r(x)\,dx \\ &= -(pf')^*(x)g(x)\big|_a^b + f^*(x)pg'(x)\big|_a^b + \int_a^b f^*(x)\frac{1}{r(x)}\left[-(pg')'(x) + q(x)g(x)\right] r(x)\,dx \\ &= \langle f | \tau g\rangle + \text{boundary terms}\end{aligned} \tag{2.101}$$

Definition 2.5.8 is very general, and we will mostly be concerned with the simpler case of

$$\tau f(x) = -f''(x) + Q(x)f(x) \quad \text{for} \quad x \in (a,b),\ -\infty \le a < b \le \infty\,. \tag{2.102}$$

The basic assumptions on τ reduce to

1. Q is real-valued and measurable on (a,b), and
2. Q is locally integrable on (a,b).

Let us discuss how one generates operators from τ. One defines the maximal operator $\hat{T}$ through the largest domain in $\mathcal{H}$ on which τ may act.

Definition 2.5.9 *The* maximal operator $\hat{T}$ *has as its domain*

$$\mathrm{dom}(\hat{T}) = \left\{ f \in L^2((a,b),\, r(x)\,dx)\ :\ f, pf' \in AC(a,b),\ \tau f \in L^2((a,b),\, r(x)\,dx)\right\} \tag{2.103}$$

$AC(a,b)$ denotes the set of absolutely continuous functions on the interval (a,b). The minimal operator $\hat{T}_0$, which is in a sense the smallest symmetric operator that one may construct, is defined as follows:

Definition 2.5.10 *The* minimal operator $\hat{T}_0$ *has as its domain*

$$\mathrm{dom}(\hat{T}_0) = \left\{ f \in \mathrm{dom}(\hat{T})\ :\ [f,g]_a = [f,g]_b = 0 \quad \forall\, g \in \mathrm{dom}(\hat{T})\right\} \tag{2.104}$$

The previous definition makes use of the Lagrange bracket.

Definition 2.5.11 *For $f, g \in \mathrm{dom}(\hat{T})$, the* Lagrange bracket *at a point $x \in (a,b)$ is defined as*

$$[f,g]_x := f^*(x)pg'(x) - (pf'(x))^* g(x). \tag{2.105}$$

The Lagrange brackets at the endpoints are given by the limits

$$[f,g]_a = \lim_{x\to a^+}[f,g]_x \qquad \textit{and} \qquad [f,g]_b = \lim_{x\to b^-}[f,g]_x, \tag{2.106}$$

which are guaranteed to exist.

One immediately notices that it is possible to rewrite equation (2.101) using the Lagrange bracket:

$$\langle \tau f | g \rangle = [f, g]_b - [f, g]_a + \langle f | \tau g \rangle \tag{2.107}$$

Since the boundary terms must vanish for an operator to be self-adjoint, one may rightly guess that the self-adjoint extensions of the minimal operator $\hat{T}_0$ may be characterized in terms of the Lagrange bracket. It turns out that $\hat{T}_0$ may have deficiency indices $(0,0)$, $(1,1)$, or $(2,2)$ [33]. Furthermore, a powerful way to deduce which set of deficiency indices some given Sturm-Liouville minimal operator has is to examine the endpoints a and b and to determine whether they are *limit point case* (LPC) or *limit circle case* (LCC).

To understand the LPC and LCC characterization, we need an additional definition.

Definition 2.5.12 *A function $f \in L^2((a,b),\, r(x)\,dx)$ is said to* lie left *(resp. right) in $L^2((a,b),\, r(x)\,dx)$ if f restricted to the interval (a,c) (resp. (c,b)) for all $c \in (a,b)$ is in $L^2((a,c),\, r(x)\,dx)$ (resp. $L^2((c,b),\, r(x)\,dx)$).*

The Weyl Alternative then classfies endpoints as LPC or LCC.

Theorem 2.5.13 (Weyl Alternative) *Let τ denote a Sturm-Liouville differential expression. Then for the endpoint a (resp. b), one of the following is true:*

- *For every $z \in \mathbb{C}$, all solutions of $(\tau - z)u = 0$ lie left (resp. right) in $\mathcal{H}$. One says that τ is LCC at a (resp. b).*
- *For every $z \in \mathbb{C} \setminus \mathbb{R}$, there is a single solution of $(\tau - z)u = 0$ which lies left (resp. right) in $\mathcal{H}$. One says that τ is LPC at a (resp. b).*

Alternatively, if for every $z \in \mathbb{C}$ there is at least one solution of $(\tau - z)u = 0$ which does not lie left (resp. right), then τ is LPC at a (resp. b). Otherwise, τ is LCC at a (resp. b).

Finally, one has that the deficiency indices of $\hat{T}_0$ are as follows:

- $(0,0)$: τ is LPC at both endpoints
- $(1,1)$: τ is LPC at one endpoint and LCC at the other
- $(2,2)$: τ is LCC at both endpoints

In this thesis, we will mainly be concerned with Sturm-Liouville operators that have deficiency indices $(1,1)$. Thus, in closing we note the following parametrization of the self-adjoint extensions of $\hat{T}_0$ when its deficiency indices are $(1,1)$.

Proposition 2.5.14 *Let τ be a Sturm-Liouville differential expression such that $\hat{T}_0$ has deficiency indices $(1,1)$. Then, all of the self-adjoint extensions $\hat{A}$ of $\hat{T}_0$ are given by*

$$\mathrm{dom}(\hat{A}) \equiv \mathrm{dom}(\hat{A}_g) = \left\{ f \in \mathrm{dom}(\hat{T}) \;:\; [f,g]_b - [f,g]_a = 0 \right\}, \tag{2.108}$$

where $g(x)$ is real-valued on (a,b) and $g \in \mathrm{dom}(\hat{T}) \setminus \mathrm{dom}(\hat{T}_0)$.

In particular, if τ is LCC at a and LPC at b, one may parametrize all self-adjoint extensions by writing

$$\mathrm{dom}(\hat{A}_g) = \left\{ f \in \mathrm{dom}(\hat{T}) \;:\; [f,g]_a = 0 \right\}, \tag{2.109}$$

where $g \neq 0$ is any real-valued solution of $(\tau - \lambda)u = 0$ on (a,b) for some $\lambda \in \mathbb{R}$.

Chapter 3

Results on Two-Point Functions in Quantum Field Theory

We have already encountered one example of a two-point function, namely, the Feynman propagator $G_F(x,y) \equiv \langle 0|T\hat{\phi}(x)\hat{\phi}(y)|0\rangle$. Two-point functions are ubiquitous in quantum field theory. The Feynman propagator in particular is of great interest for this thesis, since our aim is to study how the Feynman propagator is modified by the covariant cutoff. As such, let us study two-point functions in quantum field theory in a bit more detail.

In sections 3.1 and 3.2, we will examine how two-point functions are calculated in the Heisenberg operator picture and in the path integral picture respectively. While the operator picture excels in producing clean formulas for two-point functions, the path integral picture will later reveal how one imposes the covariant cutoff on the Feynman propagator. We will also examine new results on how the choice of vacuum enters into path integral calculations in flat spacetime. Finally, we will see in section 3.3 how to calculate the Feynman propagator in a way that will be useful for imposing the covariant cutoff later.

3.1 Two-Point Functions from the Operator Approach

In the last chapter, we expressed the Feynman propagator as a time-ordered expectation value. In general, one may build different two-point functions out of the basic expectation values

$$G^+(x,y) \equiv \langle 0|\hat{\phi}(x)\hat{\phi}(y)|0\rangle \qquad \text{and} \qquad G^-(x,y) \equiv \langle 0|\hat{\phi}(y)\hat{\phi}(x)|0\rangle. \tag{3.1}$$

$G^+(x,y)$ and $G^-(x,y)$ are called the *positive* and *negative Wightman functions* respectively. For example, in this notation, we may write $G_F(x,y) = \theta(t-s)G^+(x,y) + \theta(s-t)G^-(x,y)$. As another example, the Pauli-Jordan function, which is also known as the retarded Green's function $G_R(x,y)$, is given by $G_R(x,y) = \theta(t-s)\left(G^+(x,y) - G^-(x,y)\right)$ [25, Chapter 2].

Using field expectation values to compute two-point functions is exceptionally useful for obtaining clean, closed-form expressions. Recall, for example, the expression that we found for the Feynman propagator of

a scalar field in a FLRW spacetime in equation (2.71). In particular, we can read off its Fourier transform with respect to $\mathbf{x}-\mathbf{y}$:

$$G_F(t,s,k) = \frac{1}{(2\pi)^{3/2}}\frac{1}{2}\left[\theta(t-s)v_k^*(t)v_k(s) + \theta(s-t)v_k(t)v_k^*(s)\right] \tag{3.2}$$

Here, we still define $k := |\mathbf{k}|$. For example, for flat spacetime, where $v_k(t) = \omega_k^{-1/2}\exp\{i\omega_k t\}$, $\omega_k^2 = |\mathbf{k}|^2 + m^2$, one easily finds that

$$G_F(t,s,k) = \frac{1}{(2\pi)^{3/2}}\frac{1}{2\omega_k}e^{-i\omega_k|t-s|}. \tag{3.3}$$

As was noted in the previous chapter, $G_F(t=s,k)$ may be used to calculate the fluctuation spectrum of a field $\hat{\phi}$.

The fact that we have been calling certain two-point functions "propagators" or "Green's functions" is no coincidence. Indeed, certain two-point functions in quantum field theory are the integral kernels of inverses of the Klein-Gordon operator $(\Box - m^2)$. Others, such as G^+ and G^-, satisfy the homogeneous equation $(\Box - m^2)G^{\pm}(x,y) = 0$.

In particular, for a globally-hyperbolic spacetime (M,g), the Feynman propagator of a scalar field obeys [27, Chapter 3.2]

$$(\Box_x - m^2)G_F(x,y) = i\frac{\delta^4(x-y)}{\sqrt{|g(x)|}}. \tag{3.4}$$

(The subscript x on the d'Alembertian denotes that derivatives are to be taken with respect to x.) The Feynman propagator is thus clearly a Green's function of the Klein-Gordon operator.

Since we will be exclusively concerned with FLRW spacetimes, let us demonstrate that equation (3.4) holds in this case.

Proposition 3.1.1 *In a FLRW spacetime M with the line element $ds^2 = -dt^2 + a^2(t)d\mathbf{x}^2$, the time-ordered expectation value $\langle 0|T\hat{\phi}(t,\mathbf{x})\hat{\phi}(s,\mathbf{y})|0\rangle$ obeys*

$$(\Box_x - m^2)\langle 0|T\hat{\phi}(t,\mathbf{x})\hat{\phi}(s,\mathbf{y})|0\rangle = i\frac{\delta^4(x-y)}{a^3(t)}. \tag{3.5}$$

Proof:

Recall the ansatz (2.25) for $\hat{\phi}(t,\mathbf{x})$ in a FLRW spacetime, where $u_{\mathbf{k}}(t,\mathbf{x}) = (1/\sqrt{2})\,v_k^*(t)\exp(i\mathbf{k}\cdot\mathbf{x})$. We thus have that

$$\begin{aligned} G^+(t,\mathbf{x},s,\mathbf{y}) &= \frac{1}{(2\pi)^3}\int d^3k\, u_k(t,\mathbf{x})u_k^*(s,\mathbf{y}) \\ &= \left[G^-(t,\mathbf{x},s,\mathbf{y})\right]^* \end{aligned} \tag{3.6}$$

Consequently, the left-hand side of equation (3.5) reads

$$\begin{aligned} \text{LHS} &= (-a^{-3}(t)\partial_t a^3(t)\partial_t + a^{-2}(t)\triangle - m^2)\left[\theta(t-s)G^+(t,\mathbf{x},s,\mathbf{y}) + \theta(s-t)G^-(t,\mathbf{x},s,\mathbf{y})\right] \\ &= -a^{-3}\partial_t a^3\partial_t\left[\theta(t-s)G^+ + \theta(s-t)G^-\right] \\ &\quad + \theta(t-s)(a^{-2}\triangle - m^2)G^+ + \theta(s-t)(a^{-2}\triangle - m^2)G^-. \end{aligned} \tag{3.7}$$

The square brackets in the last line of (3.7) may be expanded as

$$-\left[\dot{\delta}(t-s)G^{+}+2\delta(t-s)\dot{G}^{+}+\theta(t-s)\ddot{G}^{+}-\dot{\delta}(t-s)G^{-}-2\delta(t-s)\dot{G}^{-}+\theta(s-t)\ddot{G}^{-}\right]$$
$$-a^{-3}(\partial_t a^3)\left[\delta(t-s)G^{+}+\theta(t-s)\dot{G}^{+}-\delta(t-s)G^{-}+\theta(s-t)\dot{G}^{-}\right],$$

whence

$$\begin{aligned}\text{LHS} &= -\left[\dot{\delta}(t-s)(G^{+}-G^{-})+2\delta(t-s)(\dot{G}^{+}-\dot{G}^{-})\right]-a^{-3}(\partial_t a^3)\delta(t-s)(G^{+}-G^{-})\\ &\quad+\theta(t-s)\underbrace{(-a^{-3}\partial_t a^3\partial_t+a^{-2}\triangle-m^2)G^{+}}_{=0}+\theta(s-t)\underbrace{(-a^{-3}\partial_t a^3\partial_t+a^{-2}\triangle-m^2)G^{-}}_{=0}\\ &=\dot{\delta}(t-s)(G^{-}-G^{+})+2\delta(t-s)(\dot{G}^{-}-\dot{G}^{+})+3a^{-1}\dot{a}\,\delta(t-s)(G^{-}-G^{+}).\end{aligned}$$

From integration by parts, it follows that $\partial_t\delta(t-s)=-\delta(t-s)\partial_t$. Therefore,

$$\text{LHS}=\delta(t-s)\left[(\dot{G}^{-}-\dot{G}^{+})+3a^{-1}\dot{a}\,(G^{-}-G^{+})\right]. \tag{3.8}$$

Next, consider the following:

$$\begin{aligned}G^{-}-G^{+}&=\frac{1}{(2\pi)^3}\int d^3k\,[u_k^{*}(t,\mathbf{x})u_k(s,\mathbf{y})-u_k(t,\mathbf{x})u_k^{*}(s,\mathbf{y})]\\ &=\frac{1}{(2\pi)^3}\frac{1}{2}\int d^3k\left[v_k(t)v_k^{*}(s)e^{-i\mathbf{k}\cdot(\mathbf{x}-\mathbf{y})}-v_k^{*}(t)v_k(s)e^{i\mathbf{k}\cdot(\mathbf{x}-\mathbf{y})}\right]\end{aligned}$$

In equation (3.8), since LHS is the kernel of an integral operator and has a prefactor of $\delta(t-s)$, we can set $t=s$ in the previous line. Thus,

$$\begin{aligned}(G^{-}-G^{+})\big|_{t=s}&=\frac{1}{(2\pi)^3}\frac{1}{2}\left|v_k(t)\right|^2\left[\int d^3k\;e^{-i\mathbf{k}\cdot(\mathbf{x}-\mathbf{y})}-\int d^3k\;e^{i\mathbf{k}\cdot(\mathbf{x}-\mathbf{y})}\right]\\ &=0.\end{aligned}$$

Likewise,

$$\begin{aligned}\dot{G}^{-}-\dot{G}^{+}&=\frac{1}{(2\pi)^3}\int d^3k\,[\dot{u}_k^{*}(t,\mathbf{x})u_k(s,\mathbf{y})-\dot{u}_k(t,\mathbf{x})u_k^{*}(s,\mathbf{y})]\\ &=\frac{1}{(2\pi)^3}\frac{1}{2}\int d^3k\left[\dot{v}_k(t)v_k^{*}(s)e^{-i\mathbf{k}\cdot(\mathbf{x}-\mathbf{y})}-\dot{v}_k^{*}(t)\tilde{v}_k(s)e^{i\mathbf{k}\cdot(\mathbf{x}-\mathbf{y})}\right].\end{aligned}$$

Next, we set $t=s$ again and we use the Wronskian condition (2.42):

$$\begin{aligned}(\dot{G}^{-}-\dot{G}^{+})\Big|_{t=s}&=\frac{1}{(2\pi)^3}\frac{1}{2}\int d^3k\left[\dot{v}_k(t)\tilde{v}_k^{*}(t)e^{-i\mathbf{k}\cdot(\mathbf{x}-\mathbf{y})}+\left(2ia^{-3}(t)-\dot{v}_k(t)v_k^{*}(t)\right)e^{i\mathbf{k}\cdot(\mathbf{x}-\mathbf{y})}\right]\\ &=\frac{i}{(2\pi)^3}\frac{1}{a^3(t)}\int d^3k e^{i\mathbf{k}\cdot(\mathbf{x}-\mathbf{y})}+\frac{1}{(2\pi)^3}\frac{1}{2}\dot{\tilde{v}}_k(t)\tilde{v}_k^{*}(t)\left[\int d^3k\;e^{-i\mathbf{k}\cdot(\mathbf{x}-\mathbf{y})}-\int d^3k\;e^{i\mathbf{k}\cdot(\mathbf{x}-\mathbf{y})}\right]\\ &=i\frac{\delta^3(\mathbf{x}-\mathbf{y})}{a^3(t)}\end{aligned}$$

So, we recover

$$\text{LHS} = i\frac{\delta^4(x-y)}{a^3(t)}$$

as required. □

3.2 Two-Point Functions from the Path Integral Approach

While expressing two-point functions as vacuum expectation values produces clean formulas, it turns out that it is not a useful formalism in which to understand and implement the covariant cutoff. Instead, we will make use of insight into two-point functions that the path integral formulation of quantum field theory offers.

In terms of path integrals, the Feynman propagator of a scalar field $\hat{\phi}$ is given by

$$G_F(x,y) \equiv \frac{\int \phi(x)\phi(y)e^{iS[\phi]}\,\mathcal{D}[\phi]}{\int e^{iS[\phi]}\,\mathcal{D}[\phi]}. \tag{3.9}$$

Although this definition is somewhat unwieldy, it will prove to be very useful for us. For now, however, we can use it to re-derive the equation of motion (3.4).

We begin by considering the following path integral. Since it is the integral of a total functional derivative, the path integral can only be given by boundary terms, which vanish since we are integrating over all of the field's configuration space:

$$0 = \int \frac{\delta}{\delta\phi(x)}\left(\phi(y)e^{iS[\phi]}\right)\,\mathcal{D}[\phi] \tag{3.10}$$

Expanding the integrand, one has that

$$0 = \int \left(\delta^4(x-y) + i\phi(y)\frac{\delta S[\phi]}{\delta\phi(x)}\right)e^{iS[\phi]}\,\mathcal{D}[\phi]. \tag{3.11}$$

From the action (2.19) with $V(\phi) = \frac{1}{2}m^2\phi^2$, one readily finds that $\delta S[\phi]/\delta\phi(x) = \sqrt{|g(x)|}(\Box_x - m^2)\phi(x)$. Making this substitution into the equation above and dividing through by $\sqrt{|g(x)|}$ yields

$$\begin{aligned} 0 &= \int \left(\frac{\delta^4(x-y)}{\sqrt{|g(x)|}} + i\phi(y)(\Box_x - m^2)\phi(x)\right)e^{iS[\phi]}\,\mathcal{D}[\phi] \\ &= \frac{\delta^4(x-y)}{\sqrt{|g(x)|}}\int e^{iS[\phi]}\,\mathcal{D}[\phi] + i(\Box_x - m^2)\int \phi(x)\phi(y)e^{iS[\phi]}\,\mathcal{D}[\phi]. \end{aligned} \tag{3.12}$$

Then, we simply divide the last line by $\int e^{iS[\phi]}\,\mathcal{D}[\phi]$ and rearrange the result to arrive at equation (3.4).

In the operator formalism, we began with a definition of G_F in terms of expectation values and we subsequently found that, rather fortuitously, G_F obeys equation (3.4). In the path integral formalism, the definition of G_F immediately implies (3.4). So, starting with a path integral definition of G_F, one could

view (3.4) as an equation of motion and take it as the starting point for computing G_F. The problem in this case is to solve equation (3.4) for $G_F(x,y)$ using whatever means are available. We will refer to this last procedure as "computing $G_F(x,y)$ using the path integral approach," even though strictly speaking we do not evaluate any path integrals.

Example 3.2.1 *Flat Spacetime*

As an example, let us solve equation (3.4) for G_F for a scalar field in flat spacetime. The following approach may be found in any good text on quantum field theory (*e.g.*, [25, Chapter 2.4]). The equation of motion reads

$$\left(-\frac{\partial^2}{\partial t^2} + \triangle - m^2\right) G_F(x,y) = i\delta^4(x-y). \tag{3.13}$$

Let $\Box_x$ denote the d'Alembertian where derivatives are taken with respect to x. One immediately notices that $\Box_x = \Box_{x-y}$ in flat spacetime. Therefore, from the line above it follows that we may take G_F to be a function of the separation $x-y$. In other words, $G_F(x,y) = G_F(x-y)$ in flat spacetime. As such, let us take the Fourier transform of (3.13) with respect to $x-y$:

$$\left((k^0)^2 - |\mathbf{k}|^2 - m^2\right) G_F(k^0,\mathbf{k}) = \frac{i}{(2\pi)^2}$$

Or, rearranging this last line, one has that

$$G(k^0,\mathbf{k}) = \frac{i}{(2\pi)^2}\frac{1}{((k^0)^2 - |\mathbf{k}|^2 - m^2)}. \tag{3.14}$$

Upon performing an inverse Fourier transform, the last line reads

$$G(x,y) = \frac{i}{(2\pi)^4}\int dk^0 d^3k\, \frac{1}{(k^0)^2 - \mathbf{k}^2 - m^2}\, e^{-ik^0(t-s)+i\mathbf{k}\cdot(\mathbf{x}-\mathbf{y})}. \tag{3.15}$$

Notice that the subscript F does not appear in the last two lines. This is intentional, as the previous expressions do not describe a unique propagator. This is because the right-hand side of (3.14) has poles at $k^0 = \pm\sqrt{|\mathbf{k}|^2 + m^2}$, and so one must specify how they are integrated over when performing an inverse Fourier transform. For example, one obtains the Feynman propagator if one performs the k^0 integration along the contour shown in figure 3.1. Of course, one lets the semicircular portions of the contour shrink down to the poles after integrating. Equivalently, one may compactly write

$$G_F(x,y) = \lim_{\epsilon\to 0}\frac{i}{(2\pi)^4}\int dk^0 d^3k\, \frac{1}{(k^0)^2 - \mathbf{k}^2 - m^2 + i\epsilon}\, e^{-ik^0(t-s)+i\mathbf{k}\cdot(\mathbf{x}-\mathbf{y})}. \tag{3.16}$$

If we were to evaluate the k^0 integral alone, we would indeed recover expression (3.3) for $G_F(t,s,k)$. To illustrate that different integration contours give different Green's functions, consider that the retarded Green's function is given by

$$G_R(x,y) = \lim_{\epsilon\to 0}\frac{i}{(2\pi)^4}\int dk^0 d^3k\, \frac{1}{(k^0+i\epsilon)^2 - \mathbf{k}^2 - m^2}\, e^{-ik^0(t-s)+i\mathbf{k}\cdot(\mathbf{x}-\mathbf{y})}. \tag{3.17}$$

▷

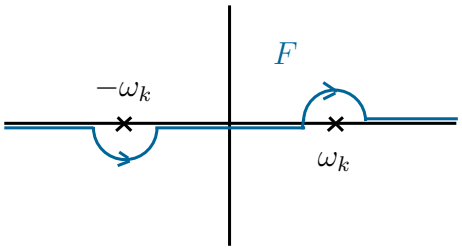

Figure 3.1: Feynman propagator contour

An important question that has not been addressed is how the choice of vacuum enters these last calculations that involve contour integrals. In the operator formalism, the choice of vacuum clearly enters into the calculation of two-point functions since the two-point functions are defined in terms of vacuum expectation values. Concretely, using the operator formalism, we found that G_F is given by equation (3.3) in flat spacetime. This was for the particular choice of mode functions (2.32) with $A_k = 1/\sqrt{\omega_k}$ and $B_k = 0$. Although there are very good reasons to make this choice – this vacuum state is the state of minimal energy in Minkowski space, for instance – in principle we could have chosen any A_k and B_k which satisfy the Wronskian condition (2.35). Writing $v_k(t) = A_k \exp(i\omega_k t) + B_k \exp(-i\omega_k t)$, equation (3.2) gives us a much more general Feynman propagator:

$$G_F(t,s,k) = \frac{1}{(2\pi)^{3/2}} \frac{1}{2} \left\{ |A_k|^2 e^{-i\omega_k|t-s|} + |B_k|^2 e^{i\omega_k|t-s|} + A_k B_k^* e^{i\omega_k(t+s)} + A_k^* B_k e^{-i\omega_k(t+s)} \right\} \tag{3.18}$$

The question is how does one obtain this last expression for G_F when one uses a path integral approach?

As far as the author is aware, what follows are original calculations. We can gain some intuition by effectively working backwards and re-writing equation (3.18) as follows:

$$\begin{aligned} G_F(t,s,k) = \omega_k |A_k|^2 \frac{i}{(2\pi)^{5/2}} \int dk^0 \, \frac{e^{-ik^0(t-s)}}{(k^0)^2 - \omega_k^2 + i\epsilon} - \omega_k |B_k|^2 \frac{i}{(2\pi)^{5/2}} \int dk^0 \, \frac{e^{-ik^0(t-s)}}{(k^0)^2 - \omega_k^2 - i\epsilon} \\ + \omega_k A_k B_k^* \frac{i}{(2\pi)^{5/2}} \int_{\Gamma^-} dz \, \frac{e^{-iz(t+s)}}{z^2 - \omega_k^2} + \omega_k A_k^* B_k \frac{i}{(2\pi)^{5/2}} \int_{-\Gamma^+} dz \, \frac{e^{-iz(t+s)}}{z^2 - \omega_k^2} \end{aligned} \tag{3.19}$$

In all cases a limit as $\epsilon \to 0$ is implied. The contours $-\Gamma^+$ and Γ^- are the loops which go around the poles $z = \pm\omega_k$ respectively, as shown in figure 3.2 below. The minus sign in front of Γ^+ is to indicate that we go around the loop in the clockwise direction.

Ignoring the prefactor of $\omega_k |A_k|^2$, the first term of equation (3.19) is the usual expression for the Feynman propagator. The second term corresponds to an "anti-Feynman" contour, shown in figure 3.3. The last two terms do not possess the right integrand to properly be compared to the representation (3.15). However, it does illustrate that they are homogeneous solutions of the Klein-Gordon equation. In other words,

$$(-\partial_t^2 - \omega_k^2) e^{\pm i\omega_k(t+s)} = 0. \tag{3.20}$$

Therefore, we may add any linear combination of the last two terms to a given Green's function and still have it remain a Green's function, since it will still satisfy equation (3.13).

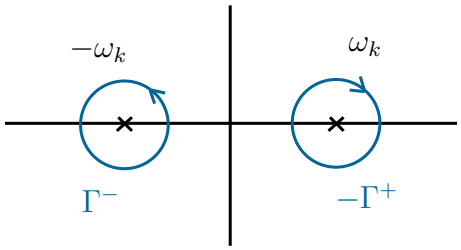

Figure 3.2: Homogeneous contours

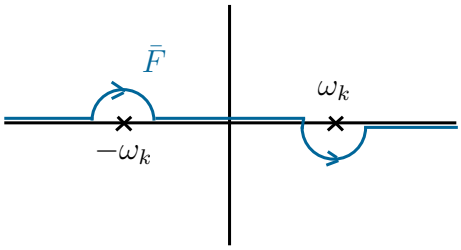

Figure 3.3: Anti-Feynman propagator contour

Our conclusion is that in the path integral picture, when calculating the Feynman propagator, the specification of different vacua amounts to taking different linear combinations of the Feynman contour integral, the anti-Feynman contour integral, and then appending two-point functions which are homogeneous solutions of the Klein-Gordon equation. Also note that we could write the anti-Feynman contour $\bar{F}$ as $F - \Gamma^- - \Gamma^+$. This lets us express the integration contour for a given choice of vacuum in terms of the usual Feynman contour and the homogeneous contours.

Notice that to choose a vacuum other than the standard Minkowski vacuum requires that we have terms containing the homogeneous two-point functions $e^{\pm i\omega_k(t+s)}$ in the Feynman propagator. Furthermore, as we noted earlier, these terms cannot be obtained by choosing a suitable contour C for the integral

$$\int_C dk^0 \, \frac{e^{-ik^0(t-s)}}{(k^0)^2 - \omega_k^2}. \tag{3.21}$$

This is an important feature of the choice of vacuum, versus the determination of which Green's function is calculated. One may obtain different Green's functions purely by modifying the contour C in the integral above. To choose different vacuum states, however, one must necessarily add to a Green's function computed using the contour integral (3.21) homogeneous two-point functions which cannot be obtained by modifying the contour C.

Interestingly, the requirement that the Feynman propagator be a Green's function of the Klein-Gordon operator, *i.e.*, that equation (3.13) hold, gives us the same condition on A_k and B_k that we normally obtain from the Wronskian condition. Explicitly, if we apply $(-\partial_t^2 - \omega_k^2)$ to either equation (3.18) or (3.19), we find that

$$(-\partial_t^2 - \omega_k^2) G_F(t, s, \mathbf{k}) = \frac{i}{(2\pi)^{3/2}} \omega_k \left(|A_k|^2 - |B_k|^2 \right) \delta(t - s). \tag{3.22}$$

Therefore, in order for G_F to be a Green's function, it must be that $|A_k|^2 - |B_k|^2 = \omega_k^{-1}$.

Perhaps the most important lesson to learn from the considerations above is that the pole prescription that one chooses to compute a given propagator is a very subtle matter. Not only does the pole prescription encode which Green's function is being calculated, but it also encodes information about a specific choice of vacuum.

The last step to complete this study would be to study mode mixing in the path integral approach. The general Feynman propagator (3.18) essentially describes all those propagators which are generated by transforming the mode functions according to the Bogoliubov transformation (2.37). More general Bogoliubov transformations where the mode numbers mix are possible, however. We may write such a general transformation as

$$v_k(t) = \int \left(A(k,\ell)\tilde{v}_\ell(t) + B(k,\ell)\tilde{v}_\ell^*(t)\right)\, d\ell. \tag{3.23}$$

The final issue is to understand the effect that such a transformation has on propagators in terms of path integrals and contours. This is the subject of future work.

In closing and for convenient reference, a catalogue of the two-point functions in flat spacetime that we have discussed is given below in table 3.1.

$$K(t,s,\mathbf{k}) = \frac{i}{(2\pi)^{5/2}} \int_X ds \frac{e^{-iz(t-s)}}{z^2 - \omega_k^2}$$

function K	contour X	canonical	evaluated
$G^+(t,s,\mathbf{k})$	$-\Gamma^+$	$\langle 0\|\hat{\phi}_k(t)\hat{\phi}_k(s)\|0\rangle$	$\frac{1}{(2\pi)^{3/2}}\frac{1}{2\omega_k}e^{-i\omega_k(t-s)}$
$G^-(t,s,\mathbf{k})$	Γ^-	$\langle 0\|\hat{\phi}_k(s)\hat{\phi}_k(t)\|0\rangle$	$\frac{1}{(2\pi)^{3/2}}\frac{1}{2\omega_k}e^{i\omega_k(t-s)}$
$G_F(t,s,\mathbf{k})$	F	$\langle 0\|T\hat{\phi}_k(t)\hat{\phi}_k(s)\|0\rangle$ $\theta(t-s)G^+(t,s,\mathbf{k}) + \theta(s-t)G^-(t,s,\mathbf{k})$	$\frac{1}{(2\pi)^{3/2}}\frac{1}{2\omega_k}e^{-i\omega_k\|t-s\|}$
$G_{\bar{F}}(t,s,\mathbf{k})$	$\bar{F}$	$-\langle 0\|\bar{T}\hat{\phi}_k(t)\hat{\phi}_k(s)\|0\rangle$ $-\theta(s-t)G^+(t,s,\mathbf{k}) - \theta(t-s)G^-(t,s,\mathbf{k})$	$-\frac{1}{(2\pi)^{3/2}}\frac{1}{2\omega_k}e^{i\omega_k\|t-s\|}$

Table 3.1: Selected two-point functions

3.3 Results on More General Spacetimes

Flat spacetime is a somewhat special case for solving equation (3.4) because of its tight compatibility with the Fourier transform. In more general spacetimes, the Fourier transform may not simplify the

mathematics, or it may only partially help. This is the case, for instance, for FLRW spacetimes. If M is a FLRW spacetime with the line element $ds^2 = -dt^2 + a^2(t)d\mathbf{x}^2$ in comoving coordinates, then (3.4) reads

$$(\Box - m^2)G_F(x,y) = i\frac{\delta^4(x-y)}{a^3(t)}. \tag{3.24}$$

Again, recall that $\Box = a^{-3}(t)(-\partial_t a^3(t)\partial_t + a(t)\triangle)$ is the d'Alembertian on M. One may still take a spatial Fourier transform of the last equation with respect to $\mathbf{x} - \mathbf{x}'$, giving

$$(\Box_k - m^2)G_F(t,s,k) = \frac{i}{(2\pi)^{3/2}}\frac{\delta(t-s)}{a^3(t)}. \tag{3.25}$$

Taking a Fourier transform with respect to t is not terribly useful, however. To proceed any further, we must examine the linear operator natures of $\Box_k$ and of $G_F(t,s,k)$.

Formally, the objects $(\Box_k - m^2)$ and $G_F(t,s,k)$ are the integral kernels of operators that act on suitable domains contained in $\mathcal{H} = L^2\left((t_i,t_f), a^3(t)\,dt\right)$, with the understanding that one or both of t_i and t_f may be infinite. Denote these operators by $\hat{D}_k$ and $\hat{G}_k$ respectively. For $f \in \mathrm{dom}(\hat{D}_k)$ and $g \in \mathrm{dom}(\hat{G}_k)$, one explicitly has that

$$(\hat{D}_k f)(t) = \int_{t_i}^{t_f} \frac{\delta(t-s)}{a^3(t)}\left[(\Box_k(s) - m^2)f(s)\right]\, a^3(s)\, ds \tag{3.26}$$

and

$$(\hat{G}_k g)(t) = \int_{t_i}^{t_f} G_F(t,s,k)g(s)\, a^3(s)\, ds. \tag{3.27}$$

The notation $\Box_k(s)$ indicates that the derivatives in this k-d'Alembertian are to be taken with respect to the variable s.

It is clear that equation (3.25) is a representation of the operator equation[1]

$$\hat{D}_k\hat{G}_k = \frac{i}{(2\pi)^{3/2}}\hat{\mathbb{1}}. \tag{3.29}$$

While this operator equation is essentially equivalent to equation (3.25), studying $\hat{D}_k$ and $\hat{G}_k$ as operators will let us write down a particularly useful spectral expression for $G_F(t,s,k)$.

To this end, suppose that $\hat{D}_k$ is essentially self-adjoint, or that we have chosen a particular self-adjoint extension if it is only symmetric. Then, there exists an orthonormal eigenbasis for $L^2\left((t_i,t_f), a^3(t)\,dt\right)$ consisting of eigenfunctions of $(\Box_k - m^2)$. Denote these eigenfunctions by $\{\phi_{\lambda,k}(t)\}_{\lambda\in\mathrm{spec}(D_k)}$, where we have that $(\Box_k - m^2)\phi_{\lambda,k}(t) = \lambda\phi_{\lambda,k}(t)$. Note that to be completely correct, each λ should come with a small subscript k. For the sake of tidiness, however, let us suppress this subscript with the understanding that the spectrum of $\hat{D}_k$ depends on the choice of fixed mode k.

[1]Note that $a^{-3}(t)\delta(t-s)$ is indeed a representation of the identity operator $\hat{\mathbb{1}}$, since

$$(\hat{\mathbb{1}}f)(t) = \int_{t_i}^{t_f}\frac{\delta(t-s)}{a^3(t)}f(s)\, a^3(s)\, ds = f(t) \tag{3.28}$$

By the Spectral Theorem (see, e.g., [34, Chapters 6-7] or [35, Chapter 2]), we may expand a function of $\hat{D}_k$ using the eigenbasis $\{|\phi_{\lambda,k})\}_{\lambda\in\mathrm{spec}(D_k)}$ with the appropriate weight $\sigma(\lambda)$ as follows:[2]

$$f(\hat{D}_k) = \int_{\mathrm{spec}(\hat{D}_k)} f(\lambda)\,|\phi_{\lambda,k})\,(\phi_{\lambda,k}|\;d\sigma(\lambda) \tag{3.30}$$

In particular, if it exists, the inverse of $\hat{D}_k$ is given by

$$\hat{D}_k^{-1} = \int_{\mathrm{spec}(\hat{D}_k)} \frac{1}{\lambda}\;|\phi_{\lambda,k})\,(\phi_{\lambda,k}|\;d\sigma(\lambda), \tag{3.31}$$

or equivalently,

$$D_k^{-1}(t,s) = \int_{\mathrm{spec}(\hat{D}_k)} \frac{1}{\lambda}\,\phi_{\lambda,k}(t)\phi^*_{\lambda,k}(s)\,d\sigma(\lambda). \tag{3.32}$$

Equation (3.29) makes it clear that $\hat{G}_k$ is, up to a multiplicative constant, *an* inverse of $\hat{D}_k$. It is not necessarily *the* inverse of $\hat{D}_k$, however. A unique inverse of $\hat{D}_k$ may not even exist. Rather, equation (3.29) indicates that $\hat{G}_k$ is a right inverse of $\hat{D}_k$. In other words, if $(\hat{D}_k f)(t) = g(t)$, then the action of $\hat{G}_k$ on g is $(\hat{G}_k g)(t) = f(t) + h(t)$, where $h(t)$ in principle could be any function for which $(\Box_k - m^2)h(t) = 0$. The function $h(t)$ does not even need to be in the Hilbert space.

What, then, is the appropriate spectral expansion of $G_F(t,s,k)$? Given the orthonormal eigenbasis $\{\phi_{\lambda,k}(t)\}_{\lambda\in\mathrm{spec}(D_k)}$, suppose that one knew the action of $\hat{G}_k$ on each eigenfunction. To this end, let us write

$$(\hat{G}_k\phi_{\lambda,k})(t) = \frac{i}{(2\pi)^{3/2}}\left(\frac{1}{\lambda}\phi_{\lambda,k}(t) + C^{(1)}_{\lambda,k}h^{(1)}_k(t) + C^{(2)}_{\lambda,k}h^{(2)}_k(t)\right). \tag{3.33}$$

The functions $h^{(1)}_k$ and $h^{(2)}_k$ are two linearly independent solutions of the homogeneous equation $(\Box_k - m^2)u = 0$, and we suppose that the constants $C^{(1)}_{\lambda,k}, C^{(2)}_{\lambda,k} \in \mathbb{C}$ are known. The right-hand side of equation (3.33) is the most general object to which an eigenfunction could be mapped by $\hat{G}_k$. The first term is necessary because $\hat{G}_k$ is proportional to an inverse of $\hat{D}_k$. The map could also append to this term any function from the solution space of $(\Box_k - m^2)u = 0$, which is spanned by $\{h^{(1)}_k, h^{(2)}_k\}$. We may then exploit the orthonormality condition

$$\int_{t_i}^{t_f} \phi_{\lambda,k}(t)\phi^*_{\mu,k}(t)\,a^3(t)\,dt = \delta(\lambda-\mu) \tag{3.34}$$

to write

$$\begin{aligned} G_F(t,s,k) = \frac{i}{(2\pi)^{3/2}}\int_{\mathrm{spec}(\hat{D}_k)} \Bigg[&\frac{1}{\lambda}\,\phi_{\lambda,k}(t)\phi^*_{\lambda,k}(s) \\ &+ C^{(1)}_{\lambda,k}h^{(1)}_k(t)\phi^*_{\lambda,k}(s) + C^{(2)}_{\lambda,k}h^{(2)}_k(t)\phi^*_{\lambda,k}(s)\Bigg]\,d\sigma(\lambda). \end{aligned} \tag{3.35}$$

[2]The integrals appearing in this section should be interpreted as Riemann-Stieltjes integrals. This interpretation is necessary so that in certain cases, such as when $-\infty < t_i < t_f < \infty$, an integral reduces to a discrete sum. More precisely, the integrals here must be able to accommodate both integration over the continuous spectrum and summation over the point spectrum.

The previous equation completely and correctly determines the action of $\hat{G}_k$ on any functions in its domain. This is because any $f \in L^2\left((t_i, t_f), a^3(t)\,dt\right)$, and thus any $g \in \mathrm{dom}(\hat{G}_k) \subset L^2\left((t_i, t_f), a^3(t)\,dt\right)$, can be expanded in terms of the basis of eigenfunctions of $\hat{D}_k$. Then, the orthonormality relation (3.34) together with the second orthonormality relation[3]

$$\int_{\mathrm{spec}(\hat{D}_k)} \phi_{\lambda,k}(t)\phi^*_{\lambda,k}(s)\,d\sigma(\lambda) = \delta(t-s) \tag{3.37}$$

determines the action of $\hat{G}_k$ on g from its eigenfunction expansion.

The expression for $G_F(t,s,k)$ given by equation (3.35) may be further simplified. If we split this expression into three integrals, we may evaluate the last two integrals. Defining

$$F^{(j)}_k(s) := \int_{\mathrm{spec}(\hat{D}_k)} C^{(j)}_{\lambda,k}\phi^*_{\lambda,k}(s)\,d\sigma(\lambda) \qquad ; \qquad j = 1, 2\,, \tag{3.38}$$

the Feynman propagator takes the form

$$G_F(t,s,k) = \frac{i}{(2\pi)^{3/2}}\left[\int_{\mathrm{spec}(\hat{D}_k)} \frac{1}{\lambda}\,\phi_{\lambda,k}(t)\phi^*_{\lambda,k}(s)\,d\sigma(\lambda) + h^{(1)}_k(t)F^{(1)}_k(s) + h^{(2)}_k(t)F^{(2)}_k(s)\right]. \tag{3.39}$$

Recall, however, that the Feynman propagator is symmetric in t and s (*cf.* equation (3.2)). Therefore, we must have that $F^{(1)}_k(s) = A_k h^{(1)}_k(s) + C_k h^{(2)}_k(s)$ and $F^{(2)}_k(s) = B_k h^{(2)}_k(s) + C_k h^{(1)}_k(s)$ for some $A_k, B_k, C_k \in \mathbb{C}$. We conclude that the most general spectral expression for the Feynman propagator is

$$\begin{aligned} G_F(t,s,k) = {} & \frac{i}{(2\pi)^{3/2}}\int_{\mathrm{spec}(\hat{D}_k)} \frac{1}{\lambda}\,\phi_{\lambda,k}(t)\phi^*_{\lambda,k}(s)\,d\sigma(\lambda) \\ & + \frac{i}{(2\pi)^{3/2}}\left[A_k h^{(1)}_k(t)h^{(1)}_k(s) + B_k h^{(2)}_k(t)h^{(2)}_k(s) + C_k\left(h^{(1)}_k(t)h^{(2)}_k(s) + h^{(2)}_k(t)h^{(1)}_k(s)\right)\right]. \end{aligned} \tag{3.40}$$

In the case of flat spacetime, we saw that the choice of pole prescription, or integration contour, corresponds to a choice of which Green's function is calculated. Then, by modifying the integration contour and appending different two-point functions that are homogeneous solutions of the Klein-Gordon equation, we could also choose different vacuum states. In FLRW spacetimes, we see the resurgence of homogeneous two-point functions, namely, $h^{(1)}_k(t)h^{(1)}_k(s)$, $h^{(2)}_k(t)h^{(2)}_k(s)$, $h^{(1)}_k(t)h^{(2)}_k(s)$, and $h^{(2)}_k(t)h^{(1)}_k(s)$. Here, it must be that the choice of coefficients in front of these terms affects both the choice of vacuum and the choice of Green's function that is computed. For instance, if we had not required that $h^{(1)}_k(t)h^{(2)}_k(s)$ and $h^{(2)}_k(t)h^{(1)}_k(s)$ appear in a symmetric combination, we would not have computed the Feynman propagator.

[3] How one writes this second orthonormality condition is slightly ambiguous, as it depends on how one treats $\int_0^\infty \delta(x)\,dx$. Alternatively, it depends on the value of the Heaviside step function at the origin. In this thesis we adopt the convention $\int_0^\infty \delta(x)\,dx = \frac{1}{2}$, $\theta(0) = \frac{1}{2}$. In the case of $t_i > -\infty$ and $t_f < \infty$, one should thus more properly write

$$\int_{\mathrm{spec}(\hat{D}_k)} \phi_{\lambda,k}(t)\phi^*_{\lambda,k}(s)\,d\sigma(\lambda) = \delta(t-s) + \delta(t+s-2t_i) + \delta(t+s-2t_f). \tag{3.36}$$

Also note that we have written the first orthonormality condition (3.34) with the continuous spectrum in mind. In the case of discrete eigenvalues, the Dirac delta function $\delta(\lambda-\mu)$ is of course replaced with a Kronecker delta $\delta_{\lambda\mu}$.

A rigorous reason for why this must be so is because it may happen that $0 \notin \text{spec}(\hat{D}_k)$. If 0 in fact *is* in the spectrum of $\hat{D}_k$, then one will be forced to specify a pole prescription for handling the point $\lambda = 0$ in the first line of (3.40). This pole prescription will of course affect which Green's function is computed. Should 0 not be in the spectrum of $\hat{D}_k$, then there is no pole prescription to make, and so one must be able to obtain different Green's functions purely by changing the coefficients of the homogeneous two-point functions.

Furthermore, an additional complication that is not present in Minkowski space arises in FLRW spacetimes. This complication is the fact that the minimal operator corresponding to $(\Box_k - m^2)$ may not be essentially self-adjoint. In this case, one must also choose a particular self-adjoint extension of this minimal operator in order to obtain a self-adjoint operator $\hat{D}_k$. This choice of self-adjoint extension enters into the choice of vacuum.

Later, it will be the case that we will need to choose a self-adjoint extension of the Klein-Gordon operator in a curved FLRW spacetime. As such, let us examine here the simplest case of a scalar quantum field theory where the minimal operator corresponding to $(\Box_k - m^2)$ is not essentially self-adjoint.

Example 3.3.1 *Flat Spacetime with a Finite Start Time*

Let M be a flat spacetime with the line element $ds^2 = -dt^2 + d\mathbf{x}^2$, where $\mathbf{x} \in \mathbb{R}^3$, but where $t \in [0, \infty)$. M is thus a flat spacetime which has an abrupt beginning at $t = 0$. Let us construct $G_F(t, s, k)$ according to equation (3.40), setting $A_k = B_k = C_k = 0$ for convenience.

Consider the Klein-Gordon differential expression $(\Box_k - m^2) = (-\partial_t^2 - \omega_k^2)$, where $\omega_k^2 = |\mathbf{k}|^2 + m^2$. Let us also assume that $m > 0$ so that the $k = 0$ mode is no different from any other modes. Let $\hat{D}_k^0$ denote the minimal operator corresponding to the differential expression $\Box_k - m^2$, with $\text{dom}(\hat{D}_k^0) \subset L^2[0, \infty)$. It is straightforward to show that $\hat{D}_k^0$ has deficiency indices $(1, 1)$. One can see this by directly inspecting the eigenfunctions for the eigenvalues $-\omega_k^2 \pm i$. The eigenvalue equation reads

$$\begin{aligned} (\Box_k - m^2)u &= (-\omega_k^2 \pm i)u \\ -\ddot{u}(t) - \omega_k^2 u(t) &= -\omega_k^2 u(t) \pm iu(t) \\ 0 &= \ddot{u}(t) \pm iu(t), \end{aligned} \tag{3.41}$$

for which the general solution is

$$\begin{aligned} \phi_{\pm i}(t) &= C_1 e^{i(\pm 1 + i)t/\sqrt{2}} + C_2 e^{-i(\pm 1 + i)t/\sqrt{2}} \\ &= C_1 e^{-t/\sqrt{2}} e^{\pm it/\sqrt{2}} + C_2 e^{t/\sqrt{2}} e^{\mp it/\sqrt{2}}. \end{aligned} \tag{3.42}$$

The solution which contains $e^{-t/\sqrt{2}}$ is normalizable in $L^2[0, \infty)$ for both eigenvalues $-\omega_k^2 \pm i$, while the other solution is not normalizable for either eigenvalue. Therefore, the deficiency spaces of $\hat{D}_k^0$ are each one-dimensional subspaces of $L^2[0, \infty)$. As such, $\hat{D}_k^0$ has deficiency indices $(1, 1)$.

At this point, we could proceed from first principles and construct the self-adjoint extensions of $\hat{D}_k^0$ according to Proposition 2.5.14. Instead, let us use a simpler parametrization for the case of $\hat{D}_k^0$ with deficiency indices $(1, 1)$ from [36, Chapter VI.21] and [37, Chapter 11.2]. This approach is valid for $\hat{D}_k^0$ that are associated with second order Sturm-Liouville differential expressions on (a, b) where the endpoint a is regular.

Let τ be a Sturm-Liouville differential expression of the form of (2.100). Then, all of the self-adjoint realizations $\hat{A}_\theta$ of τ are described by a Robin boundary condition:

$$\mathrm{dom}(\hat{A}_\theta) = \left\{ f \in L^2(a,b) \ : \ pf'(a)/f(a) = \theta \right\} \tag{3.43}$$

The real number θ parametrizes the self-adjoint realizations. The case $\theta \to \infty$ corresponds to the Dirichlet boundary condition $f(a) = 0$. Intuitively, we see that this must be a correct parametrization of self-adjoint extensions by examining the boundary terms in equation (2.101). (Recall that the boundary terms must vanish for the operator to be self-adjoint.)

Let $u_1(t;z)$ and $u_2(t;z)$ be the solutions of $(\tau - z)u = 0$ such that

$$\begin{array}{ll} u_1(a;z) = 1 & u_2(a;z) = 0 \\ pu_1'(a;z) = 0 & pu_2'(a;z) = 1 \end{array} .$$

Next, define

$$u_\theta(t;z) := \begin{cases} u_1(t;z) + \theta u_2(t;z) & \theta < \infty \\ u_2(t;z) & \text{otherwise} \end{cases} . \tag{3.44}$$

Then, one has that $\{u_\theta(t;\lambda)\}_{\lambda \in \mathrm{spec}(\hat{A}_\theta) \subseteq \mathbb{R}}$ is an orthonormal basis of eigenfunctions for $L^2(a,b)$. For $f \in L^2(a,b)$, the forward and inverse spectral transforms are given by

$$F(\lambda) = \int_a^b f(t) u_\theta^*(t;\lambda)\, dt \qquad \text{and} \qquad f(t) = \int_{-\infty}^{\infty} F(\lambda) u_\theta(t;\lambda)\, d\sigma(\lambda) \tag{3.45}$$

respectively. The weight $\sigma(\lambda)$ is given by

$$\frac{\sigma(\lambda^+) - \sigma(\lambda^-)}{2} = C + \lim_{y \to 0^+} \frac{1}{\pi} \int_0^\lambda \Im\left(m_\theta(x+iy)\right)\, dx\,. \tag{3.46}$$

The constant C is irrelevant, since we are ultimately only interested in the weight $d\sigma(\lambda)$. For $z \in \mathbb{C}$, $\Re(z) > 0$, the function $m_\theta(z)$ is defined through the condition $m_\theta(z) u_\theta(t;z) - u_2(t;z) \in L^2(a,b)$. Since by assumption $\hat{D}_k^0$ has deficiency indices $(1,1)$, $m_\theta(z)$ exists and is uniquely defined.

We now apply the theory above to $\tau = -\partial_t^2 - \omega_k^2$ with $t \in [0,\infty)$. We have that u_1 and u_2 are given by

$$u_1(t;z) = \cos\left(\sqrt{z+\omega_k^2}\, t\right) \qquad \text{and} \qquad u_2(t;z) = \frac{1}{\sqrt{z+\omega_k^2}} \sin\left(\sqrt{z+\omega_k^2}\, t\right) \tag{3.47}$$

respectively. One may also show that $m_\theta(z)$ is given by

$$m_\theta(z) = \frac{1}{\theta - i\sqrt{z+\omega_k^2}}. \tag{3.48}$$

For $x > -\omega_k^2$, one finds that

$$\Im\left(m_\theta(x+iy)\right) = \frac{1}{2}\left[\frac{\sqrt{x+\omega_k^2 - iy} + \sqrt{x+\omega_k^2+iy}}{\theta^2 + i\theta\left(\sqrt{x+\omega_k^2-iy} - \sqrt{x+\omega_k^2+iy}\right) + \sqrt{(x+\omega_k^2)^2+y^2}} \right]. \tag{3.49}$$

Here, it turns out that we may take the limit into the integral in equation (3.46). Doing so, we have

$$\frac{\sigma(\lambda^+) - \sigma(\lambda^-)}{2} = C + \frac{1}{\pi}\int_0^\lambda \frac{\sqrt{x+\omega_k^2}}{\theta^2 + x + \omega_k^2} dx\,. \tag{3.50}$$

Therefore, for $\lambda > -\omega_k^2$, it follows that

$$d\sigma(\lambda) = \frac{1}{\pi}\frac{\sqrt{\lambda+\omega_k^2}}{\theta^2+\lambda+\omega_k^2}\,d\lambda\,. \tag{3.51}$$

The case of $\lambda < -\omega_k^2$ is slightly more complicated. To begin, consider the following:

$$\lim_{y\to 0^+} m_\theta(x+iy) = \frac{1}{\theta - i\sqrt{x+\omega_k^2}} \tag{3.52}$$

If $\theta > 0$, then $\lim_{y\to 0^+} m_\theta(x+iy)$ is purely real and well-defined for all $x < -\omega_k^2$. Therefore, the integrand in equation (3.46) vanishes and we have that $d\sigma(\lambda) = 0$. If $\theta < 0$, however, observe that there is a pole in $\lim_{y\to 0^+} m_\theta(x+iy)$ at $x = -\theta^2 - \omega_k^2$. It is still true that $\Im(\lim_{y\to 0^+} m_\theta(x+iy)) = 0$ for $-\theta^2-\omega_k^2 < x < -\omega_k^2$ and $x < -\theta^2 - \omega_k^2$. After much tedious complex analysis, one may show that this pole causes a jump in $\sigma(\lambda)$ at $\lambda = -\theta^2 - \omega_k^2$ given by

$$\frac{\sigma\left((-\theta^2-\omega_k^2)^+\right) - \sigma\left((-\theta^2-\omega_k^2)^-\right)}{2} = -\theta. \tag{3.53}$$

Therefore, for $\lambda < -\omega_k^2$, it follows that $d\sigma(\lambda) = 0$, unless $\theta < 0$ in which case

$$d\sigma(\lambda)|_{\theta<0} = \begin{cases} -2\theta\,\delta(\lambda+\theta^2+\omega_k^2)\,d\lambda & \lambda = -\theta^2-\omega_k^2 \\ 0 & \text{otherwise} \end{cases}. \tag{3.54}$$

The forward and inverse spectral transforms are thus given by

- Case 1: $\theta \geq 0$

$$F(\lambda) = \int_0^\infty f(t)u_\theta(t;\lambda)\,dt \tag{3.55}$$

$$f(t) = \frac{1}{\pi}\int_{-\omega_k^2}^\infty F(\lambda)u_\theta(t;\lambda)\frac{\sqrt{\lambda+\omega_k^2}}{\theta^2+\lambda+\omega_k^2}\,d\lambda \tag{3.56}$$

- Case 2: $\theta < 0$

$$F(\lambda) = \int_0^\infty f(t)u_\theta(t;\lambda)\,dt \tag{3.57}$$

$$f(t) = -2\theta F(-\theta^2-\omega_k^2)e^{\theta t} + \frac{1}{\pi}\int_{-\omega_k^2}^\infty F(\lambda)u_\theta(t;\lambda)\frac{\sqrt{\lambda+\omega_k^2}}{\theta^2+\lambda+\omega_k^2}\,d\lambda \tag{3.58}$$

Let us now compute the Feynman propagator $G_F(t,s,k)$. From (3.40), we have the following:

$$-i(2\pi)^{3/2}G_F(t,s,k) = \int_{-\omega_k^2}^{\infty} \frac{1}{\lambda} u_\theta(t;\lambda)u_\theta^*(s;\lambda)\, d\sigma(\lambda) \tag{3.59}$$

First, let us assume that $\theta \geq 0$. The last line then reads

$$\begin{aligned} -i(2\pi)^{3/2}G_F(t,s,k) = \int_{-\omega_k^2}^{\infty} \frac{1}{\lambda} &\left[\cos\left(\sqrt{\lambda+\omega_k^2}\, t\right) + \frac{\theta}{\sqrt{\lambda+\omega_k^2}} \sin\left(\sqrt{\lambda+\omega_k^2}\, t\right)\right] \\ &\times \left[\cos\left(\sqrt{\lambda+\omega_k^2}\, s\right) + \frac{\theta}{\sqrt{\lambda+m^2}} \sin\left(\sqrt{\lambda+\omega_k^2}\, s\right)\right] \frac{\sqrt{\lambda+\omega_k^2}}{\theta^2+\lambda+\omega_k^2} \frac{d\lambda}{\pi}. \end{aligned} \tag{3.60}$$

Let $\mu := \sqrt{\lambda+\omega_k^2}$. Changing the integration variable from λ to μ and expressing the sine and cosine functions of the last line in terms of exponentials, we have the following:

$$\begin{aligned} -i(2\pi)^{3/2}G_F(t,s,k) &= \frac{1}{2\pi}\int_0^{\infty} \frac{1}{\mu^2-\omega_k^2}\left[\frac{\mu-i\theta}{\mu+i\theta}e^{i\mu(t+s)} + \frac{\mu+i\theta}{\mu-i\theta}e^{-i\mu(t+s)} + e^{i\mu(t-s)} + e^{-i\mu(t-s)}\right] d\mu \\ &= \frac{1}{2\pi}\int_{-\infty}^{\infty} \frac{e^{-i\mu(t-s)}}{\mu^2-\omega_k^2}\, d\mu + \frac{1}{2\pi}\int_{-\infty}^{\infty} \frac{e^{-i\mu(t+s)}}{\mu^2-\omega_k^2}\, d\mu - \frac{i\theta}{\pi}\int_{-\infty}^{\infty} \frac{e^{i\mu(t+s)}}{(\mu^2-\omega_k^2)(\mu+i\theta)}\, d\mu \end{aligned}$$

All of the integrands in the last line have poles at $\mu = \pm\omega_k$. We regulate them according to the usual Feynman prescription of $\omega_k^2 \to \omega_k^2 - i\epsilon$. The first two integrals are just like the integrals that we saw before when computing the Feynman propagator in full Minkowski spacetime. Since $t+s \geq 0$, by Jordan's Lemma we evaluate the last integral by closing the integration contour in the upper complex plane. Since $\theta > 0$ by assumption, the only pole of the last integrand is at $\mu = -\sqrt{\omega_k^2 - i\epsilon}$. Therefore, we have that

$$\lim_{\epsilon\to 0}\int_{-\infty}^{\infty} \frac{e^{i\mu(t+s)}}{(\mu^2-\omega_k^2+i\epsilon)(\mu+i\theta)}\, d\mu = 2\pi i \frac{e^{-i\omega_k(t+s)}}{-2\omega_k(-\omega_k+i\theta)}. \tag{3.61}$$

The full Feynman propagator thus reads

$$G_F(t,s,k) = \frac{1}{(2\pi)^{3/2}}\left[\frac{1}{2\omega_k}e^{-i\omega_k|t-s|} + \frac{1}{2\omega_k}e^{-i\omega_k(t+s)} + \frac{i\theta}{\omega_k(\omega_k-i\theta)}e^{-i\omega_k(t+s)}\right]. \tag{3.62}$$

If $\theta < 0$, then the right hand side of equation (3.60) acquires the following additional term:

$$\frac{1}{\lambda}u_\theta(t;\lambda)u_\theta^*(s;\lambda)\cdot(-2\theta)\Big|_{\lambda=-\theta^2-\omega_k^2} = \frac{2\theta}{\theta^2+\omega_k^2}e^{\theta(t+s)}$$

We also have, however, that the integral (3.61) acquires an extra term because its integrand now has a pole in the upper complex plane at $\mu = i|\theta|$:

$$\begin{aligned} \lim_{\epsilon\to 0}\int_{-\infty}^{\infty} \frac{e^{i\mu(t+s)}}{(\mu^2-\omega_k^2+i\epsilon)(\mu+i\theta)}\, d\mu &= 2\pi i\left[\frac{e^{-i\omega_k(t+s)}}{-2\omega_k(-\omega_k+i\theta)} + \frac{e^{-|\theta|(t+s)}}{-\theta^2-\omega_k^2}\right] \\ &= 2\pi i\left[\frac{e^{-i\omega_k(t+s)}}{2\omega_k(\omega_k-i\theta)} - \frac{e^{\theta(t+s)}}{\theta^2+\omega_k^2}\right] \end{aligned} \tag{3.63}$$

These two additional terms exactly cancel each other, so we again obtain expression (3.62) for $G_F(t,s,k)$. ▷

Flat spacetime with a finite start time is the simplest example of a d'Alembertian that has deficiency indices $(1,1)$. Additionally, the calculation of the Feynman propagator shown above reveals a very important feature of scalar quantum field theories in flat spacetime with a start time. We discover that canonical quantization is incompatible with flat spacetime that has a finite start time. In other words, there is no ansatz for the scalar field $\hat{\phi}(t,\mathbf{x})$ of the form (2.30) such that we obtain the expression (3.62) for $G_F(t,s,k)$ from the vacuum expectation value $\langle 0|T\hat{\phi}_k(t)\hat{\phi}_k(s)|0\rangle$. The essential reason for this is that the canonical mode functions $v_k(t)$ cannot satisfy both the Wronskian condition (2.34) and the boundary condition $f'(0)/f(0) = \theta$.

Canonical quantization demands that the mode functions obey the Wronskian condition. The following line of reasoning, however, demonstrates that they must also satisfy $\dot{v}_k(0)/v_k(0) = \theta$. Writing $G_F(t,s,k) = i/(2\pi)^{3/2}\int \lambda^{-1}u_\theta(t;\lambda)u_\theta(s;\lambda)\,d\sigma(\lambda)$, we have that

$$\begin{aligned}\partial_t G_F(t,s,k)|_{t=0} &= \frac{i}{(2\pi)^{3/2}}\int \frac{1}{\lambda}\dot{u}_\theta(0;\lambda)u_\theta(s;\lambda)\,d\sigma(\lambda)\\ &= \frac{i}{(2\pi)^{3/2}}\int \frac{1}{\lambda}\left(\theta\, u_\theta(0;\lambda)\right)u_\theta(s;\lambda)\,d\sigma(\lambda)\\ &= \theta G_F(0,s,k)\end{aligned}$$

Therefore, $\partial_t G_F(0,s,k)/G_F(0,s,k) = \theta$. We can check this fact using equation (3.62). For $s > 0$, we have that

$$G_F(0,s,k) = \frac{1}{(2\pi)^{3/2}}\frac{1}{\omega_k - i\theta}e^{-i\omega_k s}$$

and

$$\begin{aligned}\partial_t G_F(t,s,k)|_{t=0} &= \frac{1}{(2\pi)^{3/2}}\left[\frac{-i}{2}\left(H(t-s)-H(s-t)\right)e^{-i\omega_k|t-s|} - \frac{i}{2}e^{-i\omega_k(t+s)} + \frac{\theta}{\omega_k - i\theta}e^{-i\omega_k(t+s)}\right]_{t=0}\\ &= \frac{1}{(2\pi)^{3/2}}\frac{\theta}{\omega_k - i\theta}e^{-i\omega_k s}\end{aligned}$$

(Here we are using $H(t-s)$ to denote the Heaviside step function so as to avoid confusion with the boundary condition parameter θ.) It thus clearly follows that $\partial_t G_F(0,s,k)/G_F(0,s,k) = \theta$.

On the other hand, canonical quantization implies that we may compute $\partial_t G_F(0,s,k)$ and $G_F(0,s,k)$ according to equation (3.2). Again assuming that $s > 0$, we have that

$$G_F(0,s,k) = \frac{1}{(2\pi)^{3/2}}\frac{1}{2}v_k(0)v_k^*(s)$$

and

$$\begin{aligned}\partial_t G_F(t,s,k)|_{t=0} &= \frac{1}{(2\pi)^{3/2}}\frac{1}{2}\left[\delta(t-s)v_k^*(t)v_k(s) + H(t-s)\dot{v}_k^*(t)v_k(s)\right.\\ &\qquad\left. -\delta(t-s)v_k(t)v_k^*(s) + H(s-t)\dot{v}_k(t)v_k^*(s)\right]_{t=0}\\ &= \frac{1}{(2\pi)^{3/2}}\frac{1}{2}\dot{v}_k(0)v_k^*(s)\,.\end{aligned}$$

It follows that

$$\frac{\partial_t G_F(0,s,k)}{G_F(0,s,k)} = \frac{\dot{v}_k(0)}{v_k(0)} = \theta. \tag{3.64}$$

We therefore conclude that the mode functions $v_k(t)$ also obey the Robin boundary condition at $t = 0$.

The contradiction comes when we try to evaluate the Wronskian condition at $t = 0$. The left hand side of (2.34) reads

$$\dot{v}_k(0)v_k^*(0) - v_k(0)\dot{v}_k^*(0) = [\theta v_k(0)]\, v_k^*(0) - v_k(0)\,[\theta v_k^*(0)] = 0.$$

This is never equal to $2i$, as is required to satisfy the Wronskian condition. Therefore, there is no way to choose $v_k(t)$ that satisfies the Robin boundary condition so that the Wronskian condition is also satisfied. We conclude that canonical quantization is incompatible with flat spacetime that possesses a finite start time.

These considerations from $L^2([0,\infty)\times\mathbb{R}^3)$ suggest that path integral quantization is more fundamental than canonical quantization, at least in its ability to accommodate arbitrary spacetimes. We see that in flat spacetime having a start time, we can construct the Feynman propagator by starting with the "equation of motion" (3.4). This equation directly follows from the path integral definition of G_F. On the other hand, it is impossible to construct the Feynman propagator canonically using equation (3.2). While it may be possible to repair the ansatz (2.30) so as to modify the requirements on mode functions, it remains that canonical quantization fails in the case of Minkowski space with a start time. Even though this spacetime has only limited physical significance, it illustrates a limitation of canonical quantization.

Chapter 4

Review of the Covariant Cutoff

We now turn to the topic of the covariant UV cutoff itself. In preparation for studying the effect of the covariant cutoff on the Feynman propagator of a scalar field, let us review the nature of the cutoff here.

Recall what was stated in the introduction: that the covariant cutoff, applied to a scalar field, is a cutoff on the field's degrees of freedom in time. The cutoff is thus inherently information-theoretic. As such, we will begin by reviewing the fundamentals of sampling theory in section 4.1 so that we may define the covariant cutoff in section 4.2. Then, we will make explicit the notion that the covariant cutoff is a cutoff on the temporal degrees of freedom of a field, first in flat spacetime (section 4.3), and then in FLRW spacetime (section 4.4).

All of the results of this section are featured in greater detail in [38]. Many proofs and technical details are deferred to this publication.

4.1 Review of Sampling Theory

Sampling theory is the branch of information theory that is concerned with the reconstruction of functions that are defined on continuous domains from the values that the functions take on discrete sets of points. As such, sampling theory constitutes the link between continuous information and discrete information.

Central to sampling theory is the notion of a bandlimited function, which is defined below for a function on the real line.

Definition 4.1.1 *Let $f \in L^2(\mathbb{R})$. The function f is said to be* bandlimited *if it is the Fourier transform of a function that has compact support. In other words, there exists $F \in L^2[-\Omega, \Omega]$ such that*

$$f(t) = \frac{1}{\sqrt{2\pi}} \int_{-\Omega}^{\Omega} F(\omega) e^{i\omega t} \, d\omega \, . \tag{4.1}$$

The maximum Fourier frequency Ω is called the *bandlimit*. We will denote the space of Ω-bandlimited functions on the real line by $B(\mathbb{R}, \Omega)$.

Crucially, bandlimited functions obey the Shannon Sampling Theorem [39].

Theorem 4.1.2 (Shannon Sampling) *An Ω-bandlimited function $f \in B(\mathbb{R}, \Omega)$ is perfectly reconstructible from the values that it takes on the discrete set of points $\{t_n := \frac{n\pi}{\Omega}\}_{n\in\mathbb{Z}}$. The reconstruction formula is given by*

$$f(t) = \sum_{n\in\mathbb{Z}} f(t_n) \frac{\sin\left(\Omega(t - t_n)\right)}{\Omega(t - t_n)}. \tag{4.2}$$

The Shannon Sampling Theorem makes use of an equidistantly-spaced set of sample points $\{t_n\}$. In practical science and engineering, one usually chooses a set of equidistant sample points. However, one is in principle free to choose a more general set of sampling for reconstructing a bandlimited function. This freedom of choice is clarified in the following definition:

Definition 4.1.3 *A set of points $\Lambda = \{t_n\}_{n\in\mathbb{Z}}$ is a* set of sampling *provided that Λ is a strictly increasing sequence, that there is a finite minimum spacing between the points of Λ, and that a bandlimited function f can be stably reconstructed from the set of values $\{f(t_n)\}$.*

That a bandlimited function can be stably reconstructed from its sampled values means that any bounded errors in the sampled values only produces bounded errors in the reconstructed function.

To determine when a set of points Λ is a set of sampling, one may appeal to Beurling's Theorem. In order to state the theorem, however, we must first define the Beurling density.

Definition 4.1.4 *Let $\Lambda \subset \mathbb{R}$ be a discrete set of points, and let $n(r)$ be the minimum number of points of Λ that lie in any interval of length r on the real line. The* Beurling density *is defined as*

$$D(\Lambda) := \lim_{r\to\infty} \frac{n(r)}{r}. \tag{4.3}$$

One then has the following theorem [40]:

Theorem 4.1.5 (Beurling) *$\Lambda \subset \mathbb{R}$ is a set of sampling for $B(\mathbb{R}, \Omega)$ if $D(\Lambda) > \frac{\Omega}{\pi}$. Conversely, if Λ is a set of sampling, then $D(\Lambda) \geq \frac{\Omega}{\pi}$.*

Note that the equidistant set of sampling $\{t_n := \frac{n\pi}{\Omega}\}_{n\in\mathbb{Z}}$ saturates the converse inequality in Beurling's Theorem. This theorem is very nice, as it makes precise the notion that bandlimited functions possess a finite density of degrees of freedom in time.

The notion of a bandlimited function and of reconstruction from sets of sampling naturally generalizes to $\mathbb{R}^n$. For a function on $\mathbb{R}^n$, bandlimitation is defined as follows.

Definition 4.1.6 *Let $f \in L^2(\mathbb{R}^n)$. The function f is said to be* bandlimited *if its Fourier transform $F(\mathbf{k})$ has compact support in $\mathbb{R}^n$. In other words, $F \in L^2(S)$ where $S \subset \mathbb{R}^n$ is compact, and we may write*

$$f(\mathbf{x}) = \frac{1}{(2\pi)^{n/2}} \int_S F(\mathbf{k}) e^{i\mathbf{k}\cdot\mathbf{x}}\, d^n k\,. \tag{4.4}$$

Let $X(\Omega) \subset \mathbb{R}^n$ be the smallest ball such that $S \subseteq X(\Omega)$, where Ω is the radius of the ball. This Ω defines a bandlimit in $\mathbb{R}^n$. We will denote the set of Ω-bandlimited functions in $\mathbb{R}^n$ by $B(\mathbb{R}^n, \Omega)$.

Lastly, in $\mathbb{R}^n$, sets of sampling are characterized by Landau's theorem [40]:

Theorem 4.1.7 (Landau) *If $S \subset \mathbb{R}^n$ is a set of sampling for $B(\mathbb{R}^n, \Omega)$, then $D(S) \geq \frac{\text{vol}(S)}{(2\pi)^n}$. In $\mathbb{R}^n$, density is defined as*

$$D(S) := \lim_{r \to \infty} \frac{n(r)}{r}, \tag{4.5}$$

where $n(r)$ is the minimum number of points of S that lie in any ball of radius r.

4.2 Definition of the Covariant Cutoff

Next, we will see how the notion of a bandlimit and of bandlimited functions can be generalized to Riemannian, and then Lorentzian manifolds (or in other words, spacetimes). This generalization relies on the observation that a bandlimit is equivalent to a cutoff on the spectrum of the Laplacian.

Consider for a moment the case of one-dimensional sampling. Notice that the plane waves $\exp(i\omega t)$ are eigenfunctions of the second derivative operator $-\frac{d^2}{dt^2}$. The corresponding eigenvalues are $\omega^2 \in [0, \infty)$. Therefore, the Fourier transform (4.1) is a (continuous) linear combination of eigenfunctions of the second derivative operator whose eigenvalues are less than or equal to Ω^2.

The second derivative operator $-\frac{d^2}{dt^2}$ is the Laplacian in $\mathbb{R}$. In $\mathbb{R}^n$, the Laplacian reads $-\sum_{j=1}^n \frac{\partial^2}{\partial x^{j\,2}}$. Its eigenfunctions are now the plane waves $\exp(i\mathbf{k} \cdot \mathbf{x})$, with corresponding eigenvalues $|\mathbf{k}|^2$. Moreover, any bandlimited function $f \in B(\mathbb{R}^n, \Omega)$ is still a linear combination of eigenfunctions of the Laplacian with eigenvalues less than or equal to Ω^2. Therefore, instead viewing a bandlimit as a maximum Fourier frequency, one may equivalently view a bandlimit as being a cutoff on the spectrum of the Laplacian. Explicitly, one has that $B(\mathbb{R}^n, \Omega) = \text{span}\left\{\exp(i\mathbf{k} \cdot \mathbf{x}) \ : \ \mathbf{k} \in \mathbb{R}^n, \ |\mathbf{k}|^2 \in [0, \Omega^2]\right\}$.

These last two examples motivate the following definition of a bandlimit and the space of bandlimited functions for a Riemannian manifold. Given a Riemannian manifold M, we may assume that its scalar Laplacian is self-adjoint or that we have chosen a particular self-adjoint extension of the Laplacian should it be necessary to specify boundary conditions. The Laplacian is thus equipped with an orthonormal basis for $L^2(M)$ consisting of its eigenfunctions. Furthermore, the spectrum of the Laplacian is strictly non-negative. We thus have the following definition:

Definition 4.2.1 *Let M be a Riemannian manifold with a self-adjoint Laplacian $\triangle$. Given a bandlimit $\Omega \in \mathbb{R}$, the space of Ω-bandlimited functions on M is*

$$B(M, \Omega) := \text{span}\left\{\phi_\lambda \ : \ \lambda \in \text{spec}(\triangle), \ \lambda \in [0, \Omega^2]\right\} \tag{4.6}$$

This bandlimit is covariant because the spectrum of the Laplacian is a set of scalar quantities, which is independent of the choice of coordinates for M. Therefore, a cutoff on $\text{spec}(\triangle)$ is also covariant. Furthermore, one still finds that $B(M, \Omega)$ possesses sampling properties that are analogous to the case of $\mathbb{R}^n$. For a study of sampling on Riemannian manifolds the reader is referred to [41].

This last definition is very nice, because the Laplacian has a natural generalization to Lorentzian-signature manifolds: the d'Alembertian. As such, it was proposed in [9, 10] that a fully covariant bandlimit may be obtained by cutting off the spectrum of the d'Alembertian. This is the covariant ultraviolet cutoff that we study in this thesis:

Definition 4.2.2 *Let M be a Lorentzian manifold with a self-adjoint d'Alembertian $\Box$. Given a bandlimit $\Omega \in \mathbb{R}$, the space of Ω-bandlimited functions on M is*

$$B(M,\Omega) := \text{span}\left\{\phi_\lambda \ : \ \lambda \in \text{spec}(\Box),\, \lambda \in [-\Omega^2, \Omega^2]\right\} \tag{4.7}$$

Note that the d'Alembertian of a Lorentzian manifold is no longer positive definite, so spec($\Box$) is no longer strictly nonnegative.

4.3 The Covariant Cutoff in Flat Spacetime

Let us first turn our attention to flat spacetime and study the effect of the covariant cutoff on the kinematics of scalar fields here. Let M denote flat $1+3$ dimensional spacetime. Recall that in flat spacetime, the d'Alembertian reads $\Box = -\frac{\partial^2}{\partial t^2} + \triangle$. Its eigenfunctions are the plane waves $e^{-ik^0 t + i\mathbf{k}\cdot\mathbf{x}}$, with corresponding eigenvalues $(k^0)^2 - |\mathbf{k}|^2$. Therefore, the space of covariantly bandlimited fields is

$$B(M,\Omega) = \text{span}\left\{e^{-ik^0 t + i\mathbf{k}\cdot\mathbf{x}} \ : \ \left|(k^0)^2 - |\mathbf{k}|^2\right| \leq \Omega^2\right\}. \tag{4.8}$$

These fields' Fourier transforms thus only have support on the region

$$S = \left\{(k^0, \mathbf{k}) \in \mathbb{R}^4 \ : \ \left|(k^0)^2 - |\mathbf{k}|^2\right| \leq \Omega^2\right\}. \tag{4.9}$$

This region is shown below in figure 4.1.

One immediately notices two important points. First, points with arbitrarily large k^0 and $|\mathbf{k}|$ lie in the region S. Second, one may easily check that the volume of S is infinite. Therefore, by Landau's theorem, there is no set of sampling for $B(M,\Omega)$ that has a finite density. What sort of cutoff is Ω, then?

Let us address the second issue first. Instead of considering a full field $\hat{\phi}(t,\mathbf{x})$, one could instead examine the spatial modes of the field,

$$\hat{\phi}(t,\mathbf{k}) \equiv \frac{1}{(2\pi)^{3/2}} \int e^{-i\mathbf{k}\cdot\mathbf{x}} \hat{\phi}(t,\mathbf{x})\, d^3x, \tag{4.10}$$

with $\mathbf{k}$ held fixed. We will call these the fixed spatial modes of a field $\hat{\phi}$. For a fixed spatial mode, the condition $|(k^0)^2 - |\mathbf{k}|^2| \leq \Omega^2$ reads

$$r_1 := \Re\left(\sqrt{|\mathbf{k}|^2 - \Omega^2}\right) \leq |k^0| \leq \sqrt{|\mathbf{k}|^2 + \Omega^2} =: r_2\,. \tag{4.11}$$

Therefore, we see that each fixed spatial mode is bandlimited in time, with its Fourier transform having support on the compact interval

$$S_{\mathbf{k}} := \begin{cases} [-r_2, r_2] & |\mathbf{k}| \leq \Omega \\ [-r_2, -r_1] \cup [r_1, r_2] & |\mathbf{k}| > \Omega \end{cases}. \tag{4.12}$$

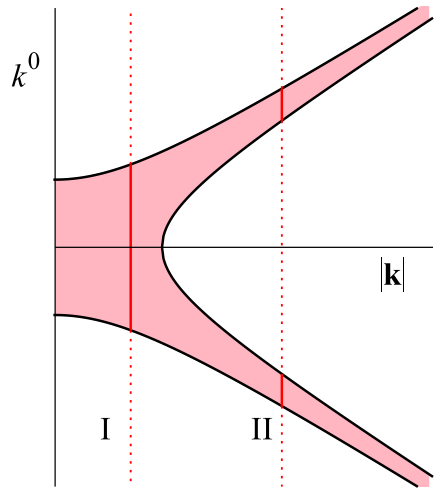

Figure 4.1: The bandwidth region S (shaded). The solid red lines are examples of $S_{\mathbf{k}}$ for (I) $k \leq \Omega$ and (II) $k > \Omega$.

The solid red lines in figure 4.1 are examples of different $S_{\mathbf{k}}$.

Notice that for any $\mathbf{k} \in \mathbb{R}^3$, the volume (or rather, length) of $S_{\mathbf{k}}$ is finite. Therefore, each fixed spatial mode has sampling properties in time. Furthermore, it is clear that

$$\lim_{|\mathbf{k}|\to\infty} \mathrm{vol}(S_{\mathbf{k}}) = 0\,.$$

Therefore, the density of degrees of freedom in time of fixed spatial modes that possess large spatial wavevectors is very small. Furthermore, this density tends to zero as $|\mathbf{k}|$ grows unboundedly large. This resolves the first issue raised above.

In summary, we see that the covariant cutoff causes each fixed spatial mode of a scalar field to possess a finite density of degrees of freedom in time. Consistent with Lorentz contractions, we find that modes with arbitrarily large $|\mathbf{k}|$ still exist. The density of degrees of freedom in time of arbitrarily large fixed spatial modes is infinitesimally small, however. In other words, one must only sample large-$|\mathbf{k}|$ modes very infrequently in order to know their behaviour for all time. The reader is referred to [38] for a more detailed discussion of the sampling properties of fixed spatial modes, as well as a discussion of fixed temporal modes.

Finally, we can explicitly demonstrate how this covariant cutoff is consistent with Lorentz contractions. Suppose that in some reference frame O we are given a set of sampling $\Lambda = \{t_n\}_{n\in\mathbb{Z}}$ for a fixed spatial mode $\mathbf{k}$. Suppose that we then boost to a new frame O' where, according to time dilation, the set Λ' is now less dense. At first, it would seem that we have a contradiction. How can it be that this sparser set Λ' is a still a set of sampling in the frame O'? Of course, the answer is that the mode $\mathbf{k}$ gets boosted to a new mode $\mathbf{k}'$ which, according to length contraction, is such that $|\mathbf{k}'| > |\mathbf{k}|$. Therefore, the boosted fixed spatial mode has less bandwidth in time, so the set of sampling in the frame O' does not need to be as dense as the set of sampling in O.

4.4 The Covariant Cutoff in Expanding FLRW Spacetimes

Next, we turn our attention to the covariant cutoff in expanding FLRW spacetimes. Motivated by our studies in flat spacetime, here as well we will consider the fixed spatial modes of a scalar field. In other words, we will study the differential expressions $\Box_k = -a^{-3}(t)\left(\partial_t a^3(t)\partial_t + k^2 a(t)\right)$ and the operators that they generate. The main result of this section will be to show that like in flat spacetime, a similar freezing out of the degrees of freedom in time occurs for modes with large $|\mathbf{k}|$.

First, note that if $\lambda \in \text{spec}(\Box)$, *i.e.*, $\Box\phi_\lambda(t,\mathbf{x}) = \lambda\phi_\lambda(t,\mathbf{x})$ for some $\phi_\lambda(t,\mathbf{x})$, then $\Box_k\phi_\lambda(t,\mathbf{k}) = \lambda\phi_\lambda(t,\mathbf{k})$ as well, where $\phi_\lambda(t,\mathbf{k})$ is the spatial Fourier transform of $\phi_\lambda(t,\mathbf{x})$. Therefore, $\lambda \in \text{spec}(\Box_k)$. It follows that the spectra of $\Box$ and $\Box_k$ are the same modulo degeneracy. We may therefore impose the covariant cutoff by cutting off the spectrum of each k-d'Alembertian, mode-by-mode.

Here, we study the differential expressions $\Box_k$ for t in the range $-\infty \leq t_i < t_f < \infty$. In other words, we consider FLRW spacetimes that began expanding at some time t_i (which is possibly infinitely far in the past) up to some finite end time t_f. According to section 2.5.2, let $\hat{D}_k^0$ denote the minimal operator generated by $\Box_k$. (For now, we let $m = 0$.) We then make the following generic assumptions on the scale factor $a(t)$. We assume that $a(t)$ is positive and finite on $[t_i, t_f]$ and differentiable on (t_i, t_f). We also assume that either

1. $t_i > -\infty$ so that $[t_i, t_f]$ is compact, or
2. $\frac{1}{k}\int_{-\infty}^{t_f} a(t)\,dt < \infty$ for all $k > 0$.

With these assumptions, one may show that $\hat{D}_k^0$ has deficiency indices $(2,2)$ for all $k \geq 0$ if $t_i > -\infty$ and for all $k > 0$ if $t_i \to -\infty$. For simplicity let us not consider the zero mode here. The reader is referred to [38] for details about the zero mode and for the proof that $\hat{D}_k^0$ has deficiency indices $(2,2)$.

Since the minimal operator generated by $\Box_k$ is only symmetric and not self-adjoint, it is necessary to choose a particular self-adjoint extension $\hat{D}_k'$ in order to impose the covariant cutoff. One does not know generically which self-adjoint extension should be chosen. This choice should be made based on physical input. As such, here we examine results that are independent of the choice of self-adjoint extension.

First, let us collect certain facts about the operators $\hat{D}_k^0$. All of these results are discussed in greater detail in [38]. First, since $\hat{D}_k^0$ has deficiency indices $(2,2)$, it follows from Krein's Theorem that the spectrum of any self-adjoint extension $\hat{D}_k'$ of $\hat{D}_k^0$ is bounded below [36, Chapter V.19.4]. One may also show that $\text{spec}(\hat{D}_k')$ is discrete and has no finite accumulation points for any choice of self-adjoint extension. Finally, one may also show that $\hat{D}_k^0$ is simple, *i.e.*, it has no point spectrum. From this last fact, it follows that $\text{spec}(\hat{D}_k')$ consists only of a point spectrum for any choice of self-adjoint extension. Furthermore, the eigenvalues all have a multiplicity of at most 2, and, given any $\lambda \in \mathbb{R}$, there is a particular self-adjoint extension such that λ is an eigenvalue of multiplicity 2.

For each comoving mode $k := |\mathbf{k}|$, denote the space of covariantly bandlimited functions by $B_k(\Omega)$ for a given choice of self-adjoint extension. Applying the facts above, we may write

$$B_k(\Omega) = \text{span}\left\{\phi_\lambda \;:\; \lambda \in \text{spec}(\hat{D}_k'),\, |\lambda| \leq \Omega^2\right\}. \tag{4.13}$$

Furthermore, since $\mathrm{spec}(\hat{D}'_k)$ is discrete, we conclude that $N_k := \dim B_k(\Omega)$ is actually finite! In other words, in a FLRW spacetime in which we only consider a field's evolution up to some finite end time, the fixed spatial comoving modes of a scalar field only have a finite *number* of degrees of freedom in time when one imposes the covariant bandlimit. This result is independent of the choice of self-adjoint d'Alembertian.

We may now state the main result of this section, which shows that the degrees of freedom in time of a comoving mode freeze out as k grows large.

Theorem 4.4.1 *There exists a $K > 0$ such that for all $k \geq K$, $N_k = c$, where $c \in \{0, 1, 2\}$. This K is independent of the choice of self-adjoint extension $\hat{D}'_k$ that defines $B_k(\Omega)$.*

The reader is referred to [38] for the proof of this theorem.

Intuitively, we may understand Theorem 4.4.1 in terms of Planck scale and Hubble scale crossings. In any spacetime, one would intuitively expect that the dynamics of modes whose physical wavelengths are smaller than the Planck scale should be frozen out. In an expanding FLRW spacetime, one would therefore expect modes to become dynamical as their wavelengths cross the Planck scale. In an inflationary spacetime, however, modes again become frozen as they cross the Hubble horizon. With the covariant cutoff, the fact that any comoving mode thus has a finite window of time during which its dynamics are unfrozen makes is plausible that any fixed spatial mode would have only a finite number of degrees of freedom in time. Furthermore, if a fixed mode's comoving wavelength is so small (*i.e.*, k is so large) that its physical wavelength never crosses the Planck scale before the end of inflation at t_f, one would expect that it should possess no dynamics whatsoever. This last expectation corresponds to the existence of the $K > 0$ in Theorem 4.4.1. The modes for which $k > K$ are the modes which never cross the Planck scale. Unsurprisingly, then, these modes possess at most two degrees of freedom in time.

Let us investigate this intuition in the following example.

Example 4.4.2 *De Sitter Inflation with a Finite End Time*

Consider a massless scalar field in de Sitter space. We work with the flat slicing of de Sitter space so that its line element reads $ds^2 = -dt^2 + a^2(t)d\mathbf{x}^2$. The scale factor is $a(t) = e^{Ht}$, where H is the Hubble constant, and we consider $t \in (-\infty, t_f]$. Observe that $\int_{-\infty}^{t_f} a(t)\, dt = e^{Ht_f}/H$, so our assumptions hold for this scale factor.

For convenience, let us change from cosmic time to conformal time. Define the conformal time as $\eta(t) := e^{-Ht}/H$ so that $\eta \in [\eta_f, \infty)$ and $ds^2 = a^2(\eta)[-d\eta^2 + d\mathbf{x}^2]$. As t runs from $-\infty$ to t_f, η runs from ∞ down to η_f. The scale factor in conformal time is $a(\eta) = (H\eta)^{-1}$. Then, it is straightforward to show that two linearly independent solutions of the eigenfunction equation $\Box_k u = \lambda u$, where $\Box_k$ is given by equation (2.44), are

$$f_\lambda(\eta) = \sqrt{\frac{k\pi}{2}}\eta^{3/2} J_{p(\lambda)}(k\eta) \qquad \text{and} \qquad g_\lambda(\eta) = \sqrt{\frac{k\pi}{2}}\eta^{3/2} Y_{p(\lambda)}(k\eta). \tag{4.14}$$

The order of the Bessel functions is given by

$$p(\lambda) := \sqrt{\frac{9}{4} - \frac{\lambda}{H^2}}. \tag{4.15}$$

Also note that for large η, one has that

$$\begin{aligned} f_\lambda(\eta) &\sim \eta \cos\left(k\eta - p(\lambda)\frac{\pi}{2} - \frac{\pi}{4}\right), \\ g_\lambda(\eta) &\sim \eta \sin\left(k\eta - p(\lambda)\frac{\pi}{2} - \frac{\pi}{4}\right). \end{aligned} \tag{4.16}$$

For simplicity, instead of investigating the general K from Theorem 4.4.1, let us investigate the threshold K' beyond which modes have at most two degrees of freedom in time for a particular choice of self-adjoint extension. In particular, let us choose the self-adjoint extension $\hat{D}'_k$ of $\hat{D}^0_k$ for which $\lambda = 0$ is an eigenvalue of multiplicity 2. Then, for a given covariant bandlimit Ω, the threshold K' is the smallest value of k such that there are no other eigenvalues of $\hat{D}'_k$ besides $\lambda = 0$ in the interval $[-\Omega^2, \Omega^2]$.

One has the following useful lemma [38]:

Lemma 4.4.3 *Let $\hat{D}'_k$ be the self-adjoint extension of $\hat{D}^0_k$ such that $\lambda' \in \mathbb{R}$ is an eigenvalue of $\hat{D}'_k$ of multiplicity 2. Denote by f_λ and g_λ two linearly independent solutions of the eigenvalue equation $\Box_k u = \lambda u$. Also define*

$$\Delta(\lambda; \lambda', k) := \langle f_\lambda | f_{\lambda'} \rangle \langle g_\lambda | g_{\lambda'} \rangle - \langle f_\lambda | g_{\lambda'} \rangle \langle g_\lambda | f_{\lambda'} \rangle, \tag{4.17}$$

where $\langle \cdot | \cdot \rangle$ is the standard inner product on $L^2\left([\eta_f, \infty), a^4(\eta) d\eta\right)$, $\langle \psi | \phi \rangle = \int_{\eta_f}^{\infty} \psi^*(\eta)\phi(\eta)a^4(\eta)\, d\eta$. Then, if $\lambda \in \mathbb{R}$, $\lambda \neq \lambda'$ is another eigenvalue of $\hat{D}'_k$, it follows that $\Delta(\lambda; \lambda', k) = 0$.

One can also show that $\Delta(\lambda; \lambda', k)$ converges to a constant as $k \to \infty$ for any fixed $\lambda' \in \mathbb{R}$. Therefore, K' is the threshold such that $\Delta(\lambda; 0, k) \neq 0$ on $[-\Omega^2, \Omega^2]$ whenever $k \geq K'$.

So as to avoid the need later on to take the complex conjugate of Bessel functions that have an imaginary order (which considerably complicates numerics), let us equivalently consider searching for the zeros (or lack thereof) of $\Delta^*(\lambda; 0, k)$. The inner products which define $\Delta^*(\lambda; 0, k)$ are given by

$$\begin{aligned} \langle f_0 | f_\lambda \rangle &= \frac{k}{H^4}\left[\frac{\sin\delta(\lambda)}{\lambda/H^2} + \frac{\pi}{2}F(J,J)\right] \quad \langle f_0 | g_\lambda \rangle = \frac{k}{H^4}\left[\frac{\cos\delta(\lambda)}{\lambda/H^2} + \frac{\pi}{2}F(J,Y)\right] \\ \langle g_0 | f_\lambda \rangle &= \frac{k}{H^4}\left[-\frac{\cos\delta(\lambda)}{\lambda/H^2} + \frac{\pi}{2}F(Y,J)\right] \quad \langle g_0 | g_\lambda \rangle = \frac{k}{H^4}\left[\frac{\cos\delta(\lambda)}{\lambda/H^2} + \frac{\pi}{2}F(Y,Y)\right] \end{aligned} \tag{4.18}$$

The quantity $\delta(\lambda)$ is given by $\delta(\lambda) = p(\lambda)\frac{\pi}{2} + \frac{\pi}{4}$. The function $F(\cdot, \cdot)$ is defined as

$$F(A,B) := k\eta_f \frac{A_{3/2}(k\eta_f)B_{p(\lambda)-1}(k\eta_f) - A_{1/2}(k\eta_f)B_{p(\lambda)}(k\eta_f)}{\lambda/H^2} + \frac{A_{3/2}(k\eta_f)B_{p(\lambda)}(k\eta_f)}{p(\lambda) + 3/2}. \tag{4.19}$$

J and Y are placeholders for the Bessel J and Bessel Y functions, and $A, B \in \{J, Y\}$.

If we let $z = k\eta_f$ and $\ell = \lambda/H^2$, then we see that $\Delta^*(\lambda; 0, k)$ is really only a function of these two variables. Therefore, let us write

$$\frac{H^8}{k^2}\Delta^*(\lambda; 0, k) := G(z, \ell). \tag{4.20}$$

We may equivalently search for the threshold Z such that $G(z,\ell) \neq 0$ for $\ell \in \left[-\frac{\Omega^2}{H^2}, \frac{\Omega^2}{H^2}\right]$ whenever $z \geq Z$. As such, we have that

$$Z\left(\frac{\Omega}{H}\right) = \min_{z>0}\left\{ z_\star \;\middle|\; G(z,\ell) \neq 0 \quad \forall\, \ell \in \left[-\frac{\Omega^2}{H^2}, \frac{\Omega^2}{H^2}\right], \forall \;\; z > z_\star \right\}. \tag{4.21}$$

Since $z = k\eta_f$, it follows that

$$K' = \frac{1}{\eta_f} Z\left(\frac{\Omega}{H}\right). \tag{4.22}$$

Because $\Delta^*(\lambda; 0, k)$ converges to a constant function of λ as $k \to \infty$, increasing k (and hence z) pushes the ℓ-zeros of $G(z,\ell)$ farther away from the origin. As such, the definition (4.21) shows that Z is a monotonically increasing function of Ω/H. A larger interval $\left[-\frac{\Omega^2}{H^2}, \frac{\Omega^2}{H^2}\right]$ requires a larger threshold Z. This behaviour is reflected in the numerical computation of $Z(\Omega/H)$ shown in figure 4.2 below.

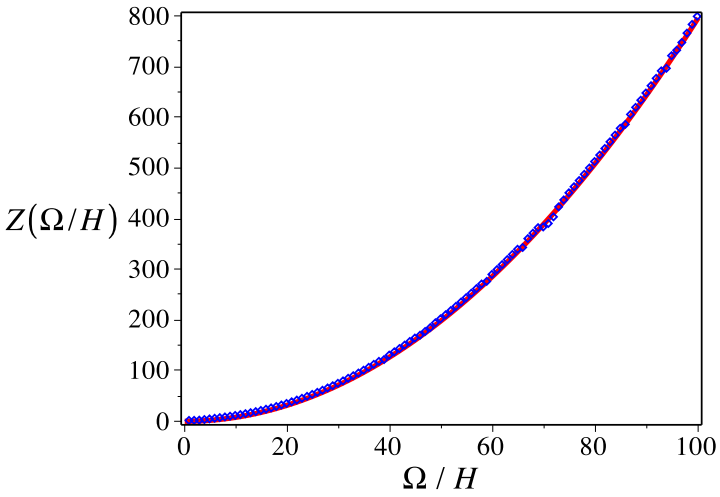

Figure 4.2: Numerical simulation of $Z(\Omega/H)$. The red curve is a fit to the numerically-generated points, given by $Z(\Omega/H) = 0.0796\,(\Omega/H)^2$.

We ultimately see that K' depends on two parameters: the conformal end time η_f and the ratio Ω/H. Furthermore, the dependence of K' on these parameters is consistent with the intuition that we developed earlier.

First, consider the dependence of K' on η_f. As η_f decreases toward zero, K' increases. This is to be expected, since decreasing the value of η_f corresponds to increasing the proper end time t_f of the de Sitter inflation. Comoving modes whose proper wavelengths were once too small to cross the Planck scale before the end of inflation can grow larger than the Planck length if inflation lasts longer. One thus naturally expects that the threshold for mode freezing K' should increase as η_f decreases.

Next, we may understand the dependence of K' on the ratio Ω/H in the following way. Holding H fixed, an increase in Ω/H corresponds to an increase in Ω. Since Ω is a frequency cutoff that operates at

the Planck scale, in essence this increase corresponds to decreasing the Planck length. If the Planck length decreases, then modes with wavelengths that were previously too small to be able to cross the Planck scale before the end of inflation may now do so. Therefore, a larger threshold for mode freezing is expected, and is indeed seen numerically.

▷

Chapter 5

Impact of the Covariant Cutoff on Field Fluctuations

We now turn our attention to our final goal: calculating the impact of the covariant UV cutoff on the quantum fluctuations of a scalar field. We will do this by calculating the impact of the covariant cutoff on the Feynman propagator of a scalar field (which directly measures the strength of the field's fluctuations).

Recall that in section 2.4.2, we found that the fluctuation spectrum of a scalar field in a FLRW spacetime is given by $\delta\phi_k(t) = \frac{1}{2\pi}k^{3/2}|v_k(t)|$. Likewise, from equation (3.2), we also have that

$$G_F(t = s, k) = \frac{1}{(2\pi)^{3/2}}\frac{1}{2}|v_k(t)|^2 \,. \tag{5.1}$$

Therefore, we relate the fluctuation spectrum to the Feynman propagator by writing

$$\delta\phi_k(t) = \frac{\sqrt{2}}{(2\pi)^{1/4}}k^{3/2}|G_F(t = s, k)|^{1/2}. \tag{5.2}$$

Then, if we denote the covariantly bandlimited Feynman propagator by G_F^c, we have that the covariantly bandlimited fluctuation spectrum, $\delta\phi_k^c(t)$, is given by

$$\delta\phi_k^c(t) = \frac{\sqrt{2}}{(2\pi)^{1/4}}k^{3/2}|G_F^c(t = s, k)|^{1/2}. \tag{5.3}$$

The question that we must answer is how the covariant cutoff enters into the calculation of the Feynman propagator. In other words, what is G_F^c? To answer this question, we must recall the path integral definition of $G_F(x, y)$ (equation (3.9)). If one assumes the existence of the covariant UV cutoff in nature, then one is assuming that all fields in nature, *i.e.*, on a given spacetime manifold M, are covariantly bandlimited. The set of covariantly bandlimited fields, $B(M, \Omega)$, is only a subset of all fields. Therefore, in the path integral picture, the covariantly bandlimited Feynman propagator is obtained by only integrating

over the space of covariantly bandlimited fields, instead of integrating over all possible field configurations. Symbolically, $G_F^c(x,y)$ is therefore defined as

$$G_F^c(x,y) := \frac{\int_{B(M,\Omega)} \phi(x)\phi(y)e^{iS[\phi]}\,\mathcal{D}[\phi]}{\int_{B(M,\Omega)} e^{iS[\phi]}\,\mathcal{D}[\phi]}. \tag{5.4}$$

More practically, given some Feynman propagator, recall that $G_F(x,y)$ is really the integral kernel of an operator, call it $\hat{G}_F$, that acts on functions in $L^2(M,g)$. Then, if we denote by $\hat{P}_{B(M,\Omega)}$ the projector onto the space of covariantly bandlimited fields, we have that

$$\hat{G}_F^c = \hat{P}_{B(M,\Omega)}\hat{G}_F\hat{P}_{B(M,\Omega)}. \tag{5.5}$$

Or, equivalently we may use the notation

$$G_F^c(x,y) = (P_{B(M,\Omega)}G_F P_{B(M,\Omega)})(x,y). \tag{5.6}$$

The details of how one constructs the projector $P_{B(M,\Omega)}$ and of how one computes G_F^c of course depend on the spacetime manifold M.

In section 5.1, we will first calculate G_F^c in the case where M is flat spacetime. Then, in section 5.2, we will discuss a general strategy for computing G_F^c when M is a FLRW spacetime. We will apply this strategy to the case of power-law FLRW spacetime in section 5.3. Since power-law spacetime is a model for early-universe inflation, our findings on the strength of the covariant cutoff's effect here will let us appraise the possible observational effect that the covariant cutoff could have in the CMB.

A question that one might ask is why power-law inflation? Why not a simpler spacetime such as de Sitter spacetime? Furthermore, power-law inflation has been ruled out by the Planck experiment [42]. As such, why not study another inflationary model, such as ϕ^2 inflation [43] or R^2 inflation [44, 45]? The answer to these questions is that power-law inflation is the simplest and best-understood inflationary scenario that still yields interesting physical results.

In particular, the case of de Sitter spacetime is somewhat less interesting. Recall that during de Sitter inflation, the (proper) Hubble radius is constant. It follows that the fluctuations of field modes that cross the Hubble horizon are scale invariant. One would thus expect the covariant cutoff to cause a constant shift in the strength field fluctuations, but to otherwise impart no other observational signatures. This constant shift *is* still of interest, since it reveals the strength at which the covariant cutoff operates. In the case of power-law inflation, however, it has been shown that more distinguishing features can appear in the presence of a (hard) cutoff [46].

Very generally, one would expect the strength of the covariant cutoff's effect to scale like σ^β for some $\beta > 0$. We denote by σ the ratio of the Planck length to the Hubble length at the end of inflation, *i.e.*, $\sigma := \ell_P/\ell_H$. During inflation, these two relevant characteristic length scales are only thought to have been separated by 5 to 6 orders of magnitude [11, 12]. As such, our ability to experimentally measure the effect of the covariant cutoff crucially depends on β. If β is much greater than 1, then the experimental signature would likely be too weak to detect.

5.1 Calculation of the Covariantly Bandlimited Feynman Propagator in Flat Spacetime

Let us first consider the case of a flat spacetime M. Recall expression (3.16) that we found for $G_F(x,y)$ by working in the path integral formalism, reproduced below for convenience:

$$G_F(x,y) = \frac{i}{(2\pi)^4}\int dk^0\, d^3\mathbf{k}\, \frac{e^{-ik^0(t-s)+i\mathbf{k}\cdot(\mathbf{x}-\mathbf{y})}}{(k^0)^2 - |\mathbf{k}|^2 - m^2 + i\epsilon} \tag{5.7}$$

(Recall that a limit as $\epsilon \to 0$ after integration is implied.) The plane waves $e^{-ik^0(t-s)+i\mathbf{k}\cdot(\mathbf{x}-\mathbf{y})}$, $(k^0,\mathbf{k}) \in \mathbb{R}^4$, are the eigenfunctions of the flat d'Alembertian $\Box = -\frac{\partial^2}{\partial t^2} + \triangle$, where as before $\triangle := \sum_{j=1}^3 \frac{\partial^2}{\partial x^{j\,2}}$. Therefore, equation (5.7) is manifestly a linear combination of eigenfunctions of the d'Alembertian.

Imposing the covariant cutoff amounts to projecting G_F onto the space spanned by the eigenfunctions of the d'Alembertian whose eigenvalues lie in the interval $[-\Omega^2, \Omega^2]$. The eigenvalues corresponding to the plane waves above are $(k^0)^2 - |\mathbf{k}|^2$. Thus, it follows that the covariantly bandlimited Feynman propagator, $G_F^c(x,y) := (P_{B(M,\Omega)} G_F P_{B(M,\Omega)})(x,y)$, is given by

$$G_F^c(x,y) = \frac{i}{(2\pi)^4}\int_{|(k^0)^2 - |\mathbf{k}|^2| \leq \Omega^2} dk^0\, d^3\mathbf{k}\, \frac{e^{-ik^0(t-s)+i\mathbf{k}\cdot(\mathbf{x}-\mathbf{y})}}{(k^0)^2 - |\mathbf{k}|^2 - m^2 + i\epsilon}. \tag{5.8}$$

Since we are after the fluctuation spectrum of a scalar field, we are most interested in the equal-time, spatial Fourier transform of the covariantly bandlimited Feynman propagator. The Fourier transform of the last line with respect to $\mathbf{x} - \mathbf{y}$ reads

$$G_F^c(t,s,k) = \frac{i}{(2\pi)^{5/2}}\int_{S_\mathbf{k}} dk^0\, \frac{e^{-ik^0(t-s)}}{(k^0)^2 - |\mathbf{k}|^2 - m^2 + i\epsilon}, \tag{5.9}$$

where $k := |\mathbf{k}|$ and where the interval $S_\mathbf{k}$ (*cf.* figure 4.1) is given by

$$S_\mathbf{k} := \begin{cases} \left[-\sqrt{|\mathbf{k}|^2 + \Omega^2}, \sqrt{|\mathbf{k}|^2 + \Omega^2}\right] & |\mathbf{k}| \leq \Omega \\ \left[-\sqrt{|\mathbf{k}|^2 + \Omega^2}, -\sqrt{|\mathbf{k}|^2 - \Omega^2}\right] \cup \left[\sqrt{|\mathbf{k}|^2 - \Omega^2}, \sqrt{|\mathbf{k}|^2 + \Omega^2}\right] & |\mathbf{k}| > \Omega \end{cases}. \tag{5.10}$$

This interval has two qualitatively different forms depending on whether $|\mathbf{k}|$ is less than or greater than Ω.

Consider first the case where $|\mathbf{k}| \leq \Omega$. Notice that the poles of the integrand in equation (5.9) occur at $k^0 = \pm\omega := \pm\sqrt{|\mathbf{k}|^2 + m^2}$. These poles thus lie in $S_\mathbf{k}$ provided $m < \Omega$, which is a reasonable assumption since particle masses beyond the Planck scale should not exist. As such, we evaluate the right hand side of equation (5.9) for equal times as follows:

$$\begin{aligned} G_F^c(t=s,k) &= \frac{i}{(2\pi)^{5/2}}\int_{-r_2}^{r_2} dk^0\, \frac{1}{(k^0)^2 - \omega^2} \\ &= \frac{i}{(2\pi)^{5/2}}\left[\int_{-\infty}^{\infty} dk^0\, \frac{1}{(k^0)^2 - \omega^2} - \int_{r_2}^{\infty} dk^0\, \frac{1}{(k^0)^2 - \omega^2} - \int_{-\infty}^{-r_2} dk^0\, \frac{1}{(k^0)^2 - \omega^2}\right] \end{aligned}$$

The first integral is easily evaluated using complex residues. The last two integrals may be combined and then evaluated using standard methods.

$$\begin{aligned} G_F^c(t=s,k) &= \frac{1}{(2\pi)^{3/2}}\frac{1}{2\omega} - \frac{2i}{(2\pi)^{5/2}} \lim_{R\to\infty} \int_{r_2}^{R} dk^0 \, \frac{1}{(k^0)^2-\omega^2} \\ &= \frac{1}{(2\pi)^{3/2}}\frac{1}{2\omega} - \frac{2i}{(2\pi)^{5/2}} \lim_{R\to\infty} \frac{1}{2\omega} \left(\ln|k^0-\omega| - \ln|k^0+\omega| \right) \Big|_{r_2}^{R} \\ &= \frac{1}{(2\pi)^{3/2}}\frac{1}{2\omega} - \frac{i}{(2\pi)^{5/2}}\frac{1}{\omega} \ln\left(\frac{r_2+\omega}{r_2-\omega}\right) \end{aligned} \tag{5.11}$$

Here, we have defined $r_2 := \sqrt{|\mathbf{k}|^2+\Omega^2}$. For completeness, let us also evaluate the right hand side of (5.9) for $m > \Omega$. In this case, we may simply evaluate the first line of (5.11) using the Fundamental Theorem of Calculus:

$$\begin{aligned} G_F^c(t=s,k) &= \frac{i}{(2\pi)^{5/2}} \int_{-r_2}^{r_2} dk^0 \, \frac{1}{(k^0)^2-\omega^2} \\ &= \frac{i}{(2\pi)^{5/2}} \frac{1}{2\omega} \left(\ln|k^0-\omega| - \ln|k^0+\omega| \right) \Big|_{-r_2}^{r_2} \\ &= -\frac{i}{(2\pi)^{5/2}}\frac{1}{\omega} \ln\left(\frac{\omega+r_2}{\omega-r_2}\right) \end{aligned} \tag{5.12}$$

The second case, where $|\mathbf{k}| > \Omega$, is completely analogous. Again assuming that $m < \Omega$, we have

$$\begin{aligned} G_F^c(t=s,k) &= \frac{i}{(2\pi)^{5/2}} \left[\int_{-r_2}^{-r_1} dk^0 \, \frac{1}{(k^0)^2-\omega^2} + \int_{r_1}^{r_2} dk^0 \, \frac{1}{(k^0)^2-\omega^2} \right] \\ &= \frac{i}{(2\pi)^{5/2}} \left[\int_{-\infty}^{\infty} dk^0 \, \frac{1}{(k^0)^2-\omega^2} - \int_{-\infty}^{-r_2} dk^0 \, \frac{1}{(k^0)^2-\omega^2} \right. \\ &\qquad \left. - \int_{-r_1}^{r_1} dk^0 \, \frac{1}{(k^0)^2-\omega^2} - \int_{r_2}^{\infty} dk^0 \, \frac{1}{(k^0)^2-\omega^2} \right] \\ &= \frac{1}{(2\pi)^{3/2}}\frac{1}{2\omega} - \frac{i}{(2\pi)^{5/2}}\frac{1}{\omega} \left[\ln\left(\frac{r_2+\omega}{r_2-\omega}\right) - \ln\left(\frac{\omega+r_1}{\omega-r_1}\right) \right]. \end{aligned} \tag{5.13}$$

Here, we have defined $r_1 := \sqrt{|\mathbf{k}|^2-\Omega^2}$. For completeness, if $m > \Omega$, the second case reads

$$G_F^c(t=s,k) = -\frac{i}{(2\pi)^{5/2}}\frac{1}{\omega} \left[\ln\left(\frac{\omega+r_2}{\omega-r_2}\right) - \ln\left(\frac{\omega+r_1}{\omega-r_1}\right) \right]. \tag{5.14}$$

In summary, for a scalar field of mass $m < \Omega$ in flat spacetime, the equal time, spatial Fourier transform of its covariantly bandlimited Feynman propagator reads

$$G_F^c(t=s,k) = \begin{cases} \dfrac{1}{(2\pi)^{3/2}}\dfrac{1}{2\omega} - \dfrac{i}{(2\pi)^{5/2}}\dfrac{1}{\omega} \ln\left|\dfrac{r_2+\omega}{r_2-\omega}\right| & |\mathbf{k}| \leq \Omega \\ \dfrac{1}{(2\pi)^{3/2}}\dfrac{1}{2\omega} - \dfrac{i}{(2\pi)^{5/2}}\dfrac{1}{\omega} \left(\ln\left|\dfrac{r_2+\omega}{r_2-\omega}\right| - \ln\left|\dfrac{\omega+r_1}{\omega-r_1}\right| \right) & |\mathbf{k}| > \Omega \end{cases} \tag{5.15}$$

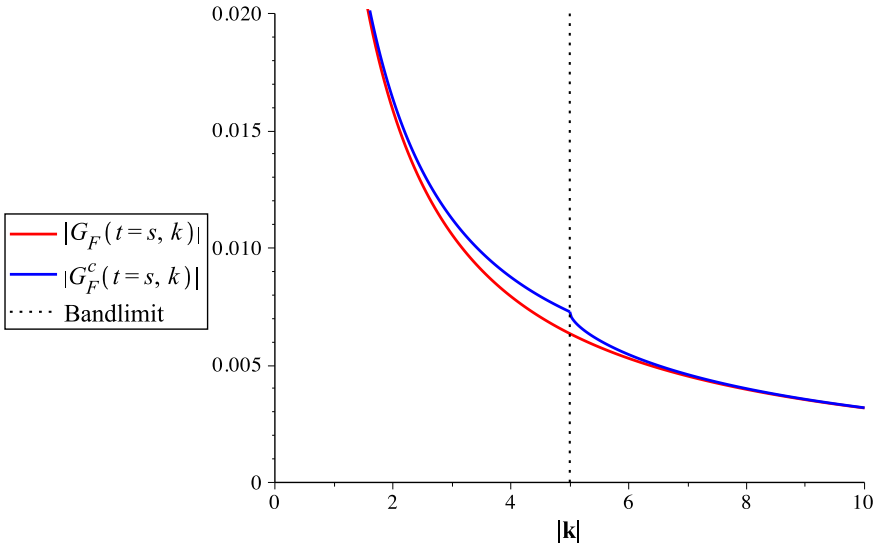

Figure 5.1: Equal-time Feynman propagator and covariantly bandlimited Feynman propagator for flat spacetime. Parameter values are $\Omega = 5$ and $m = 0.01\,\Omega$.

A plot of $G_F^c(t = s, k)$ as a function of the comoving wavenumber k is shown in figure 5.1.

From equation (5.15), we see that $G_F^c(t = s, k)$ differs from $G_F(t = s, k)$ by a purely imaginary term. Since $G_F(t = s, k)$ is itself purely real, the magnitude of $G_F^c(t = s, k)$ will always be larger than that of $G_F(t = s, k)$. This fact is indeed reflected in figure 5.1. Physically, this means that the fluctuations of a covariantly bandlimited scalar field are enhanced relative to the fluctuations in standard quantum theory. A possible interpretation of this phenomenon is that the removal of temporal modes due to the covariant cutoff eliminates destructive interference between the removed modes and the remaining modes.

Also notice that the cusp that appears in figure 5.1 is not unexpected. Indeed, referring to figure 4.1, we see that the cusp occurs at the value of $\mathbf{k}$ at which the horizontally-opening hyperbola which bounds the region $\left|(k^0)^2 - |\mathbf{k}|^2\right| \leq \Omega^2$ begins. The fact that the tangent to this hyperbola is vertical at $|\mathbf{k}| = \Omega$ implies that there will be a cusp in the graph of $G_F^c(t = s, k)$ at this point.

How do we quantify and interpret the strength of the effect of the covariant cutoff? To answer this question, let us consider the fluctuation spectrum and the relative difference between the cutoff and standard fluctuation spectra, $|\delta\phi_k^c - \delta\phi_k|/|\delta\phi_k|$. These quantities are plotted in figures 5.2 and 5.3 respectively.

Recall that the two length scales which are important for Planck scale effects in inflationary cosmology are the Hubble horizon during inflation, ℓ_H, and the Planck length, ℓ_P. During inflation, ℓ_P and ℓ_H are thought to have been separated by about five to six orders of magnitude. Referring to figure 5.3, for $|\mathbf{k}| \approx 10^{-5}\,\Omega$, or in other words for length scales five orders of magnitude away from the Planck scale, the difference between $\delta\phi_k^c$ and $\delta\phi_k$ is approximately $1 \times 10^{-9}\%$. Therefore, in the case of flat spacetime, one may estimate that experiments would need to be sensitive to better than one part in 10^{11} in order to be sensitive to the covariant cutoff. Unfortunately, such sensitivity is infeasible with the current generation of experiments. For flat spacetime, the result above seems to suggest that the strength of the covariant

cutoff's observational effect scales like σ^β with $\beta \approx 2$.

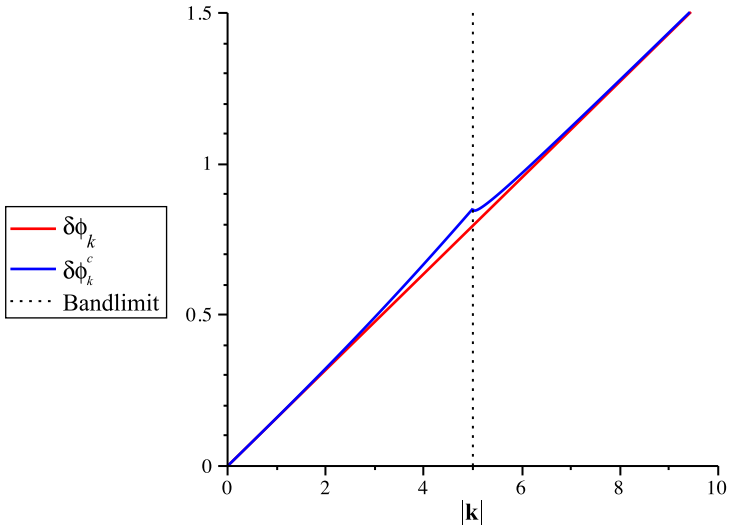

Figure 5.2: Equal time fluctuation spectrum and covariantly bandlimited fluctuation spectrum for flat spacetime. Parameter values are $\Omega = 5$ and $m = 0.01\,\Omega$.

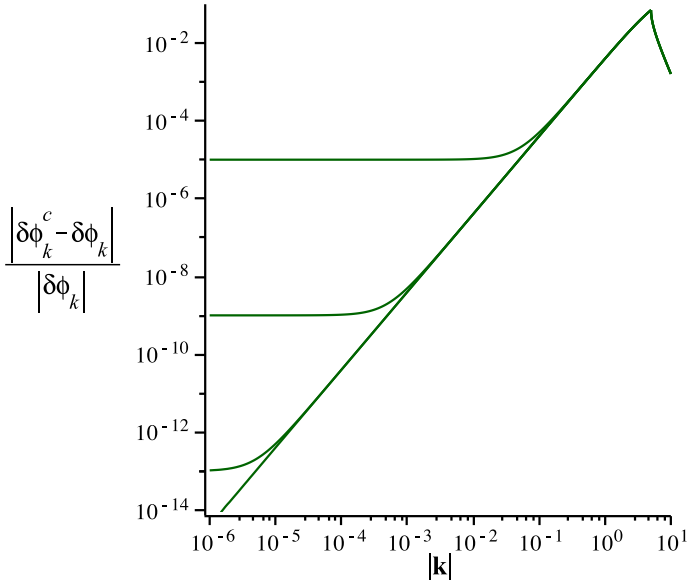

Figure 5.3: Relative difference between the usual and covariantly bandlimited fluctuation spectra for several field masses in flat spacetime. In descending order are the curves for $m = 1 \times 10^{-2}\,\Omega$, $m = 1 \times 10^{-4}\,\Omega$, $m = 1 \times 10^{-6}\,\Omega$, and $m = 0$.

5.2 Calculation of the Covariantly Bandlimited Feynman Propagator in FLRW Spacetimes

Let us now address the question of how to calculate the covariantly bandlimited Feynman propagator in a FLRW spacetime M. We will work in comoving coordinates $(t, \mathbf{x})$ so that the line element reads $ds^2 = -dt^2 + a^2(t)d\mathbf{x}^2$.

Recall that the covariant bandlimit is a cutoff on the spectrum of the d'Alembertian. Also recall that the spectrum of the d'Alembertian is, up to multiplicity, the same as the spectrum of each k-d'Alembertian. The covariant cutoff may therefore be imposed by cutting off the spectrum of each k-d'Alembertian, mode by mode. As such, here as well we will study the fixed spatial modes of the Feynman propagator, *i.e.*, $G_F(t, s, k)$.

Let $\hat{P}_{B_k(\Omega)}$ denote the projector which projects functions in $\mathcal{H}_k = L^2\left((t_i, t_f) : a^3(t)dt\right)$ onto the space of covariantly bandlimited functions $B_k(\Omega)$. Recalling the nomenclature from chapter 3.3, we see that we may write the integral kernels of the projectors as

$$P_{B_k(\Omega)}(t, s) := \int_\Lambda \phi_{\lambda,k}(t)\phi^*_{\lambda,k}(s)\, d\sigma(\lambda), \tag{5.16}$$

where $\Lambda := \{\lambda \,|\, \lambda \in \text{spec}(\hat{D}_k), \lambda + m^2 \in [-\Omega^2, \Omega^2]\}$, and with the appropriate weight $\sigma(\lambda)$. Again, $\{\phi_{\lambda,k}(t)\}_{\lambda\in\text{spec}(D_k)}$ is an orthonormal basis of eigenfunctions of the (self-adjoint) operator $\hat{D}_k$.

Given a full Feynman propagator $G_F(t, s, k)$, the covariantly bandlimited propagator is consequently

$$\begin{aligned} G^c_F(t, s, k) &= (\hat{P}_{B_k(\Omega)}\hat{G}_k\hat{P}_{B_k(\Omega)})(t, s) \\ &= \int_{t_i}^{t_f} a^3(\zeta)\, d\zeta \int_{t_i}^{t_f} a^3(\xi)\, d\xi\; P_{B_k(\Omega)}(t, \zeta)G_F(\zeta, \xi, k)P_{B_k(\Omega)}(\xi, s). \end{aligned} \tag{5.17}$$

Using the spectral expansion (3.40) for $G_F(t, s)$, we ultimately have that

$$\begin{aligned} G^c_F(t, s, k) = \frac{i}{(2\pi)^{3/2}} \int_\Lambda \frac{1}{\lambda}\, \phi_{\lambda,k}(t)\phi^*_{\lambda,k}(s)\, d\sigma(\lambda) + \frac{i}{(2\pi)^{3/2}} \Big[A_k Ph^{(1,1)}_{k,\Omega}(t, s) + B_k Ph^{(2,2)}_{k,\Omega}(t, s) \\ + C_k \left(Ph^{(1,2)}_{k,\Omega}(t, s) + Ph^{(2,1)}_{k,\Omega}(t, s) \right) \Big], \end{aligned} \tag{5.18}$$

where

$$Ph^{(i,j)}_{k,\Omega}(t, s) := \int_{t_i}^{t_f} a^3(\zeta)\, d\zeta \int_{t_i}^{t_f} a^3(\xi)\, d\xi\; P_{B_k(\Omega)}(t, \zeta)h^{(i)}_k(\zeta)h^{(j)}_k(\xi)P_{B_k(\Omega)}(\xi, s). \tag{5.19}$$

Since the mathematics are quite involved, let us illustrate the functional analytic machinery outlined above by applying it to a concrete example.

Example 5.2.1 *Flat Spacetime*

Let M be a flat spacetime. Our goal is to construct expressions for G_F and G^c_F using equations (3.40) and (5.18) respectively.

Consider again the flat k-d'Alembertians $\Box_k$ and the associated Klein-Gordon differential expressions $(\Box_k - m^2) = (-\partial_t^2 - \omega_k^2)$, where $\omega_k^2 = k^2 + m^2$. Consider a fixed spatial mode k. The largest domain in $\mathcal{H} = L^2(\mathbb{R})$ on which an operator associated with the differential expression $(\Box_k - m^2)$ may be defined is the set of functions that are mapped into L^2 functions by $\Box_k$. Define the domain of $\hat{D}_k : \mathrm{dom}(\hat{D}_k) \subset L^2(\mathbb{R}) \to L^2(\mathbb{R})$ as

$$\mathrm{dom}(\hat{D}_k) = \left\{ f \in L^2(\mathbb{R}) \ : \ \Box_k f \in L^2(\mathbb{R}) \right\}. \tag{5.20}$$

Naturally, the action of $\hat{D}_k$ on a function in its domain is to apply $(\Box_k - m^2)$ to that function.

It is straightforward to show that $\hat{D}_k$ is essentially self-adjoint, or in other words, that it has deficiency indices $(0, 0)$. One can see this by directly inspecting the eigenfunctions for the eigenvalues $-\omega_k^2 \pm i$, as we did in example 3.3.1. Referring to equation (3.42), we see that all of the solutions of the eigenvalue equation $(\Box_k - m^2)u = (-\omega_k^2 \pm i)u$ are not normalizable in $L^2(\mathbb{R})$. Therefore, there are no deficiency vectors and the dimension of both deficiency spaces is zero. The deficiency indices of $\hat{D}_k$ are thus $(0, 0)$.

The eigenfunctions of $(\Box_k - m^2)$ for an eigenvalue λ are

$$\phi_\lambda^{(\rho)}(t) := N_\lambda e^{\rho i \sqrt{\lambda + \omega_k^2} t}, \tag{5.21}$$

where $\rho \in \{+, -\}$ and where N_λ is a normalization constant. It is tedious but straightforward to show that the spectrum of $\hat{D}_k$ consists entirely of a doubly degenerate continuous spectrum on the semi-infinite line $[-\omega_k^2, \infty)$ [47, Chapter 4.1].

We obtain the same expression for $G_F(t, s, k)$ found before by setting $A_k = B_k = C_k = 0$ in equation (3.40). Alternatively, one could motivate this choice by taking the expression for $G_F(t, s, k)$ from equation (3.3) and using it to propagate any eigenfunction (normalized to unity or not) of $(\Box_k - m^2)$. This calculation is shown below:

$$\begin{aligned}
(G_F \phi_\lambda^{(\pm)})(t) &= \int_{-\infty}^{\infty} \frac{1}{(2\pi)^{3/2}} \frac{1}{2\omega_k} e^{-i\omega_k |t-s|} e^{\pm i\nu s} \, ds \qquad ; \qquad \nu := \sqrt{\lambda + \omega_k^2} \\
&= \frac{1}{(2\pi)^{3/2}} \frac{1}{2\omega_k} \left[\int_{-\infty}^{t} e^{-i\omega_k (t-s)} e^{\pm i\nu s} \, ds + \int_{t}^{\infty} e^{i\omega_k (t-s)} e^{\pm i\nu s} \, ds \right] \\
&= \frac{1}{(2\pi)^{3/2}} \frac{1}{2\omega_k} \left[e^{-i\omega_k t} \int_{-\infty}^{t} e^{i(\omega_k \pm \nu)s} \, ds + e^{i\omega_k t} \int_{t}^{\infty} e^{-i(\omega_k \mp \nu)s} \, ds \right]
\end{aligned}$$

To proceed, we introduce a Feynman regulator $\omega_k \to \omega_k - i\epsilon$ and take the limit as $\epsilon \to 0$.

$$\begin{aligned}
(G_F \phi_\lambda^{(\pm)})(t) &= \frac{1}{(2\pi)^{3/2}} \frac{1}{2\omega_k} \lim_{\epsilon \to 0} \left[e^{-i\omega_k t} \int_{-\infty}^{t} e^{i(\omega_k \pm \nu)s + \epsilon s}\, ds + e^{i\omega_k t} \int_{t}^{\infty} e^{-i(\omega_k \mp \nu)s - \epsilon s}\, ds \right] \\
&= \frac{1}{(2\pi)^{3/2}} \frac{1}{2\omega_k} \lim_{\epsilon \to 0} \left[e^{-i\omega_k t} \frac{e^{i(\omega_k \pm \nu)s + \epsilon s}}{i(\omega_k \pm \nu) + \epsilon} \bigg|_{-\infty}^{t} + e^{i\omega_k t} \frac{e^{-i(\omega_k \mp \nu)s - \epsilon s}}{-i(\omega_k \mp \nu) - \epsilon} \bigg|_{t}^{\infty} \right] \\
&= \frac{1}{(2\pi)^{3/2}} \frac{1}{2\omega_k} \left[\frac{e^{\pm i\nu t}}{i(\omega_k \pm \nu)} + \frac{e^{\pm i\nu t}}{i(\omega_k \mp \nu)} \right] \\
&= \frac{1}{(2\pi)^{3/2}} \frac{e^{\pm i\nu t}}{2i\omega_k} \left[\frac{\omega_k \mp \nu + \omega_k \pm \nu}{\omega_k^2 - \nu^2} \right] \\
&= \frac{i}{(2\pi)^{3/2}} \frac{1}{\lambda} e^{\pm i\sqrt{\lambda + \omega_k^2}\, t}
\end{aligned} \tag{5.22}$$

The calculation shows that the eigenfunctions $\phi_\lambda^{(\rho)}$ do not pick up contributions from the homogeneous solutions of $(\Box_k - m^2)u = 0$ under the action of G_F.

The last remaining task is to determine the weight $\sigma(\lambda)$ and the normalization N_λ. Since $\hat{D}_k$ has only continuous spectrum, let us set $d\sigma(\lambda) = d\lambda$ and absorb any λ dependence of the weight into N_λ. To determine the form of N_λ, we appeal to orthornomality and demand that

$$\int_{-\infty}^{\infty} [\phi_\lambda^{(\rho)}(t)]^* \phi_{\lambda'}^{(\rho')}(t)\, dt = \delta(\lambda - \lambda')\delta_{\rho\rho'}\,. \tag{5.23}$$

The inner product of two eigenfunctions reads

$$\begin{aligned}
\int_{-\infty}^{\infty} [\phi_\lambda^{(\rho)}(t)]^* \phi_{\lambda'}^{(\rho')}(t)\, dt &= N_\lambda^* N_{\lambda'} \int_{-\infty}^{\infty} e^{-i(\rho\sqrt{\lambda+\omega_k^2} - \rho'\sqrt{\lambda'+\omega_k^2})t}\, dt \\
&= N_\lambda^* N_{\lambda'}\, 2\pi\, \delta\left(\rho\sqrt{\lambda + \omega_k^2} - \rho'\sqrt{\lambda' + \omega_k^2} \right).
\end{aligned}$$

We immediately see that the line above is zero if $\rho \neq \rho'$. Therefore,

$$\int_{-\infty}^{\infty} [\phi_\lambda^{(\rho)}(t)]^* \phi_{\lambda'}^{(\rho')}(t)\, dt = N_\lambda^* N_{\lambda'} 2\pi\, \delta_{\rho\rho'}\, \delta\left(\sqrt{\lambda + \omega_k^2} - \sqrt{\lambda' + \omega_k^2} \right). \tag{5.24}$$

Next, we use the fact (see, *e.g.*, [48, Appendix C]) that

$$\delta(f(x)) = \sum_{x_\star\,:\, f(x_\star)=0} \frac{\delta(x - x_\star)}{|f'(x_\star)|} \tag{5.25}$$

to simplify the Dirac delta function appearing in equation (5.24). With $f(\lambda) = \sqrt{\lambda + \omega_k^2} - \sqrt{\lambda' + \omega_k^2}$, the only zero of f is $\lambda = \lambda'$. So, we have that

$$\begin{aligned}
\int_{-\infty}^{\infty} [\phi_\lambda^{(\rho)}(t)]^* \phi_{\lambda'}^{(\rho')}(t)\, dt &= N_\lambda^* N_{\lambda'} 2\pi \cdot 2\sqrt{\lambda'^2 + \omega_k^2}\, \delta(\lambda - \lambda')\, \delta_{\rho\rho'} \\
&= N_\lambda^* N_{\lambda'} 4\pi (\lambda^2 + \omega_k^2)^{1/4} (\lambda'^2 + \omega_k^2)^{1/4}\, \delta(\lambda - \lambda')\, \delta_{\rho\rho'}\,.
\end{aligned} \tag{5.26}$$

Note that we may freely interchange λ and μ in the last line since that expression is a distribution containing the Dirac delta $\delta(\lambda - \mu)$. Therefore, it must be that

$$N_\lambda = \frac{1}{\sqrt{4\pi}(\lambda + \omega_k^2)^{1/4}}, \tag{5.27}$$

up to an arbitrary complex phase. Let us choose N_λ to be real.

We may now write down the following expression for $G_F(t, s, k)$:

$$G_F(t, s, k) = \frac{i}{(2\pi)^{3/2}} \sum_{\rho=\pm} \int_{-\omega_k^2}^{\infty} \frac{1}{\lambda + i\epsilon} \frac{1}{4\pi} \frac{1}{\sqrt{\lambda + \omega_k^2}} e^{\rho i \sqrt{\lambda+\omega_k^2}(t-s)} \, d\lambda \tag{5.28}$$

The only additional piece of information that we had to introduce was how to treat the pole at $\lambda = 0$. For this, we follow the Feynman prescription. Likewise, $G_F^c(t = s, k)$ is given by

$$G_F^c(t = s, k) = \frac{i}{(2\pi)^{3/2}} \sum_{\rho=\pm} \int_{\alpha}^{\beta} \frac{1}{\lambda + i\epsilon} \frac{1}{4\pi} \frac{1}{\sqrt{\lambda + \omega_k^2}} \, d\lambda, \tag{5.29}$$

where $\alpha = \max\{k^2 - m^2, -\Omega^2 - m^2\}$ and $\beta = \Omega^2 + m^2$.

If we change the integration variable from λ to $k^0 := \sqrt{\lambda + \omega_k^2}$ in equation (5.28), we obtain the following:

$$\begin{aligned} G_F(t, s, k) &= \frac{i}{(2\pi)^{3/2}} \sum_{\rho=\pm} \int_0^{\infty} \frac{1}{(k^0)^2 - \omega_k^2 + i\epsilon} \frac{1}{4\pi k^0} e^{\rho i k^0 (t-s)} \, 2k^0 \, dk^0 \\ &= \frac{i}{(2\pi)^{5/2}} \int_{-\infty}^{\infty} \frac{1}{(k^0)^2 - \omega_k^2 + i\epsilon} e^{-ik^0(t-s)} \, dk^0 \, . \end{aligned} \tag{5.30}$$

This is the expression for $G_F(t, s, k)$ that was obtained earlier from the path integral formalism. Naturally, the same change of variables would give the expression for $G_F^c(t, s, k)$ that was obtained in section 5.1. ▷

5.3 Application to Power-Law Spacetimes

We now apply our formalism to FLRW spacetime with a power-law scale factor.

5.3.1 Formulation of the Problem

Consider a FLRW spacetime that is characterized by the following scale factor and range of the proper time coordinate t:

$$a(t) = ct^\alpha \, ; \qquad c > 0, \qquad \alpha \gg 1, \qquad t \in [0, \infty) \tag{5.31}$$

We will consider a massless scalar field $\hat{\phi}$ on this spacetime. In this case, the Klein-Gordon differential expression is just the d'Alembertian. As was noted in example 2.4.4, the mode functions $v_k(t)$ that one

determines via the Bunch-Davies criterion are given by[1]

$$v_k(t) = \frac{1}{a(t)}\sqrt{\frac{\pi\eta(t)}{2}}H_n^{(1)}(k\eta(t)), \tag{5.32}$$

where the conformal time $\eta(t)$ and the constant n are given by

$$\eta(t) = \frac{1}{c(\alpha-1)t^{\alpha-1}}, \qquad \text{and} \qquad n = \frac{3\alpha-1}{2(\alpha-1)}. \tag{5.33}$$

Therefore, the full Feynman propagator for a fixed mode k as given by equation (3.2) reads

$$G_F(t,s,k) = \frac{1}{(2\pi)^{3/2}}\frac{1}{2c^2(ts)^\alpha}\frac{\pi}{2}\sqrt{\eta(t)\eta(s)}\Big[\theta(t-s)H_n^{(2)}(k\eta(t))H_n^{(1)}(k\eta(s)) \\ +\theta(s-t)H_n^{(1)}(k\eta(t))H_n^{(2)}(k\eta(s))\Big] \tag{5.34}$$

The task of computing the covariantly bandlimited propagator essentially consists of two steps. First, we must diagonalize the d'Alembertian (find its orthonormal eigenfunctions). Second, we must write down the projectors $\hat{P}_{B_k(\Omega)}$ so that we may compute $G_F^c(t,s,k) = (\hat{P}_{B_k(\Omega)}\hat{G}_k\hat{P}_{B_k(\Omega)})(t,s)$.

The task of diagonalizing the d'Alembertian is quite nontrivial for two reasons. First, the eigenfunctions of the d'Alembertian are not known in closed form; they may only be computed numerically. Second, the minimal operator defined through the action of $\Box_k$ is only symmetric and not self-adjoint. Therefore, we must choose a self-adjoint extension of each k-d'Alembertian. It is not immediately clear how to correctly (in a physical sense) make this choice.

In comoving coordinates, the eigenvalue equation $\Box_k u(t) = \lambda u(t)$ reads

$$-\frac{1}{a^3(t)}\left(\frac{d}{dt}\left(a^3(t)\frac{du}{dt}\right) + k^2 a(t)u(t)\right) = \lambda u(t)$$

$$\Rightarrow \quad \ddot{u}(t) + \frac{3\alpha}{t}\dot{u}(t) + \left(\frac{k^2}{c^2}\frac{1}{t^{2\alpha}} + \lambda\right)u(t) = 0. \tag{5.35}$$

The Hilbert space of functions that we consider is $L^2([0,\infty),\, a^3(t)\,dt)$. In order to simplify the mathematics, let us introduce a unitary transformation which will rid us of the integration weight $a^3(t)$. Let

$$\begin{array}{rccc} \hat{U}\ : & L^2([0,\infty),\, a^3(t)\,dt) & \longrightarrow & L^2[0,\infty) \\ & f(t) & \longmapsto & a^{3/2}(t)f(t) \end{array}. \tag{5.36}$$

[1]Notice that we do not simply define the mode functions $v_k(t)$ as $v_k(\eta(t))$, but rather as $v_k(t) := v_k^*(\eta(t))$. This is because the conformal time η runs opposite to t, so that $\theta(\eta(t)-\eta(s)) = \theta(s-t)$. Writing

$$G_F(\eta,\eta',k) = \frac{1}{(2\pi)^{3/2}}\frac{1}{2}\left[\theta(\eta-\eta')v_k^*(\eta)v_k(\eta') + \theta(\eta'-\eta)v_k(\eta)v_k^*(\eta')\right],$$

with this definition one has that $G_F(\eta(t),\eta(s),k) = G_F(t,s,k)$, where $G_F(t,s,k)$ is evaluated according to equation (3.2). Also note that with this definition, $v_k(t)$ possesses the correct early-time asymptotic behaviour, *i.e.*, $v_k(t) \sim k^{-1/2}\exp(ikt)$ as t tends to 0.

The action of $\hat{U}^*$ is $(\hat{U}^* g)(t) = a^{-3/2}(t) g(t)$. With this unitary transformation, we define a new differential expression

$$H_k = U \Box_k U^* = -\frac{d^2}{dt^2} + \left(\frac{3\alpha}{2} \left(\frac{3\alpha}{2} - 1 \right) \frac{1}{t^2} - \frac{k^2}{c^2} \frac{1}{t^{2\alpha}} \right). \tag{5.37}$$

We will study the differential operators that H_k generates. The eigenvalue problem (5.35) becomes $H_k w(t) = \lambda w(t)$ and reads

$$\ddot{w}(t) + \left(\frac{k^2}{c^2} \frac{1}{t^{2\alpha}} - \frac{3\alpha}{2} \left(\frac{3\alpha}{2} - 1 \right) \frac{1}{t^2} + \lambda \right) w(t) = 0, \tag{5.38}$$

where $w(t) := (\hat{U} u)(t) = a^{3/2}(t) u(t)$.

As was noted, closed-form solutions of equations (5.35) and (5.38) are not known for general $\lambda \in \mathbb{C}$. As far as this author knows, a closed-form solution is only known for the case of $\lambda = 0$, which corresponds to the mode functions of the quantum field theory. In other words, the mode functions for a massive scalar field in a power-law FLRW spacetime are unknown. Furthermore, Frobenius series solutions about the endpoints $t = 0$ and $t = \infty$ are impossible, as these points are irregular singular points of the ODE (see for example [49, Chapter 6.3] or [50, Chapter 1.4]). It was found that it is possible to construct divergent series solutions for arbitrary λ when $\alpha \in \mathbb{Q}^+$; however, these solutions are not of much computational use for the task at hand. An overview of this techinique is given in appendix A.

We now turn to constructing operators from the differential expression (5.37) so that we may proceed with diagonalization. In what follows, H_k will denote the differential expression (5.37), while symbols with a circumflex $\hat{}$ will denote operators. The action of all the operators that we will consider will be to apply the differential expression H_k to functions in their domains. The operators will only differ by their domains.

Following the theory of [33], as we did in chapter 2.5.2, let us define the maximal operator $\hat{H}_k$ and the minimal operator $\hat{H}_k^0$ as follows:

$$\mathrm{dom}(\hat{H}_k) = \left\{ f \in L^2[0,\infty) \,:\, f, \partial_t f \in AC[0,\infty),\, H_k f \in L^2[0,\infty) \right\} \tag{5.39}$$

$$\mathrm{dom}(\hat{H}_k^0) = \left\{ f \in \mathrm{dom}(\hat{H}_k) \,:\, [f,g]_0 = [f,g]_\infty = 0 \quad \forall\, g \in \mathrm{dom}(\hat{H}_k) \right\} \tag{5.40}$$

$\hat{H}_k^0$ is a symmetric operator, and we can demonstrate that it has deficiency indices $(1,1)$. Therefore, $\hat{H}_k^0$ has a one-parameter family of self-adjoint extensions. It is necessary to choose a particular self-adjoint extension in order to construct an orthonormal basis of eigenfunctions for $L^2[0,\infty)$. Let us prove that the deficiency indices of $\hat{H}_k^0$ are $(1,1)$. The following proof strategy is initially due to Martin [51], and we formalize it here.

To prove that $\hat{H}_k^0$ has deficiency indices $(1,1)$, we will show that the endpoint $t = 0$ is LCC and that the endpoint $t = \infty$ is LPC. It is actually easier to show that $\Box_k$ is LCC at $t = 0$, so first we establish that an endpoint's nature is preserved under the unitary map $\hat{U}$.

Proposition 5.3.1 *Consider the Sturm-Liouville differential expression* $\tau f(t) = \frac{1}{r(t)} \left[-(pf')'(t) + q(t) f(t) \right]$ *with the basic assumptions 2.5.8, and define* $\omega := U \tau U^*$, *where*

$$\begin{aligned} \hat{U} \,:\quad L^2((a,b),\, r(t)\,dt) &\longrightarrow L^2(a,b) \\ f(t) &\longmapsto r^{1/2}(t) f(t) \end{aligned}$$

Then ω is LPC at a (resp. b) if and only if τ is LPC at a (resp. b), and ω is LCC at a (resp. b) if and only if τ is LCC at a (resp. b).

Proof: Suppose τ is LPC at a. Then for each $z \in \mathbb{C}$, there exists a function ϕ_z for which $(\tau - z)\phi_z = 0$ but for which $\int_a^c |\phi_z(t)|^2 r(t)\, dt$ diverges for some $c \in (a, b)$. Define $\psi_z(t) := (\hat{U}\phi_z)(t) = r^{1/2}(t)\phi_z(t)$. Then it follows that $\int_a^c |\psi_z(t)|^2\, dt$ diverges and that $(\omega - z)\psi_z = (U\tau U^* - z)U\phi_z = U(\tau - z)\phi_z = 0$. Therefore, by Weyl's Alternative, ω is LPC at a. Conversely, suppose ω is LPC at a. Then, for each $z \in \mathbb{C}$, there exists a function ψ_z for which $(\omega - z)\psi_z = 0$ but for which $\int_a^c |\psi_z(t)|^2\, dt$ diverges for some $c \in (a, b)$. Defining $\phi_z(t) := (\hat{U}^*\psi_z)(t) = r^{-1/2}(t)\psi_z(t)$, one repeats the same argument to conclude that τ is LPC at a.

Next, suppose τ is LCC at a. For each $z \in \mathbb{C}$, let $u_z^{(1)}$ and $u_z^{(2)}$ be two linearly independent solutions of $(\tau - z)u = 0$. Then, $\int_a^c |\phi_z(t)|^2 r(t)\, dt < \infty$ for all $\phi_z := C_1 u_z^{(1)} + C_2 u_z^{(2)}$, $C_1, C_2 \in \mathbb{C}$ and for all $c \in (a, b)$. Define $\psi_z(t) := (\hat{U}\phi_z)(t) = C_1 r^{1/2}(t)u_z^{(1)}(t) + C_2 r^{1/2}(t)u_z^{(2)}(t) \equiv C_1 w_z^{(1)}(t) + C_2 w_z^{(2)}(t)$. Since $r > 0$ almost everywhere by assumption, $w_z^{(1)}$ and $w_z^{(2)}$ are linearly independent, and both are solutions of $(\omega - z)w = 0$. It also follows that $\int_a^c |\psi_z(t)|^2\, dt < \infty$ for all $C_1, C_2 \in \mathbb{C}$ and for all $c \in (a, b)$. Therefore, by Weyl's Alternative, ω is LCC at a. We omit the proof of the converse, as it is completely analogous to what was done in the LPC case.

The proof for the endpoint b is the same as the proof for the endpoint a, except that the integrals run from c to b instead of from a to c. □

Next, let us show that $\Box_k$ is LCC at $t = 0$. To do this, we use [52, Corollary 8], which states that a Sturm-Liouville expression $\tau f(t) = \frac{1}{r(t)}\left[-(pf')'(t) + q(t)f(t)\right]$ on (a, b) with the basic assumptions 2.5.8 is LCC at a if

$$\int_a^d |pq|^{1/4} \left|(p(pq)^{-1/4})'\right| dt < \infty \tag{5.41}$$

and

$$\int_a^d r|pq|^{-1/2} dt < \infty \tag{5.42}$$

for all $d \in (a, b)$. For $\Box_k$, we have that $p(t) = a^3(t)$, $q(t) = -k^2 a(t)$, $w(t) = a^3(t)$, and $(a, b) = (0, \infty)$. So, (5.41) reads

$$\begin{aligned}
\int_0^d |-k^2a^4|^{1/4} \left|(a^3(-k^2a^4)^{-1/4})'\right| dt &= \int_0^d |a| \left|(a^2)'\right| dt \\
&= 2\int_0^d a^2\dot{a}\, dt \\
&= 2\int_0^d c^2 t^{2\alpha} c\alpha t^{\alpha-1}\, dt \\
&= \frac{2c^3}{3} d^{3\alpha} < \infty\,,
\end{aligned} \tag{5.43}$$

and (5.42) reads

$$\int_0^d a^3 \left|-k^2 a^4\right|^{-1/2}\, dt = \frac{1}{k}\int_0^d a\, dt$$
$$= \frac{c}{k}\frac{d^{\alpha+1}}{\alpha+1} < \infty\,. \tag{5.44}$$

Therefore, $\Box_k$ is LCC at 0 for $k > 0$. By the previous proposition, so is H_k.

Now we show that H_k is LPC at ∞. We use [33, Theorem 3.3b], which states that a differential expression $\tau f(t) = -f''(t) + Q(t)f(t)$ on (a,∞) with the basic assumptions 2.5.8 is LPC at ∞ if there exists a $C \geq 0$ such that $Q(t) \geq -C|t|^2$ as $t \to \infty$. For H_k we have that

$$Q(t) = \left(\frac{3\alpha}{2}\left(\frac{3\alpha}{2} - 1\right)\frac{1}{t^2} - \frac{k^2}{c^2}\frac{1}{t^{2\alpha}}\right) \geq 0 \;\text{ as }\; t \to \infty, \tag{5.45}$$

so we may choose $C = 0$ to conclude that H_k is LPC at ∞.

Unfortunately, the boundary point $t = 0$ is an irregular singular point of the ODE $H_k w = \lambda w$. As such, boundary conditions written in terms of Lagrange brackets at $t = 0$ are quite complicated. Consequentially, one obtains an unwieldy parametrization of the self-adjoint extensions of $\hat{H}_k^0$ according to Proposition 2.5.14. We will later employ a different method to obtain the correct self-adjoint extension of $\hat{H}_k^0$.

To summarize, for a power-law FLRW spacetime (5.31), at this stage we have the exact mode functions $v_k(t)$ as fixed by the Bunch-Davies criterion, the full Feynman propagator $G_F(t,s,k)$ given by equation (5.34), and a symmetric operator $\hat{H}_k^0 = \hat{U}\hat{\Box}_k^0\hat{U}^*$ with deficiency indicies $(1,1)$. To proceed with implementing the covariant bandlimit, we must choose a particular self-adjoint extension $\hat{H}_k'$ of $\hat{H}_k^0$ via physical criteria, and numerically solve for the self-adjoint extension's eigenfunctions $\psi_{\lambda,k}$. This lets us construct the projectors which project onto the space of covariantly bandlimited functions.

5.3.2 A Note on Computing Propagators

To simplify computations, we elect to work with the differential expression H_k and the operators that it generates. We are ultimately concerned with imposing the covariant bandlimit on $G_F(t,s,k)$, however. We must be careful when we relate propagators calculated under the unitary transformation $\hat{U}$ to the physical case, as these relationships are surprisingly delicate.

The right-hand side of equation (3.25) is (a constant times a representation of) the identity in $\mathcal{H}_k = L^2([0,\infty); a^3(t)dt)$. However, the right-hand side of equation (3.25) does not remain proportional to the identity under $\hat{U}$. Defining $K_F(t,s,k) := U(t)G_F(t,s,k)U^*(s)$, we have for $m = 0$ that

$$U\Box_k U^* U G_F U^* = \frac{i}{(2\pi)^{3/2}} U\,\mathbb{1}\,U^*$$
$$\Rightarrow \qquad H_k K_F(t,s,k) = \frac{i}{(2\pi)^{3/2}}\frac{\delta(t-s)}{a^{3/2}(t)a^{3/2}(s)}. \tag{5.46}$$

The right-hand side of this last equation is *not* a representation of the identity operator in $L^2[0,\infty)$, so $K_F(t,s,k)$ is *not* a proper Green's Function of H_k. We cannot directly write it as a spectral integral.

As such, consider the following. First, note that because of the Dirac delta in the right-hand side of equation (3.25), we may freely interchange t and s, *i.e.*,

$$\frac{\delta(t-s)}{a^3(t)} = \frac{\delta(t-s)}{a^3(s)}.$$

Next, rearrange equation (3.25) as follows:

$$\Box_k(t)\left(G_F(t,s,k)a^3(s)\right) = \frac{i}{(2\pi)^{3/2}}\delta(t-s). \tag{5.47}$$

The notation $\Box_k(t)$ is to explicitly indicate that $\Box_k$ is a differential expression in the variable t. The right-hand side of this last equation *is* mapped to a representation of the identity operator in $L^2[0,\infty)$ under the unitary $\hat{U}$. Defining $\mathcal{G}_F(t,s,k) := G_F(t,s,k)a^3(s)$ and $\mathcal{K}_F(t,s,k) := U(t)\mathcal{G}_F(t,s,k)U^*(s)$, under the unitary transformation, we correctly obtain

$$H_k\mathcal{K}_F(t,s,k) = \frac{i}{(2\pi)^{3/2}}\delta(t-s). \tag{5.48}$$

So, if $\{\psi_{\lambda,k}(t)\}$ is a complete orthonormal set of eigenfunctions of H_k, we may write

$$\begin{aligned}\mathcal{K}_F(t,s,k) &= \frac{i}{(2\pi)^{3/2}}\int \frac{1}{\lambda}\psi_{\lambda,k}(t)\psi^*_{\lambda,k}(s)\,d\lambda \\ &\quad + \frac{i}{(2\pi)^{3/2}}\left[A_k g_k^{(1)}(t)g_k^{(1)}(s) + B_k g_k^{(2)}(t)g_k^{(2)}(s) + C_k\left(g_k^{(1)}(t)g_k^{(2)}(s) + g_k^{(2)}(t)g_k^{(1)}(s)\right)\right].\end{aligned} \tag{5.49}$$

Any functional dependence of the integration measure on λ is absorbed into the eigenfunction normalization, and the homogeneous solutions $g_k^{(1)}$ and $g_k^{(2)}$ solve $H_k u = 0$. Therefore,

$$\begin{aligned}\mathcal{G}_F(t,s,k) &= U^*(t)\mathcal{K}_F(t,s,k)U(s) \\ &= \frac{i}{(2\pi)^{3/2}}\int \frac{1}{\lambda}a^{-3/2}(t)\psi_{\lambda,k}(t)\psi^*_{\lambda,k}(s)a^{3/2}(s)\,d\lambda \;+\; \text{homog. terms.}\end{aligned} \tag{5.50}$$

Note that if $\{\psi_{\lambda,k}(t)\}$ are eigenfunctions of H_k, then $\{\phi_{\lambda,k}(t) := a^{-3/2}(t)\psi_{\lambda,k}(t)\}$ are eigenfunctions of $\Box_k$. It follows that

$$\mathcal{G}_F(t,s,k) = \frac{i}{(2\pi)^{3/2}}\int \frac{1}{\lambda}\phi_{\lambda,k}(t)\phi^*_{\lambda,k}(s)a^3(s)\,d\lambda \;+\; \text{homog. terms.} \tag{5.51}$$

This is consistent with the spectral form of the propagator $G_F(t,s,k)$:

$$G_F(t,s,k) = \frac{i}{(2\pi)^{3/2}}\int \frac{1}{\lambda}\phi_{\lambda,k}(t)\phi^*_{\lambda,k}(s)\,d\lambda \;+\; \text{homog. terms} \tag{5.52}$$

We also see that $G_F(t,s,k)$ is indeed a propagator, whilst $\mathcal{G}_F(t,s,k)$ is not *per se*:

$$\begin{aligned}(G_F f)(t) &= \int_0^\infty G_F(t,s,k)f(s)a^3(s)\,ds \\ &= \frac{i}{(2\pi)^{3/2}}\int_0^\infty\int \frac{1}{\lambda}\phi_{\lambda,k}(t)\phi^*_{\lambda,k}(s)a^3(s)f(s)\,d\lambda ds \;+\; \text{homog. terms} \\ &= \int_0^\infty \mathcal{G}_F(t,s,k)f(s)\,ds\end{aligned}$$

Note that we could have elected to rearrange the right-hand side of equation (5.46) instead and defined $\mathcal{K}_F(t,s,k) := K_F(t,s,k)a^3(s)$. This would have led to the same result. From equation (5.50), we have that $G_F(t,s,k)a^3(s) = U^*(t)\mathcal{K}_F(t,s,k)U(s)$, so in terms of $\mathcal{K}_F$, G_F is given by

$$G_F(t,s,k) = a^{-3/2}(t)\,\mathcal{K}_F(t,s,k)\,a^{-3/2}(s). \tag{5.53}$$

At this point, we may also use the general parametrization of self-adjoint extensions given in Proposition 2.5.14 to show that it may not be that $A_k = B_k = C_k = 0$ in equation (5.49) for the case of power-law FLRW spacetime. Let us briefly recall this parametrization. Since H_k is LCC at $t = 0$ and LPC at $t = \infty$, we may parametrize the self-adjoint extensions of $\hat{H}_k^0$ by writing $\mathrm{dom}((\hat{H}_k)_{g_\mu}) := \left\{ f \in \mathrm{dom}(\hat{H}_k) \;:\; [f, g_\mu]_0 = 0 \right\}$. We obtain different self-adjoint extensions by taking different real-valued solutions g_μ of $(H_k - \mu)w = 0$ and different $\mu \in \mathbb{R}$.

Now, suppose that we are given the integral kernel $\mathcal{K}_F(t,s,k)$ of some propagator for a particular self-adjoint extension $(\hat{H}_k)_{g_\mu}$. Suppose, however, that we do not know which self-adjoint extension this is, *i.e.*, we do not know to which g_μ the self-adjoint extension corresponds. Let us also make the assumption (which will prove to be faulty) that $A_k = B_k = C_k = 0$. Then, we can use $\mathcal{K}_F$ to determine the boundary condition that g_μ must obey.

We do so as follows. First, note that we may write $-i(2\pi)^{3/2}\mathcal{K}_F(t,s,k) = \int \lambda^{-1}\psi_{\lambda,k}(t)\psi^*_{\lambda,k}(s)\,d\lambda$ and $-i(2\pi)^{3/2}\partial_s\mathcal{K}_F(t,s,k) = \int \lambda^{-1}\psi_{\lambda,k}(t)\psi^{*\prime}_{\lambda,k}(s)\,d\lambda$. It follows that

$$\begin{aligned} -i(2\pi)^{3/2} &\lim_{s\to 0^+} \left[\mathcal{K}_F(t,s,k)g'_\mu(s) - (\partial_s\mathcal{K}_F(t,s,k))g_\mu(s)\right] \\ &= \lim_{s\to 0^+} \int \frac{1}{\lambda}\psi_{\lambda,k}(t)\left[\psi^*_{\lambda,k}(s)g'_\mu(s) - \psi^{*\prime}_{\lambda,k}(s)g_\mu(s)\right]\,d\lambda \\ &= 0 \end{aligned} \tag{5.54}$$

Therefore, if $A_k = B_k = C_k = 0$, the constraint (5.54) fixes the condition that g_μ must obey at $t = 0$.

Example 5.3.2 *Half real line*

As an illustration, consider the differential expression $\tau = -\partial_t^2 - k^2$ for $t \in [0,\infty)$ which we studied in example 3.3.1. Recall that its self-adjoint realizations $\hat{A}_\theta$, with $\theta \in \mathbb{R}$, are characterized by the boundary condition $f \in \mathrm{dom}(\hat{A}_\theta) \Leftrightarrow f'(0)/f(0) = \theta$. Alternatively, we may define $g^\sigma_\mu(t) := \cos(\sqrt{\mu + k^2}t) + \sigma\sin(\sqrt{\mu + k^2}t)$ for $\mu \in [-k^2,\infty)$ and $\sigma \in \{+1,-1\}$ to parametrize the self-adjoint realizations of τ according to Proposition 2.5.14. Observe that the Lagrange bracket $[f, g^\sigma_\mu]_0 = 0$ gives

$$\begin{aligned} [f, g^\sigma_\mu]_0 = f^*(0)\cdot\sigma\sqrt{\mu + k^2} - f^{*\prime}(0)\cdot 1 = 0 \\ \Rightarrow \quad \frac{f'(0)}{f(0)} = \sigma\sqrt{\mu + k^2}. \end{aligned}$$

The right-hand side of the last line may be any real number, so we see that we recover the usual parametrization of τ's self-adjoint realizations.

Now, suppose that we were given a propagator

$$-i(2\pi)^{3/2}\mathcal{K}_F(t,s) = \frac{1}{2ik}e^{-ik|t-s|} + \frac{1}{2ik}e^{-ik(t+s)} + \frac{\theta}{k(k-i\theta)}e^{-ik(t+s)}, \tag{5.55}$$

and that we did not know to which g_μ^σ it corresponded. Inserting this propagator and the g_μ^σ defined above into the constraint (5.54), one finds after some algebra that the constraint reads $\sigma\sqrt{\mu+k^2}=\theta$. Therefore, we have $\sigma=\text{sign}(\theta)$ and $\mu=\theta^2-k^2$. ▷

Consider now the ODE $(H_k-\mu)w=0$. Since we ultimately just need to compute a limit as $t\to 0$, let us seek approximate solutions which are valid for t close to 0. For t close to zero, the ODE approximately reads $\ddot{w}(t)+(k^2/c^2)t^{-2\alpha}w(t)=0$. The general solution is $w(t)=C_1\sqrt{t}J_q(k\eta(t))+C_2\sqrt{t}Y_q(k\eta(t))$, $C_1,C_2\in\mathbb{C}$, where $q=(2(\alpha-1))^{-1}$. Without loss of generality, choose $g_\mu(t)\equiv g(t)=\sqrt{t}J_q(k\eta(t))+b\sqrt{t}Y_q(k\eta(t))$ with $b\in\mathbb{R}$. In fact, we may further approximate $g(t)$ by using the Bessel function asymptotics (2.89). For small t, we have that

$$g(t)\sim\sqrt{\frac{2c(\alpha-1)}{\pi k}}t^{\alpha/2}\left[\cos\left(k\eta(t)-q\frac{\pi}{2}-\frac{\pi}{4}\right)+b\sin\left(k\eta(t)-q\frac{\pi}{2}-\frac{\pi}{4}\right)\right] \tag{5.56}$$

and

$$g'(t)\sim\sqrt{\frac{2c(\alpha-1)}{\pi k}}\frac{k}{c}t^{-\alpha/2}\left[\sin\left(k\eta(t)-q\frac{\pi}{2}-\frac{\pi}{4}\right)-b\cos\left(k\eta(t)-q\frac{\pi}{2}-\frac{\pi}{4}\right)\right]. \tag{5.57}$$

Letting $\omega_q(t):=k\eta(t)-q\frac{\pi}{2}-\frac{\pi}{4}$, the boundary condition $[f,g_\mu]_0=0$ for $f\in\text{dom}(\hat{H}_k)_{g_\mu}$ thus reads

$$0=\lim_{t\to 0}\left\{f^*(t)\frac{k}{c}t^{-\alpha/2}[\sin\omega_q(t)-b\cos\omega_q(t)]-[f'(t)]^*t^{\alpha/2}[\cos\omega_q(t)+b\sin\omega_q(t)]\right\}, \tag{5.58}$$

with different choices of self-adjoint extension corresponding to different choices of $b\in\mathbb{R}$.

From equation (5.34) and the relation $\mathcal{K}_F(t,s,k)=a^{3/2}(t)\,G_F(t,s,k)a^{3/2}(s)$, we have that

$$\begin{aligned}\mathcal{K}_F(t,s,k)=\frac{1}{\sqrt{2\pi}}\frac{1}{8(\alpha-1)}\sqrt{ts}\Big[&\theta(t-s)H_n^{(2)}(k\eta(t))H_n^{(1)}(k\eta(s))\\&+\theta(s-t)H_n^{(1)}(k\eta(t))H_n^{(2)}(k\eta(s))\Big].\end{aligned} \tag{5.59}$$

In theory, then, enforcing the constraint (5.54) should give us information about the value of b which corresponds to this physical propagator. The insertion of these $\mathcal{K}_F$ and $g(t)$ into the constraint (5.54) is a lengthy and generally unenlightening calculation which we relegate to appendix B. We ultimately arrive at the condition

$$0=\lim_{s\to 0}e^{i\omega_n(s)}\frac{k}{c}\left[(1-ib)\sin\omega_q(s)-(i+b)\cos\omega_q(s)\right]. \tag{5.60}$$

This condition implies that $b=-i$; however, this contradicts the requirement that $b\in\mathbb{R}$. Therefore, we conclude that we cannot have $A_k=B_k=C_k=0$ in the case that we are studying.

5.3.3 Late-Time Approximation

One way of overcoming the problem that the eigenfunctions $\psi_{\lambda,k}$ of H_k are not known exactly is to consider an approximation for H_k valid for late times, for which the eigenfunctions are exactly known. By studying the problem at some late time, one may study field modes whose crossing times occurred well before this late time and whose fluctuations are frozen in scale. After all, it is the field modes which cross the horizon during inflation that are cosmologically important.

Consider the mode function equation $H_k w_k = 0$, *i.e.* equation (5.38) with $\lambda = 0$. We define the crossing time as that time for which the potential is zero, *i.e.*,

$$t_{cross} := \left(\frac{2k}{c\sqrt{3\alpha(3\alpha - 2)}} \right)^{1/(\alpha-1)} . \tag{5.61}$$

Note that for $t > t_{cross}$, the $t^{-2\alpha}$ term decays extremely quickly. As such, let us consider the late-time approximation

$$H_k \;\rightarrow\; \tilde{H} := -\frac{d^2}{dt^2} + \frac{3\alpha}{2}\left(\frac{3\alpha}{2} - 1\right)\frac{1}{t^2}. \tag{5.62}$$

This approximation is valid for any given mode provided that one studies the mode's dynamics at some late time t_0 that is well after the mode's crossing time. Our program will thus be to choose a sufficiently late t_0 so that we may study the impact of the covariant cutoff on the fluctuation spectrum $\delta\phi_k(t_0)$ for modes with comoving wavenumbers k that are both smaller than and larger than the cutoff Ω.

An objection that one might raise at this point is that the approximate differential expression (5.62) is now independent of k. Therefore, any correction made to the Feynman propagator due to the covariant cutoff in this approximation will just be a constant correction that is independent of k. We may argue, however, that even a constant correction is interesting, as it indicates the order of magnitude at which the covariant cutoff operates.

In the late-time approximation, the eigenvalue problem $\tilde{H}w = \lambda w$ reads

$$\ddot{w}(t) + \left(\lambda - \left(\nu^2 - \tfrac{1}{4}\right) t^{-2}\right) w(t) = 0, \tag{5.63}$$

where $\nu = \frac{1}{2}(3\alpha - 1)$. This is the Liouville form of the Bessel differential equation, and it has the general solution

$$w(t) = \begin{cases} C_1\sqrt{t}\, J_\nu(\sqrt{\lambda}t) + C_2\sqrt{t}\, Y_\nu(\sqrt{\lambda}t) & \lambda \neq 0 \\ C_1 t^{\frac{1}{2}+\nu} + C_2 t^{\frac{1}{2}-\nu} & \lambda = 0 \end{cases} . \tag{5.64}$$

For $\nu > 1$, the minimal operator generated by $\tilde{H}$ has deficiency indices (0,0), has no eigenvalues (point spectrum), and has a continuous spectrum $[0, \infty)$ [47]. Additionally, one can show that a complete orthonormal set of eigenfunctions is $\{\tilde{\psi}_\lambda(t)\}_{\lambda\in[0,\infty)}$ [53, Part I, Chapter 4.11], where

$$\tilde{\psi}_\lambda(t) = \sqrt{\frac{t}{2}} J_\nu(\sqrt{\lambda}t). \tag{5.65}$$

Therefore, we may expand $\tilde{\mathcal{K}}_F(t,s) := i/(2\pi)^{3/2}\tilde{H}^{-1}(t,s)$ as

$$\begin{aligned} \tilde{\mathcal{K}}_F(t,s) = {} & \frac{i}{(2\pi)^{3/2}} \int_0^\infty \frac{1}{\lambda} \tilde{\psi}_\lambda(t)\tilde{\psi}_\lambda(s)\, d\lambda \\ & + \frac{i}{(2\pi)^{3/2}} \left[A f_0^+(t) f_0^+(s) + B f_0^-(t) f_0^-(s) + C\left(f_0^+(t) f_0^-(s) + f_0^-(t) f_0^+(s) \right) \right], \end{aligned} \tag{5.66}$$

where $f_0^\pm(t) = t^{\frac{1}{2}\pm\nu}$ are homogeneous solutions. Using the results of [54, Section 6.574], we may evaluate

the integral in the previous line:

$$\begin{aligned}\int_0^\infty \frac{1}{\lambda}\tilde{\psi}_\lambda(t)\tilde{\psi}_\lambda(s)\,d\lambda &= \frac{(ts)^{\frac{1}{2}}}{2}\int_0^\infty \frac{1}{\lambda}J_\nu(\sqrt{\lambda}t)J_\nu(\sqrt{\lambda}s)\,d\lambda \\ &= (ts)^{\frac{1}{2}}\int_0^\infty \frac{1}{\mu}J_\nu(\mu t)J_\nu(\mu s)\,d\mu \qquad \text{where } \mu := \sqrt{\lambda} \\ &= (ts)^{\frac{1}{2}}\frac{1}{2\nu}\left[\theta(t-s)\left(\frac{s}{t}\right)^\nu + \theta(s-t)\left(\frac{t}{s}\right)^\nu\right] \end{aligned} \tag{5.67}$$

Therefore,

$$\begin{aligned}\tilde{\mathcal{K}}_F(t,s) = \frac{i}{(2\pi)^{3/2}}\Bigg\{&\frac{1}{2\nu}(ts)^{\frac{1}{2}}\left[\theta(t-s)\left(\frac{s}{t}\right)^\nu + \theta(s-t)\left(\frac{t}{s}\right)^\nu\right] \\ &+A(ts)^{\frac{1}{2}+\nu} + B(ts)^{\frac{1}{2}-\nu} + C(ts)^{\frac{1}{2}}\left[\left(\frac{s}{t}\right)^\nu + \left(\frac{t}{s}\right)^\nu\right]\Bigg\}. \end{aligned} \tag{5.68}$$

We may fix the constants A, B, and C by comparing equation (5.68) to the exact propagator $\mathcal{K}_F(t,s,k)$ approximated for large t and s using the Bessel function asymptotics (2.94). Referring to equation (5.59), for large t and s (and hence small $\eta(t)$ and $\eta(s)$), it is straightforward to show that

$$\begin{aligned}\mathcal{K}_F(t,s,k) \approx \frac{i}{(2\pi)^{3/2}}\frac{1}{4(\alpha-1)}(ts)^{\frac{1}{2}}\Bigg\{&\theta(t-s)\frac{1}{n}\left[\left(\frac{s}{t}\right)^\nu - \left(\frac{t}{s}\right)^\nu\right] + \theta(s-t)\frac{1}{n}\left[\left(\frac{t}{s}\right)^\nu - \left(\frac{s}{t}\right)^\nu\right] \\ &+\frac{i\Gamma^2(n)}{\pi}X^{2n}(ts)^\nu + \frac{i\pi}{n^2\Gamma^2(n)}\frac{1}{X^{2n}}(ts)^{-\nu}\Bigg\}, \end{aligned} \tag{5.69}$$

where $X := 2c(\alpha-1)/k$. Upon comparing equations (5.68) and (5.69), we find that

$$A = \frac{i\Gamma^2(n)X^{2n}}{4\pi(\alpha-1)}, \qquad B = \frac{i\pi}{4(\alpha-1)n^2\Gamma^2(n)X^{2n}}, \qquad \text{and} \qquad C = -\frac{1}{4\nu}. \tag{5.70}$$

The projector onto the space of covariantly bandlimited functions for a cutoff Ω is given by

$$\begin{aligned}P_\Omega(t,s) &= \int_0^{\Omega^2}\tilde{\psi}_\lambda(t)\tilde{\psi}_\lambda(s)\,d\lambda \\ &= (ts)^{\frac{1}{2}}\frac{\Omega}{t^2-s^2}\left[sJ_\nu(\Omega t)J_{\nu-1}(\Omega s) - tJ_\nu(\Omega s)J_{\nu-1}(\Omega t)\right]. \end{aligned} \tag{5.71}$$

Formally, we may write

$$\begin{aligned}\tilde{\mathcal{K}}_F^c(t,s) &= (P_\Omega\tilde{\mathcal{K}}_F P_\Omega)(t,s) \\ &= \frac{i}{(2\pi)^{3/2}}\Bigg\{\int_0^{\Omega^2}\frac{1}{\lambda}\tilde{\psi}_\lambda(t)\tilde{\psi}_\lambda(s)\,d\lambda + A(P_\Omega f_0^+)(t)(P_\Omega f_0^+)(s) \\ &\quad + B(P_\Omega f_0^-)(t)(P_\Omega f_0^-)(s) + C\left((P_\Omega f_0^+)(t)(P_\Omega f_0^-)(s) + (P_\Omega f_0^-)(t)(P_\Omega f_0^+)(s)\right)\Bigg\}. \end{aligned} \tag{5.72}$$

Note that $f_0^+(t)$ is proportional to the zero eigenfunction $\tilde{\psi}_0(t)$. One cannot simply take equation (5.65) and evaluate it for $\lambda = 0$. Rather, taking the limit as $\lambda \to 0$, one finds that

$$\tilde{\psi}_\lambda(t) \sim \sqrt{\frac{t}{2}} \frac{1}{\Gamma(\nu+1)} \left(\frac{\sqrt{\lambda}t}{2}\right)^\nu \sim t^{\frac{1}{2}+\nu}.$$

Therefore, we conclude that $(P_\Omega f_0^+)(t) = f_0^+(t)$. $(P_\Omega f_0^-)(t)$ is given by

$$(P_\Omega f_0^-)(t) = \Omega t^{1/2} \int_0^\infty \frac{s^{1-\nu}}{t^2 - s^2} \left[s J_\nu(\Omega t) J_{\nu-1}(\Omega s) - t J_\nu(\Omega s) J_{\nu-1}(\Omega t) \right] ds. \tag{5.73}$$

This integral cannot be evaluated exactly, but it can be evaluated numerically since it is a convergent integral. (In particular, note that the integrand is well defined and finite in the limits $s \to 0$, $s \to \infty$, and $s \to t$.) Finally, the spectral integral in equation (5.72) cannot be evaluated exactly for arbitrary t and s; however, when $t = s$ (which is the case of interest for us), one has that

$$\begin{aligned} \int_0^{\Omega^2} \frac{1}{\lambda} [\tilde{\psi}_\lambda(t)]^2 \, d\lambda &= t \int_0^\Omega \frac{1}{\mu} [J_\nu(\mu t)]^2 \, d\mu \\ &= \frac{t}{2\nu} \frac{1}{\Gamma^2(\nu+1)} \left(\frac{\Omega t}{2}\right)^{2\nu} {}_2F_3(\nu, \nu+\tfrac{1}{2}; \nu+1, \nu+1, 1+2\nu; -\Omega^2 t^2). \end{aligned} \tag{5.74}$$

${}_2F_3$ is a generalized hypergeometric function that is well-defined for all $z = -\Omega^2 t^2 \in \mathbb{C}$.

With all of the parts in place, we may now study the effect of the covariant cutoff on the Feynman propagator. Consider first figure 5.4a, which shows a plot of the magnitudes of the exact propagator $|\mathcal{K}_F(t = s, k_0)|$, the approximate propagator $|\tilde{\mathcal{K}}_F(t = s, k_0)|$, and the covariantly bandlimited approximate propagator $|\tilde{\mathcal{K}}_F^c(t = s, k_0)|$ as functions of the proper time t for a fixed comoving mode $k_0 = 5$. While not particularly interesting in and of itself, it does illustrate that the late-time approximation is a good approximation for sufficiently late times. In this plot, we have used the parameter values $c = 1$, $\alpha = 10$, and $\Omega = 5$. For completeness, the corresponding plots of the equal time, fixed k_0 physical Feynman propagators $|G_F|$, $|\tilde{G}_F|$, and $|\tilde{G}_F^c|$ are shown in figure 5.4b. The fluctuation spectrum $\delta\phi_{k_0}(t)$, approximate fluctuation spectrum $\delta\tilde{\phi}_{k_0}(t)$, and covariantly bandlimited approximate fluctuation spectrum $\delta\tilde{\phi}^c_{k_0}(t)$ are shown in figure 5.5a. The relative difference between $\delta\tilde{\phi}_{k_0}(t)$ and $\delta\tilde{\phi}^c_{k_0}(t)$ is shown in figure 5.5b.

What we really aim to study is the k-dependence of the covariant cutoff. As such, we would like the late-time approximation to be good for at least some $k > \Omega = 5$. Suppose we wish to study the covariant cutoff for modes up to $k = 10$. Recall that the late time t_0 must be larger than the crossing time, and that the crossing time is an increasing function of k (*cf.* equation (5.61)). Therefore, if we choose t_0 such that the late-time approximation is good for $k = 10$, then this t_0 will also produce a good approximation for the smaller comoving modes $k < 10$.

To this end, consider figure 5.6, which shows the relative difference between $\mathcal{K}_F(t = s, k_0)$ and $\tilde{\mathcal{K}}_F(t = s, k_0)$ for $k_0 = 10$. We find that $|\mathcal{K}_F - \tilde{\mathcal{K}}_F|/|\mathcal{K}_F| \approx 0.01$ for $t = 1.3$, so let us take the late time to be $t_0 = 1.3$. For comparison, the crossing time when $k = 10$ is $t_{cross} = 0.9596$.

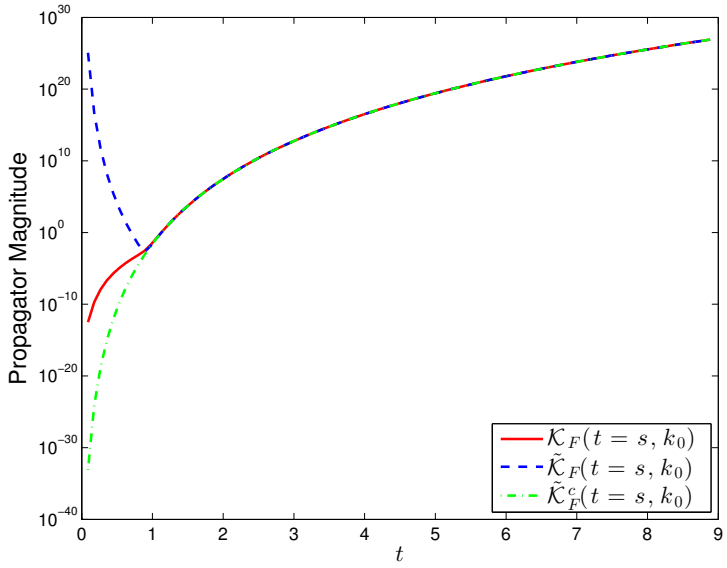

(a) $\mathcal{K}_F$ plots

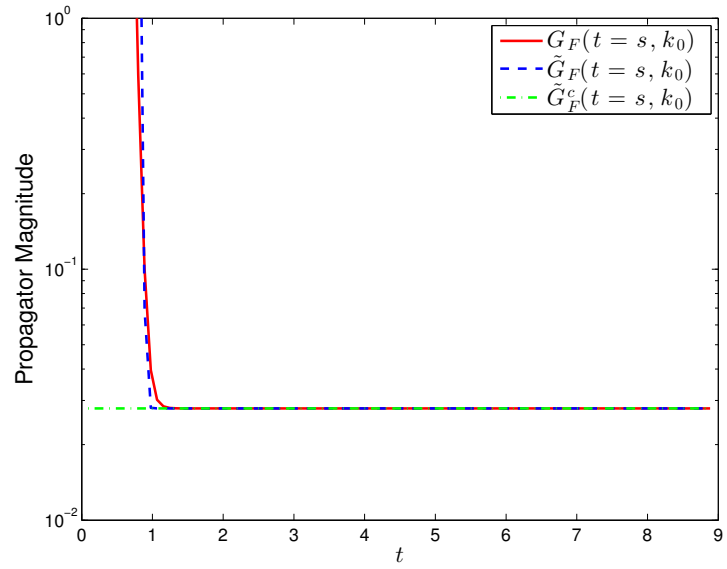

(b) G_F plots

Figure 5.4: Equal-time $\mathcal{K}_F$ and G_F for a fixed mode $k_0 = 5$. Other parameter values are $c = 1$, $\alpha = 10$, and $\Omega = 5$.

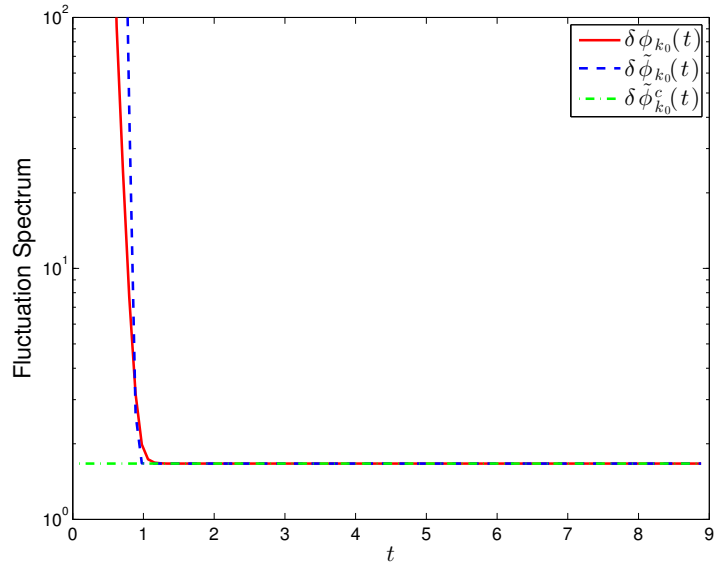

(a) Fluctuation spectum plots

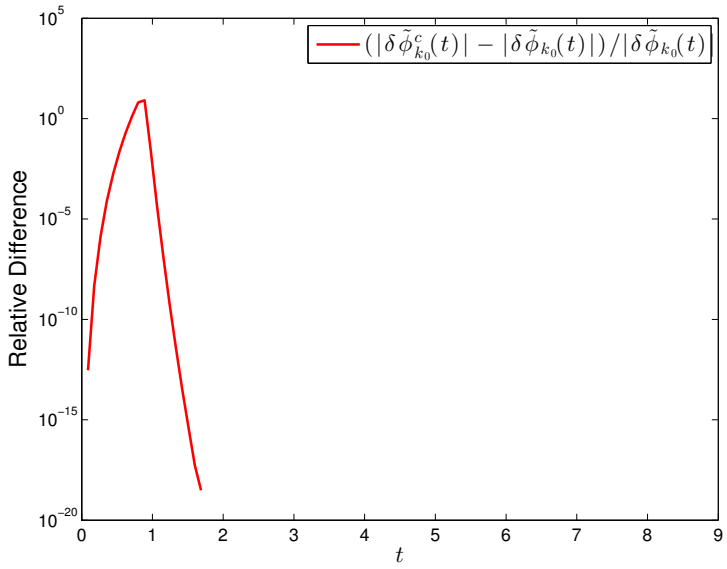

(b) Relative difference between full and cutoff fluctuation spectra

Figure 5.5: Equal-time fluctuation spectra for a fixed mode $k_0 = 5$. Other parameter values are $c = 1$, $\alpha = 10$, and $\Omega = 5$.

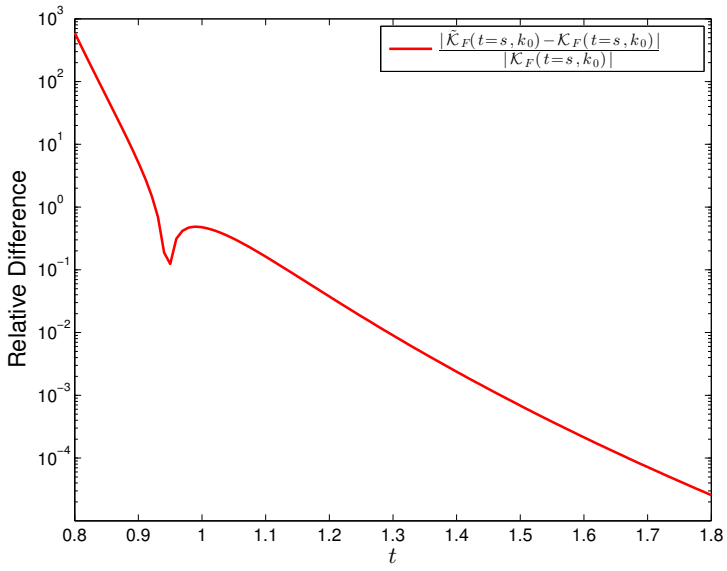

Figure 5.6: Relative difference between $\mathcal{K}_F(t=s,k_0)$ and $\tilde{\mathcal{K}}_F(t=s,k_0)$ for a fixed comoving mode $k_0 = 10$. Other parameter values are $c = 1$, and $\alpha = 10$.

Figure 5.8a shows a plot of the magnitudes of the exact propagator $|\mathcal{K}_F(t_0 = s_0, k)|$, the approximate propagator $|\tilde{\mathcal{K}}_F(t_0 = s_0, k)|$, and the covariantly bandlimited approximate propagator $|\tilde{\mathcal{K}}^c_F(t_0 = s_0, k)|$ as functions of the comoving wavenumber k evaluated at the late time $t_0 = s_0 = 1.3$. Figure 5.8b shows the corresponding plot for the physical propagators $|G_F|$, $|\tilde{G}_F|$, and $|\tilde{G}^c_F|$. Figure 5.9a shows the corresponding plot for the fluctuation spectra $\delta\phi_k(t_0)$, $\delta\tilde{\phi}_k(t_0)$, and $\delta\tilde{\phi}^c_k(t_0)$.

For reference, figure 5.7 shows the plots of the fluctuation spectra extended out as far as $k = 100$. While this is well beyond the range of validity of the late time approximation (recall that the approximation is good up to about $k \approx 10$), this plot helps us situate ourselves within the fluctuation spectrum shown in figure 2.7b.

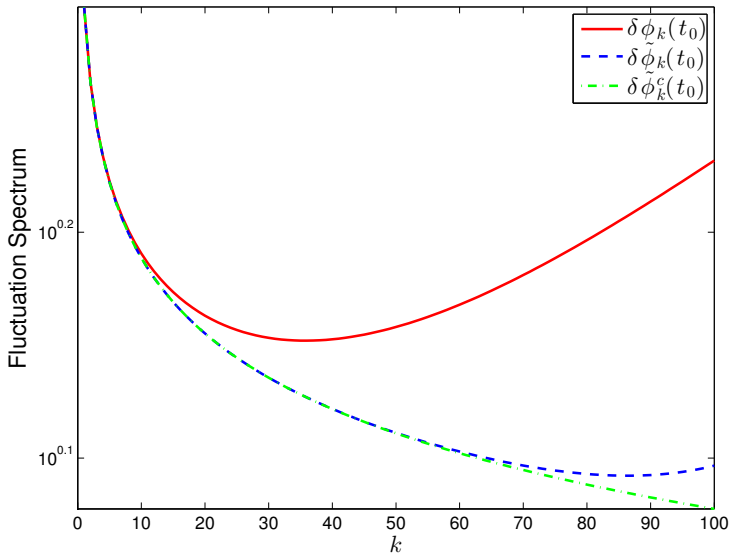

Figure 5.7: Late-time extended k-dependence of the fluctuation spectrum, evaluated at $t_0 = 1.3$. Other parameter values are $c = 1$, $\alpha = 10$, and $\Omega = 5$. Note that the late time approximations (blue and green curves) are really no longer valid beyond $k \approx 10$.

The conclusion that one draws from looking at these plots is that the effect of the covariant bandlimit on the fluctuations of the inflation field are minute. Figure 5.9b, which shows the relative differences $|\delta\tilde{\phi}^c_k(t_0) - \delta\phi_k(t_0)|/|\delta\phi_k(t_0)|$ and $|\delta\tilde{\phi}^c_k(t_0) - \delta\tilde{\phi}_k(t_0)|/|\delta\tilde{\phi}_k(t_0)|$ further support this conclusion. While the relative difference between the exact fluctuation spectrum and the covariantly bandlimited approximate fluctuation spectrum is somewhat larger than the relative difference between the approximate fluctuation spectrum and the covariantly bandlimited approximate fluctuation spectrum, the latter is likely a better estimate of the strength of the bandlimit's effect. This is because the larger effect in the first case is likely due to the error that the late-time approximation introduces.

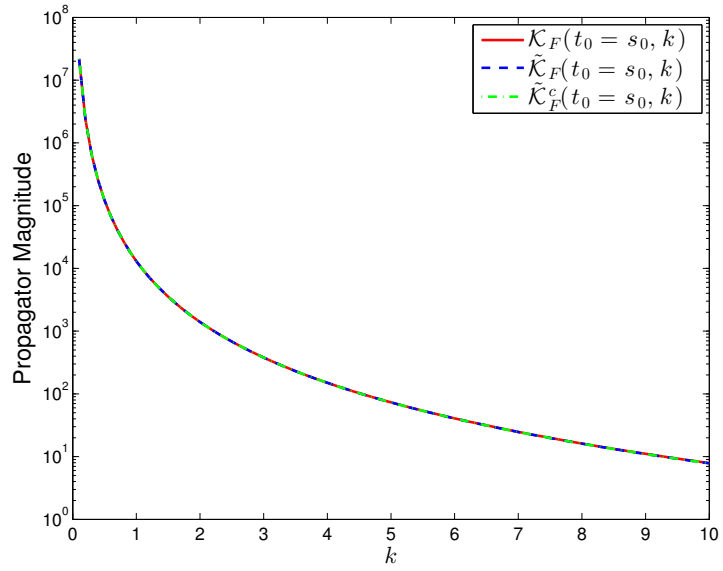

(a) $\mathcal{K}_F$ plots

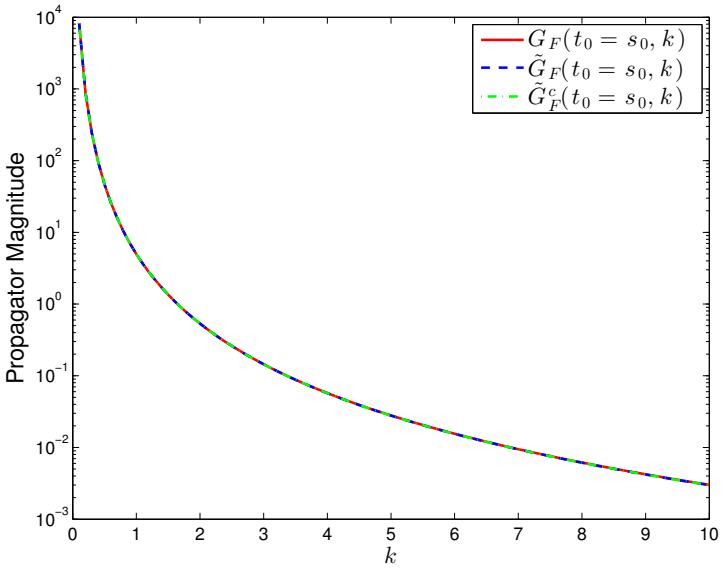

(b) G_F plots

Figure 5.8: Late-time k-dependence of $\mathcal{K}_F$ and G_F, evaluated at $t_0 = 1.3$. Other parameter values are $c = 1$, $\alpha = 10$, and $\Omega = 5$.

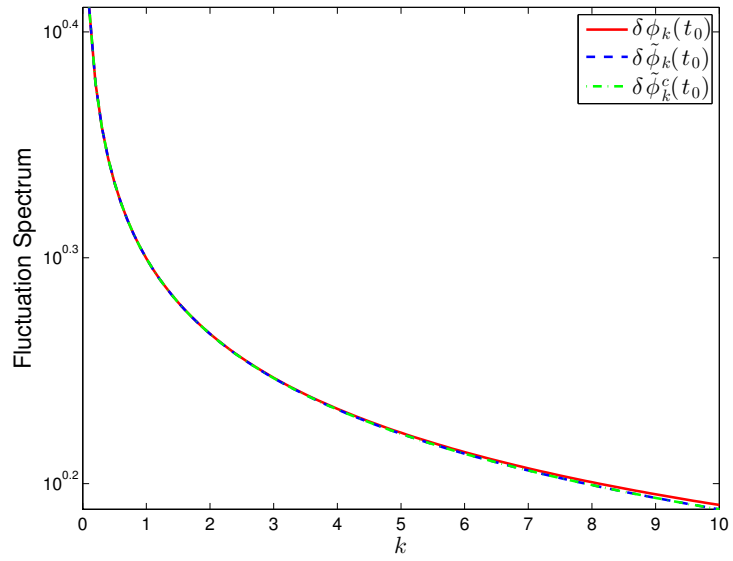

(a) Fluctuation spectum plots

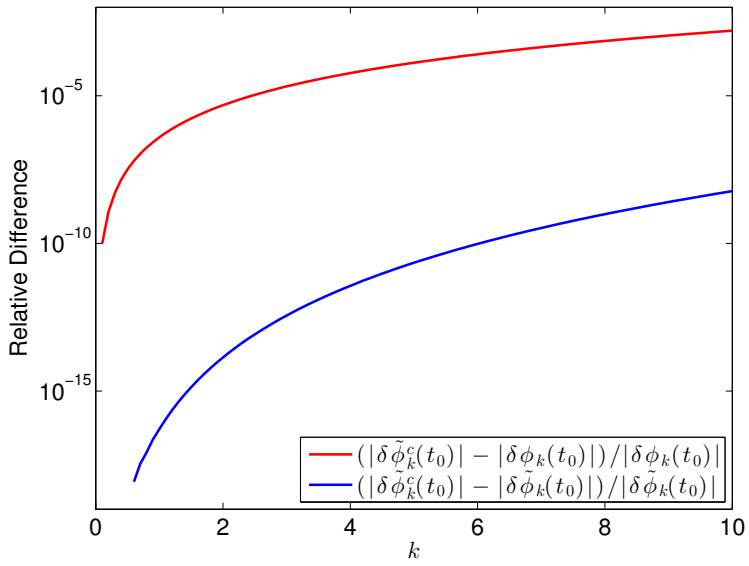

(b) Relative difference between full and cutoff fluctuation spectra

Figure 5.9: Late-time k-dependence of the fluctuation spectrum, evaluated at $t_0 = 1.3$. Other parameter values are $c = 1$, $\alpha = 10$, and $\Omega = 5$.

5.3.4 Numerical Implementation of the Cutoff: Overview

Instead of making a late-time analytic approximation, one could instead opt to construct a numerical implementation of the full problem. One reason for doing this has already been mentioned. In the late-time approximation, there is no k-dependence in the correction to the Feynman propagator that the covariant cutoff introduces. Additionally, the fact that the minimal operator $\hat{H}_k^0$ loses its deficiency indices and becomes essentially self-adjoint in the late-time approximation may be a cause for some concern.

The fact that the minimal operator generated by the d'Alembertian has deficiency indices $(1,1)$ roughly means that one boundary condition is necessary to specify a self-adjoint operator. In the case of the power-law spacetime that we are studying, this condition occurs at the boundary $t = 0$. The fact that the late-time approximation produces a problem with deficiency indices $(0,0)$ means that any boundary information at $t = 0$ is in a sense lost. Rather, one can no longer even *consider* imposing a boundary condition; the boundary behaviour is fixed by the problem. It is not surprising, however, that a late-time approximation of the problem would be insensitive to features from the start time of the problem.

The first order of business is to numerically construct the solutions of $H_k w = \lambda w$. Consider again the eigenfunction equation (5.38). In section 5.3.1, we deduced that for early times, any solution behaves asymptotically as

$$\psi_{\lambda,k}(t) \sim C_1\sqrt{t}J_q(k\eta(t)) + C_2\sqrt{t}Y_q(k\eta(t)), \qquad q := \frac{1}{2(\alpha-1)}, \tag{5.75}$$

for some $C_1, C_2 \in \mathbb{C}$. All solutions of $H_k w = \lambda w$ therefore vanish at $t = 0$ but oscillate infinitely quickly as they approach $t = 0$. For very late times, the eigenfunction equation approximately reads $\ddot{w}(t)+\lambda w(t) = 0$. This provides a convenient way of characterizing two linearly independent solutions of the full eigenfunction equation. Let us label these two solutions as follows:

$$\begin{aligned} \psi^c_{\lambda,k}(t) \ &: \ (H_k - \lambda)\psi^c_{\lambda,k}(t) = 0, \qquad \psi^c_{\lambda,k}(t) \sim \cos(\sqrt{\lambda}t) \text{ as } t \to \infty \\ \psi^s_{\lambda,k}(t) \ &: \ (H_k - \lambda)\psi^s_{\lambda,k}(t) = 0, \qquad \psi^s_{\lambda,k}(t) \sim \sin(\sqrt{\lambda}t) \text{ as } t \to \infty \end{aligned} \tag{5.76}$$

A plot of such a pair of solutions is shown in figure 5.10.

For the purpose of numerics, the problem quite naturally splits into three timescales. There is an early regime for $0 < t < t_1$, during which early-time approximations are valid. There is also a late regime for $t > t_2$, during which late-time approximations are valid. Finally, there is an intermediate regime for $t_1 < t < t_2$, during which full numerical solutions are necessary. The details of how the times t_1 and t_2 are chosen, as well as how they are used in the numerical estimation of $\psi^c_{\lambda,k}(t)$ and $\psi^s_{\lambda,k}(t)$, are discussed in section 5.3.5.

Next, we must choose the correct self-adjoint extension $\hat{H}'_k$ of $\hat{H}^0_k$ that corresponds to the physical choice of vacuum given by the Bunch-Davies criterion. In other words, we must determine which linear combination of $\psi^c_{\lambda,k}(t)$ and $\psi^s_{\lambda,k}(t)$ produces the correct eigenfunctions such that the expression for $\mathcal{K}_F(t,s,k)$ from equation (5.49) gives the propagator that is calculated in equation (5.59) according to the Bunch-Davies criterion. Since H_k is a second order differential operator, the solution space of $(H_k - \lambda)w = 0$ for any fixed λ is of course two-dimensional. The considerations of the previous section, as well as the late-time asymptotics (5.76) indicate that the spectrum of any self-adjoint extension $\hat{H}'_k$ consists entirely of a non-degenerate continuous spectrum $(0,\infty)$. (Recall that all self-adjoint extensions of a symmetric operator with

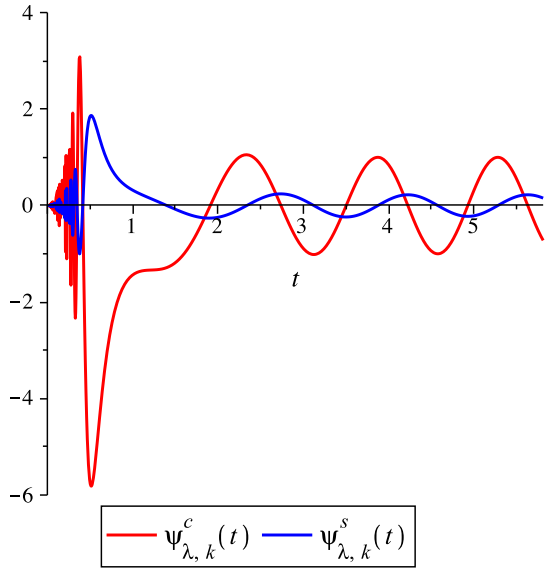

Figure 5.10: Eigenfunctions of H_k. Parameter values are $\lambda = 20$, $k = 1$, $c = 1$, and $\alpha = 4$. For this eigenfunction, we have that $t_1 \doteq 0.18$ and $t_2 \doteq 3.87$. In particular, notice that the numerical solutions are well into their sinusoidal regimes at t_2, which is when the late-time approximation begins. Also notice that both eigenfunctions oscillate infinitely quickly whilst decaying to zero as $t \to 0$.

equal deficiency indices have the same continuous spectrum [32, Theorem 1, Chapter VII.83].) Therefore, there is only one eigenfunction, which is a specific linear combination of $\psi^c_{\lambda,k}(t)$ and $\psi^s_{\lambda,k}(t)$, for any given $\lambda \in (0,\infty)$.[2] This linear combination depends on the choice of self-adjoint extension.

A prescription for numerically determining the correct eigenfunction is as follows. Define a test eigenfunction for fixed λ and k:

$$\Psi_{\lambda,k}(t) := \psi^c_{\lambda,k}(t) + b_{\lambda,k}\psi^s_{\lambda,k}(t). \tag{5.77}$$

By letting $b_{\lambda,k}$ run over $\mathbb{C}$, we cover the whole solution space of $(H_k - \lambda)w = 0$ (with the understanding that $b_{\lambda,k} \to \infty \;\Rightarrow \Psi_{\lambda,k}(t) = \psi^s_{\lambda,k}(t)$). If $\Psi_{\lambda,k}(t)$ is the correct (unnormalized) eigenfunction, then we must have

$$\begin{aligned}\frac{(2\pi)^{3/2}}{i}(\mathcal{K}_F\Psi_{\lambda,k})(t) =& \frac{1}{\lambda}\Psi_{\lambda,k}(t) + A_k f_0^J(t)\int_0^\infty f_0^J(s)\Psi_{\lambda,k}(s)\,ds + B_k f_0^Y(t)\int_0^\infty f_0^Y(s)\Psi_{\lambda,k}(s)\,ds \\ &+ C_k\left(f_0^J(t)\int_0^\infty f_0^Y(s)\Psi_{\lambda,k}(s)\,ds + f_0^Y(t)\int_0^\infty f_0^J(s)\Psi_{\lambda,k}(s)\,ds\right),\end{aligned} \tag{5.78}$$

[2] From [36, Theorem 19, Chap. 19.4, Vol. 2], since both $\psi^c_{\lambda,k}(t)$ and $\psi^s_{\lambda,k}(t)$ are nonnormalizable for $\lambda \in (0,\infty)$, we immediately have that $(0,\infty) \subseteq \sigma_c(\hat{H}'_k)$. The point $\lambda = 0$ is excluded from this interval because in this case, one of the solutions of $H_k w = 0$ actually *is* normalizable on $L^2[0,\infty)$. It remains, however, that in general this normalizable solution will not obey a boundary condition of the kind of equation (5.58), so in general $\lambda = 0$ is not in the point spectrum.

where $\mathcal{K}_{\mathcal{F}}$ is given by equation (5.59). Note that A_k, B_k, and C_k are also undetermined. We take f_0^J and f_0^Y to be the homogeneous solutions

$$f_0^J(t) := a^{1/2}(t)\sqrt{\frac{\pi\eta(t)}{2}}J_n(k\eta(t)) \qquad \text{and} \qquad f_0^Y(t) := a^{1/2}(t)\sqrt{\frac{\pi\eta(t)}{2}}Y_n(k\eta(t)). \tag{5.79}$$

This consistency equation (5.78) must hold for all $t \in [0,\infty)$. Therefore, an algorithm for determining the correct eigenfunction for any given λ is to optimize the parameters $b_{\lambda,k}$, A_k, B_k, and C_k such that equation (5.78) holds over several values of t.

To reduce numerical error, let us rework equation (5.78) by collecting integrations together. To this extent, define the following integrals:

$$\mathcal{I}_{WX}(t) := \int_0^t f_0^W(s)\psi_{\lambda,k}^X(s)\,ds \qquad W \in \{J,Y\},\ X \in \{c,s\} \tag{5.80}$$

It is straightforward to write the right hand side of (5.78) in terms of these integrals by writing $\Psi_{\lambda,k} = \psi_{\lambda,k}^c + b_{\lambda,k}\psi_{\lambda,k}^s$. For the left-hand side, in terms of f_0^J and f_0^Y we have that

$$\begin{aligned}
\frac{(2\pi)^{3/2}}{i}(\mathcal{K}_F\Psi_{\lambda,k})(t) &= \frac{1}{2i}\int_0^\infty \big[\theta(t-s)(f_0^J(t)+if_0^Y(t))(f_0^J(s)-if_0^Y(s)) \\
&\qquad +\theta(s-t)(f_0^J(t)-if_0^Y(t))(f_0^J(s)+if_0^Y(s))\big]\,\Psi_{\lambda,k}(s)\,ds \\
&= \frac{1}{2i}(f_0^J(t)+if_0^Y(t))\int_0^t (f_0^J(s)-if_0^Y(s))\Psi_{\lambda,k}(s)\,ds \\
&\qquad + \frac{1}{2i}(f_0^J(t)-if_0^Y(t))\int_t^\infty (f_0^J(s)+if_0^Y(s))\Psi_{\lambda,k}(s)\,ds \\
&= \frac{1}{2i}(f_0^J(t)+if_0^Y(t))\int_0^t (f_0^J(s)-if_0^Y(s))\Psi_{\lambda,k}(s)\,ds \\
&\qquad + \frac{1}{2i}(f_0^J(t)-if_0^Y(t))\left[\int_0^\infty (f_0^J(s)+if_0^Y(s))\Psi_{\lambda,k}(s)\,ds \right. \\
&\qquad\qquad \left. -\int_0^t (f_0^J(s)+if_0^Y(s))\Psi_{\lambda,k}(s)\,ds\right].
\end{aligned} \tag{5.81}$$

So, collecting all terms, we may rewrite equation (5.78) as follows:

$$\begin{aligned}
0 &= \mathscr{C}(A_k,B_k,C_k,b_{\lambda,k};\lambda,t) \\
&:= \frac{1}{\lambda}\left(\psi_{\lambda,k}^c(t)+b_{\lambda,k}\psi_{\lambda,k}^s(t)\right) - f_0^Y(t)\left[\mathcal{I}_{Jc}(t)+b_{\lambda,k}\mathcal{I}_{Js}(t)\right] + f_0^J(t)\left[\mathcal{I}_{Yc}(t)+b_{\lambda,k}\mathcal{I}_{Ys}(t)\right] \\
&\quad + \left(\left[A_k+\frac{i}{2}\right]f_0^J(t)+\left[C_k+\frac{1}{2}\right]f_0^Y(t)\right)\left[\mathcal{I}_{Jc}(\infty)+b_{\lambda,k}\mathcal{I}_{Js}(\infty)\right] \\
&\quad + \left(\left[C_k-\frac{1}{2}\right]f_0^J(t)+\left[B_k+\frac{i}{2}\right]f_0^Y(t)\right)\left[\mathcal{I}_{Yc}(\infty)+b_{\lambda,k}\mathcal{I}_{Ys}(\infty)\right]
\end{aligned} \tag{5.82}$$

In summary, we have a procedure for computing the covariantly bandlimited propagator $\mathcal{K}_F^c(t,s,k)$ for any fixed $k>0$. The steps are as follows:

1. For $0 < \lambda \leq \Omega^2$, optimize the consistency equation $\mathscr{C}(A_k, B_k, C_k, b_{\lambda,k}; \lambda, t)$ over several values of t to obtain $b_{\lambda,k}$.
2. Normalize the eigenfunctions obtained in the previous step.
3. Use the orthonormal eigenfunctions to write down the projector $P_{B_k(\Omega)}(t,s) = \int_0^{\Omega^2} \psi_{\lambda,k}(t)\psi^*_{\lambda,k}(s)\, d\lambda$.
4. Compute the bandlimited propagator $\mathcal{K}^c_F(t,s,k) = (P_{B_k(\Omega)}\mathcal{K}_F P_{B_k(\Omega)})(t,s,k)$.

Of course, we can only obtain $b_{\lambda,k}$ for a discrete set of eigenvalues λ, which we use to numerically approximate the projector $P_{B_k(\Omega)}$. Also note that normalizing the eigenfunctions is not a trivial task. We will discuss this in the next section, along with details about the optimization of the consistency equation.

5.3.5 Numerical Implementation of the Cutoff: Details

While clean to formulate, the algorithm we found for computing $\mathcal{K}^c_F$ is a messy numerical undertaking. Let us examine some of the algorithm's implementation details here.

The solutions $\psi^c_{\lambda,k}(t)$ and $\psi^s_{\lambda,k}(t)$

There are two numerical difficulties when it comes to constructing the solutions $\psi^c_{\lambda,k}(t)$ and $\psi^s_{\lambda,k}(t)$. The first is that both of these solutions oscillate infinitely quickly near $t = 0$. The second is that in theory we need to know these solutions out to infinity in order to evaluate integrals on $[0,\infty)$. These two considerations motivate fixing two times $0 < t_1 < t_2$ that define three time periods. For both $0 \leq t < t_1$ and $t > t_2$ we analytically approximate $\psi^c_{\lambda,k}(t)$ and $\psi^s_{\lambda,k}(t)$. For $t_1 \leq t \leq t_2$, we numerically solve for $\psi^c_{\lambda,k}(t)$ and $\psi^s_{\lambda,k}(t)$.

To make an early time approximation, t_1 should be chosen such that $\frac{k^2}{c^2}t^{-2\alpha} - \frac{3\alpha}{2}\left(\frac{3\alpha}{2} - 1\right)t^{-2} + \lambda \approx \frac{k^2}{c^2}t^{-2\alpha}$ whenever $0 \leq t < t_1$. To this extent, we define t_1 as the solution to

$$\frac{k^2}{c^2}\frac{1}{t_1^{2\alpha}} = 10^{\tau_1}\left|\lambda - \frac{3\alpha}{2}\left(\frac{3\alpha}{2} - 1\right)\frac{1}{t_1^2}\right|, \tag{5.83}$$

where the tolerance τ_1 sets the desired accuracy. To make a late time approximation, t_2 should be chosen such that $\frac{k^2}{c^2}t^{-2\alpha} - \frac{3\alpha}{2}\left(\frac{3\alpha}{2} - 1\right)t^{-2} + \lambda \approx \lambda$ whenever $t > t_2$. To this extent, we define t_2 as the solution to

$$\left|\frac{k^2}{c^2}\frac{1}{t_2^{2\alpha}} + \frac{3\alpha}{2}\left(\frac{3\alpha}{2} - 1\right)\frac{1}{t_2^2}\right| = 10^{-\tau_2}\lambda, \tag{5.84}$$

where we may choose the tolerance τ_2.

We construct $\psi^c_{\lambda,k}(t)$ and $\psi^s_{\lambda,k}(t)$ numerically as follows. For $t > t_2$, we set

$$\psi^c_{\lambda,k}(t) \approx \cos(\sqrt{\lambda}(t - t_2)), \qquad \text{and} \qquad \psi^s_{\lambda,k}(t) \approx \frac{1}{\lambda}\sin(\sqrt{\lambda}(t - t_2)). \tag{5.85}$$

$\psi^c_{\lambda,k}(t)$ and $\psi^s_{\lambda,k}(t)$ are easily obtained over the interval $[t_1, t_2]$ by numerically solving the ODE $(H_k - \lambda)w = 0$ with the initial conditions $\psi^c_{\lambda,k}(t_2) = 1$, $\partial_t\psi^c_{\lambda,k}(t_2) = 0$ and $\psi^s_{\lambda,k}(t_2) = 0$, $\partial_t\psi^s_{\lambda,k}(t_2) = 1$ respectively.

We then approximate $\psi^c_{\lambda,k}(t)$ and $\psi^s_{\lambda,k}(t)$ for $0 \le t < t_1$ with the expression from equation (5.75). Of course, this early-time approximation is matched with the numerical solution at t_1. Explicitly, we solve the systems

$$\begin{cases} \psi^c_{\lambda,k}(t_1) = C_J\sqrt{t_1}J_q(k\eta(t_1)) + C_Y\sqrt{t_1}Y_q(k\eta(t_1)) \\ \partial_t\psi^c_{\lambda,k}(t_1) = C_J\partial_t\left[\sqrt{t}J_q(k\eta(t))\right]_{t=t_1} + C_Y\partial_t\left[\sqrt{t}Y_q(k\eta(t))\right]_{t=t_1} \end{cases}$$

and

$$\begin{cases} \psi^s_{\lambda,k}(t_1) = S_J\sqrt{t_1}J_q(k\eta(t_1)) + S_Y\sqrt{t_1}Y_q(k\eta(t_1)) \\ \partial_t\psi^s_{\lambda,k}(t_1) = S_J\partial_t\left[\sqrt{t}J_q(k\eta(t))\right]_{t=t_1} + S_Y\partial_t\left[\sqrt{t}Y_q(k\eta(t))\right]_{t=t_1} \end{cases}$$

for C_J, C_Y, S_J, and S_Y.

The integrals $\mathcal{I}_{WX}(t)$

We evaluate the integrals $\mathcal{I}_{WX}(t)$ semi-analytically, using appropriate approximations for the intervals $[0, t_1)$ and (t_2, ∞). Consider first the case $t < t_1$. Then, for example,

$$\begin{aligned} \mathcal{I}_{Jc}(t) &= \int_0^t f_0^J(s)\psi^c_{\lambda,k}(s)\,ds \\ &\approx \int_0^t (cs^\alpha)^{1/2}\left(\frac{\pi\eta(s)}{2}\right)^{1/2} J_n(k\eta(s))\left[C_J\sqrt{s}J_q(k\eta(s)) + C_Y\sqrt{s}Y_q(k\eta(s))\right]\,ds\,. \end{aligned} \tag{5.86}$$

Next, we use the Bessel function asymptotics (2.89) to approximate $J_n(k\eta(s))$, $J_q(k\eta(s))$, and $Y_q(k\eta(s))$:

$$\begin{aligned} \mathcal{I}_{Jc}(t) &\approx \sqrt{\frac{c}{k}}\int_0^t s^{\alpha/2}\cos\left(\omega_n(s)\right)s^{1/2}\left[C_J\sqrt{\frac{2}{\pi k\eta(s)}}\cos\omega_q(s) + C_Y\sqrt{\frac{2}{\pi k\eta(s)}}\sin\omega_q(s)\right]\,ds \\ &= \frac{c}{k}\sqrt{\frac{2(\alpha-1)}{\pi}}\int_0^t s^\alpha\cos\omega_n(s)\left[C_J\cos\omega_q(s) + C_Y\sin\omega_q(s)\right]\,ds \end{aligned} \tag{5.87}$$

Note that $\omega_x(s) := k\eta(s) - x\frac{\pi}{2} - \frac{\pi}{4}$ as before. Since $\omega_x(s) \to \infty$ as $s \to 0$, the integrand in the last line is a linear combination of terms that oscillate extremely rapidly. Therefore, let us make the approximation $\int_0^t f(s)\cos^2(k\eta(s))\,ds \approx \frac{1}{2}\int_0^t f(s)\,ds \approx \int_0^t f(s)\sin^2(k\eta(s))\,ds$ and $\int_0^t f(s)\cos(k\eta(s))\sin(k\eta(s))\,ds \approx 0$. Expanding the cosines and sines in the last line, we obtain

$$\begin{aligned} \mathcal{I}_{Jc}(t) &\approx \frac{c}{k}\sqrt{\frac{\alpha-1}{2\pi}}\int_0^t s^\alpha\left[C_J\cos\left(\frac{\pi(3\alpha-2)}{4(\alpha-1)}\right) + C_Y\sin\left(\frac{\pi(3\alpha-2)}{4(\alpha-1)}\right)\right]\,ds \\ &= \frac{c}{k}\sqrt{\frac{\alpha-1}{2\pi}}\left[C_J\cos\left(\frac{\pi(3\alpha-2)}{4(\alpha-1)}\right) + C_Y\sin\left(\frac{\pi(3\alpha-2)}{4(\alpha-1)}\right)\right]\frac{t^{\alpha+1}}{\alpha+1}. \end{aligned} \tag{5.88}$$

Similarly, one finds that

$$\mathcal{I}_{Js}(t) \approx \frac{c}{k}\sqrt{\frac{\alpha-1}{2\pi}}\left[S_J\cos\left(\frac{\pi(3\alpha-2)}{4(\alpha-1)}\right)+S_Y\sin\left(\frac{\pi(3\alpha-2)}{4(\alpha-1)}\right)\right]\frac{t^{\alpha+1}}{\alpha+1}, \tag{5.89}$$

$$\mathcal{I}_{Yc}(t) \approx \frac{c}{k}\sqrt{\frac{\alpha-1}{2\pi}}\left[C_Y\cos\left(\frac{\pi(3\alpha-2)}{4(\alpha-1)}\right)-C_J\sin\left(\frac{\pi(3\alpha-2)}{4(\alpha-1)}\right)\right]\frac{t^{\alpha+1}}{\alpha+1}, \tag{5.90}$$

$$\mathcal{I}_{Ys}(t) \approx \frac{c}{k}\sqrt{\frac{\alpha-1}{2\pi}}\left[S_Y\cos\left(\frac{\pi(3\alpha-2)}{4(\alpha-1)}\right)-S_J\sin\left(\frac{\pi(3\alpha-2)}{4(\alpha-1)}\right)\right]\frac{t^{\alpha+1}}{\alpha+1}. \tag{5.91}$$

For the case of $t > t_1$, we write

$$\mathcal{I}_{WX}(t) = \int_0^{t_1} f_0^W(s)\psi_{\lambda,k}^X(s)\,ds + \int_{t_1}^{t} f_0^W(s)\psi_{\lambda,k}^X(s)\,ds. \tag{5.92}$$

We approximate the first integral using the early-time approximation written down above, and we evaluate the second integral numerically.

For the case of $t \to \infty$, we introduce late-time approximations to evaluate $\mathcal{I}_{WX}(\infty)$. Consider for example $\mathcal{I}_{Jc}(\infty)$. Write

$$\mathcal{I}_{Jc}(\infty) = \int_0^{t_1} f_0^J(s)\psi_{\lambda,k}^c(s)\,ds + \int_{t_1}^{t_2} f_0^J(s)\psi_{\lambda,k}^c(s)\,ds + \int_{t_2}^{\infty} f_0^J(s)\psi_{\lambda,k}^c(s)\,ds. \tag{5.93}$$

One can evaluate the first two integrals using the methods described up to this point. For the last integral, we approximate $\psi_{\lambda,k}^c$ with its asymptotic cosine form and f_0^J with the asymptotic form (2.94):

$$\begin{aligned}\int_{t_2}^{\infty} f_0^J(s)\psi_{\lambda,k}^c(s)\,ds &\approx \int_{t_2}^{\infty} a^{1/2}(s)\left(\frac{\pi\eta(s)}{2}\right)^{1/2}\frac{1}{\Gamma(n+1)}\left(\frac{k\eta(s)}{2}\right)^n\cos\left(\sqrt{\lambda}(s-t_2)\right)\,ds \\ &= \sqrt{\frac{\pi}{2(\alpha-1)}}\frac{1}{\Gamma(n+1)X^n}\left[\cos(\sqrt{\lambda}t_2)\int_{t_2}^{\infty} s^{-\frac{3\alpha}{2}+1}\cos(\sqrt{\lambda}s)\,ds\right. \\ &\qquad \left.+\sin(\sqrt{\lambda}t_2)\int_{t_2}^{\infty} s^{-\frac{3\alpha}{2}+1}\sin(\sqrt{\lambda}s)\,ds\right]\end{aligned} \tag{5.94}$$

As before, $X := 2c(\alpha-1)/k$. Since $\alpha \gg 1$ by assumption, the integrals in the last line are convergent. They may thus be computed numerically. For $\mathcal{I}_{Js}(\infty)$, we similarly have

$$\begin{aligned}\int_{t_2}^{\infty} f_0^J(s)\psi_{\lambda,k}^s(s)\,ds \approx \sqrt{\frac{\pi}{2(\alpha-1)}}\frac{1}{\Gamma(n+1)X^n}&\left[\frac{1}{\sqrt{\lambda}}\cos(\sqrt{\lambda}t_2)\int_{t_2}^{\infty} s^{-\frac{3\alpha}{2}+1}\sin(\sqrt{\lambda}s)\,ds\right. \\ &\left.-\frac{1}{\sqrt{\lambda}}\sin(\sqrt{\lambda}t_2)\int_{t_2}^{\infty} s^{-\frac{3\alpha}{2}+1}\cos(\sqrt{\lambda}s)\,ds\right].\end{aligned} \tag{5.95}$$

$\mathcal{I}_{Yc}(\infty)$ and $\mathcal{I}_{Ys}(\infty)$ are special cases, as they are not convergent integrals in the Riemannian sense. Therefore, they cannot be computed entirely numerically. Rather, we must exploit the distributional

properties of their integrands in order to evaluate them. For instance, for $\mathcal{I}_{Yc}(\infty)$, we encounter the integral

$$\begin{aligned}\int_{t_2}^{\infty} f_0^Y(s)\psi_{\lambda,k}^c(s)\,ds &\approx \int_{t_2}^{\infty} a^{1/2}(s)\left(\frac{\pi\eta(s)}{2}\right)^{1/2}\frac{(-\Gamma(n))}{\pi}\left(\frac{2}{k\eta(s)}\right)^n\cos\left(\sqrt{\lambda}(s-t_2)\right)\,ds \\ &= -\sqrt{\frac{\pi}{2(\alpha-1)}}\frac{\Gamma(n)X^n}{\pi}\left[\cos(\sqrt{\lambda}t_2)\int_{t_2}^{\infty} s^{\frac{3\alpha}{2}}\cos(\sqrt{\lambda}s)\,ds\right. \\ &\qquad \left.+\sin(\sqrt{\lambda}t_2)\int_{t_2}^{\infty} s^{\frac{3\alpha}{2}}\sin(\sqrt{\lambda}s)\,ds\right]. \end{aligned} \tag{5.96}$$

If we write each integral that runs from t_2 to ∞ in the last line as the difference of an integral from 0 to ∞ and an integral from 0 to t_2, we are forced to deal with integrals of the form

$$\int_0^{\infty} s^{\frac{3\alpha}{2}}\cos(\sqrt{\lambda}s)\,ds \qquad \text{and} \qquad \int_0^{\infty} s^{\frac{3\alpha}{2}}\sin(\sqrt{\lambda}s)\,ds. \tag{5.97}$$

For simplicity, let us introduce the additional assumption that $\alpha \in \frac{2}{3}\mathbb{N}$ so that $\frac{3\alpha}{2} \in \mathbb{N}$, $\frac{3\alpha}{2} \geq 2$. We have the following proposition.

Proposition 5.3.3 *Let $n \in \mathbb{N}$ and $\nu \in \mathbb{R}$. Then the following identities hold:*

$$\int_0^{\infty} t^n\cos(\nu t)\,dt = \begin{cases} (-1)^{n/2}\pi\delta^{(n)}(\nu) & n \text{ even} \\ (-1)^{(n+1)/2}\dfrac{n!}{\nu^{n+1}} & n \text{ odd} \end{cases} \tag{5.98}$$

$$\int_0^{\infty} t^n\sin(\nu t)\,dt = \begin{cases} (-1)^{n/2}\dfrac{n!}{\nu^{n+1}} & n \text{ even} \\ (-1)^{(n+1)/2}\pi\delta^{(n)}(\nu) & n \text{ odd} \end{cases} \tag{5.99}$$

$\delta^{(n)}$ denotes the n^{th} derivative of the Dirac delta function.

Proof: Consider first the cosine integral. Notice that we can rewrite it as follows:

$$\begin{aligned}\int_0^{\infty} t^n\cos(\nu t)\,dt &= \int_{-\infty}^{\infty}\theta(t)t^n\frac{1}{2}\left(e^{i\nu t}+e^{-i\nu t}\right)\,dt \\ &= \frac{1}{2}\left[\int_{-\infty}^{\infty}\theta(t)t^n e^{i\nu t}\,dt+\int_{-\infty}^{\infty}\theta(t)t^n e^{-i\nu t}\,dt\right]\end{aligned} \tag{5.100}$$

Here, $\theta(t)$ denotes the Heaviside step function. The last line is really a sum of two Fourier transforms, each of which we can evaluate using the convolution theorem and readily known Fourier transforms [54, Section 17.23]. For example,

$$\begin{aligned}\int_{-\infty}^{\infty}\theta(t)t^n e^{-i\nu t}\,dt &= \frac{1}{2\pi}\int_{-\infty}^{\infty}\pi\left(\frac{1}{i\pi(\nu-\nu')}+\delta(\nu-\nu')\right)2\pi i^n\delta^{(n)}(\nu')\,d\nu' \\ &= i^n\pi(-1)^n\frac{\partial^n}{\partial\nu'^n}\left[\frac{1}{i\pi(\nu-\nu')}\right]_{\nu'=0}+i^n\pi\delta^{(n)}(\nu) \\ &= i^{n-1}(-1)^n\frac{n!}{\nu^{n+1}}+i^n\pi\delta^{(n)}(\nu)\end{aligned} \tag{5.101}$$

The result (5.98) immediately follows from equations (5.100) and (5.101). Similarly, we can rewrite the sine integral as

$$\begin{aligned}\int_0^\infty t^n \sin(\nu t)\,dt &= \int_{-\infty}^\infty \theta(t) t^n \frac{1}{2i}\left(e^{i\nu t} - e^{-i\nu t}\right)\,dt \\ &= \frac{1}{2i}\left[\int_{-\infty}^\infty \theta(t) t^n e^{i\nu t}\,dt - \int_{-\infty}^\infty \theta(t) t^n e^{-i\nu t}\,dt\right], \end{aligned} \tag{5.102}$$

whence we obtain the result (5.99).

Additionally, we can obtain these results a second way using Feynman's integration trick. We have that

$$\int_0^\infty t^n \cos(\nu t)\,dt = \begin{cases} (-1)^{n/2}\dfrac{\partial^n}{\partial \nu^n}\displaystyle\int_0^\infty \cos(\nu t)\,dt & n \text{ even} \\ (-1)^{(n-1)/2}\dfrac{\partial^n}{\partial \nu^n}\displaystyle\int_0^\infty \sin(\nu t)\,dt & n \text{ odd} \end{cases}. \tag{5.103}$$

It is well known that $\int_0^\infty \cos(\nu t)\,dt = \pi\delta(\nu)$ [48, Appendix C]. We may compute $\int_0^\infty \sin(\nu t)\,dt$ by abusing the Laplace transform of $\sin(\nu t)$ [54, Section 17.13]:

$$\mathcal{L}\left[\sin(\nu t)\right](s) := \int_0^\infty e^{-st}\sin(\nu t)\,dt = \frac{\nu}{s^2+\nu^2} \quad ; \quad \Re(s) > 0 \tag{5.104}$$

Evaluating this Laplace transform at $s = 0$ gives $\int_0^\infty \sin(\nu t)\,dt = \nu^{-1}$. The result (5.98) then follows from equation (5.103). Similarly, we may write

$$\int_0^\infty t^n \sin(\nu t)\,dt = \begin{cases} (-1)^{n/2}\dfrac{\partial^n}{\partial \nu^n}\displaystyle\int_0^\infty \sin(\nu t)\,dt & n \text{ even} \\ (-1)^{(n+1)/2}\dfrac{\partial^n}{\partial \nu^n}\displaystyle\int_0^\infty \cos(\nu t)\,dt & n \text{ odd} \end{cases}, \tag{5.105}$$

whence we obtain the result (5.99). □

Note that $\delta^{(n)}(\nu) = 0$ for $\nu \neq 0$. Therefore, for $\lambda \neq 0$, it follows that $\int_{t_2}^\infty f_0^Y(s)\psi_{\lambda,k}^c(s)\,ds$ is approximated by

- $m = \frac{3\alpha}{2}$ even:

$$\begin{aligned} -\sqrt{\frac{\pi}{2(\alpha-1)}}\frac{\Gamma(n)X^n}{\pi}\Bigg[&-\cos(\sqrt{\lambda}t_2)\int_0^{t_2} s^m\cos(\sqrt{\lambda}s)\,ds \\ &+\sin(\sqrt{\lambda}t_2)\left\{(-1)^{m/2}\frac{m!}{\lambda^{(m+1)/2}} - \int_0^{t_2} s^m\sin(\sqrt{\lambda}s)\,ds\right\}\Bigg] \end{aligned} \tag{5.106}$$

- $m = \frac{3\alpha}{2}$ odd:

$$\begin{aligned} -\sqrt{\frac{\pi}{2(\alpha-1)}}\frac{\Gamma(n)X^n}{\pi}\Bigg[&\cos(\sqrt{\lambda}t_2)\left\{(-1)^{(m+1)/2}\frac{m!}{\lambda^{(m+1)/2}} - \int_0^{t_2} s^m\cos(\sqrt{\lambda}s)\,ds\right\} \\ &-\sin(\sqrt{\lambda}t_2)\int_0^{t_2} s^m\sin(\sqrt{\lambda}s)\,ds\Bigg] \end{aligned} \tag{5.107}$$

Similarly, $\int_{t_2}^{\infty} f_0^Y(s)\psi_{\lambda,k}^s(s)\,ds$ is approximated by

- $m = \frac{3\alpha}{2}$ even:

$$-\sqrt{\frac{\pi}{2(\alpha-1)}}\frac{\Gamma(n)X^n}{\pi}\left[\frac{1}{\sqrt{\lambda}}\sin(\sqrt{\lambda}t_2)\int_0^{t_2} s^m\cos(\sqrt{\lambda}s)\,ds \right. \\ \left. +\frac{1}{\sqrt{\lambda}}\cos(\sqrt{\lambda}t_2)\left\{(-1)^{m/2}\frac{m!}{\lambda^{(m+1)/2}} - \int_0^{t_2} s^m\sin(\sqrt{\lambda}s)\,ds\right\}\right] \tag{5.108}$$

- $m = \frac{3\alpha}{2}$ odd:

$$-\sqrt{\frac{\pi}{2(\alpha-1)}}\frac{\Gamma(n)X^n}{\pi}\left[-\frac{1}{\sqrt{\lambda}}\sin(\sqrt{\lambda}t_2)\left\{(-1)^{(m+1)/2}\frac{m!}{\lambda^{(m+1)/2}} - \int_0^{t_2} s^m\cos(\sqrt{\lambda}s)\,ds\right\}\right. \\ \left. -\frac{1}{\sqrt{\lambda}}\cos(\sqrt{\lambda}t_2)\int_0^{t_2} s^m\sin(\sqrt{\lambda}s)\,ds\right] \tag{5.109}$$

Optimizing $\mathscr{C}(A_k, B_k, C_k, b_{\lambda,k}; \lambda, t)$

For fixed λ and k, the correct choice of $b_{\lambda,k}$ (*i.e.*, the correct choice of self-adjoint extension) is that $b_{\lambda,k}$ for which $\mathscr{C}(A_k, B_k, C_k, b_{\lambda,k}; \lambda, t) = 0$ for all $t \in [0, \infty)$. In practice, a good way to determine $b_{\lambda,k}$ is as follows. Choosing a set of some times $\{T_j\}_{j=1}^N$, minimize

$$\overline{\mathscr{C}}(A_k, B_k, C_k, b_{\lambda,k}; \lambda) := \frac{1}{N}\sum_{j=1}^{N} |\mathscr{C}(A_k, B_k, C_k, b_{\lambda,k}; \lambda, T_j)| \tag{5.110}$$

over the parameter space $A_k, B_k, C_k, b_{\lambda,k} \in \mathbb{C}$. A consistency check, or alternatively a constraint, is that one should find the same A_k, B_k, and C_k in this way for different values of λ.

A good choice of minimization method is to use the Nelder-Mead, or nonlinear simplex method for solving a nonlinear program [55]. Aside from being a flexible and robust, the Nelder-Mead method has the advantage that it does not require the computation of derivatives of $\overline{\mathscr{C}}(A_k, B_k, C_k, b_{\lambda,k}; \lambda)$ during its minimization.

Normalizing the eigenfunction

Once the correct $b_{\lambda,k}$ has been found, we must still normalize the eigenfunction $\Psi_{\lambda,k} = \psi_{\lambda,k}^c + b_{\lambda,k}\psi_{\lambda,k}^s$. Let $\psi_{\lambda,k}$ denote the normalized eigenfunction and write $\psi_{\lambda,k}(t) = N_{\lambda,k}\Psi_{\lambda,k}(t)$. Of course, we could evaluate $N_{\lambda,k} = |\langle\Psi_{\lambda,k}|\Psi_{\lambda,k}\rangle|^{-1/2}$ using the semi-analytic methods outlined in the previous subsection. Instead, however, consider the following analytic reasoning. (In this way, the semi-analytic methods could still be used to check the orthogonality of the computed eigenfunctions.)

For a moment, write $\psi_{\lambda,k}(t) = C_\lambda \psi^c_{\lambda,k}(t) + D_\lambda \psi^s_{\lambda,k}(t)$. Let us suppress the small subscript k that should appear on C_λ and D_λ for tidiness. We must have that

$$\begin{aligned}
\delta(\lambda-\mu) = \langle \psi_{\lambda,k} | \psi_{\mu,k} \rangle &= \int_0^\infty \psi^*_{\lambda,k}(t)\psi_{\mu,k}(t)\,dt \\
&= \int_0^{t_2} \psi^*_{\lambda,k}(t)\psi_{\mu,k}(t)\,dt + \int_{t_2}^\infty \psi^*_{\lambda,k}(t)\psi_{\mu,k}(t)\,dt \\
&\approx \int_0^{t_2} \psi^*_{\lambda,k}(t)\psi_{\mu,k}(t)\,dt + \int_{t_2}^\infty \tilde{\psi}^*_{\lambda,k}(t)\tilde{\psi}_{\mu,k}(t)\,dt \\
&= \int_0^{t_2} \psi^*_{\lambda,k}(t)\psi_{\mu,k}(t)\,dt + \int_0^\infty \tilde{\psi}^*_{\lambda,k}(t)\tilde{\psi}_{\mu,k}(t)\,dt - \int_0^{t_2} \tilde{\psi}^*_{\lambda,k}(t)\tilde{\psi}_{\mu,k}(t)\,dt\,.
\end{aligned}$$

In the last computation, a tilde over a ψ indicates that we approximate it using the asymptotic cosine and sine forms of $\psi^c_{\lambda,k}$ and $\psi^s_{\lambda,k}$. This approximation becomes exact as we take $t_2 \to \infty$.

Notice in the last line that the integrals which run from 0 to t_2 are both finite, Riemannian integrals. In other words, the only integral from which we can obtain the required Dirac delta, $\delta(\lambda-\mu)$, is $\int_0^\infty \tilde{\psi}^*_{\lambda,k}(t)\tilde{\psi}_{\mu,k}(t)\,dt$. Moreover, when evaluated, the coefficient of the resulting Dirac delta must be 1. Explicitly, this integral reads

$$\int_0^\infty \left(C^*_\lambda \cos(\sqrt{\lambda}t) + \frac{D^*_\lambda}{\sqrt{\lambda}}\sin(\sqrt{\lambda}t)\right)\left(C_\mu \cos(\sqrt{\mu}t) + \frac{D_\mu}{\sqrt{\mu}}\sin(\sqrt{\mu}t)\right)\,dt\,.$$

After a bit of algebra, one finds that this integral reduces to

$$\pi\left((\lambda\mu)^{1/4}C^*_\lambda C_\mu + \frac{D^*_\lambda D_\mu}{(\lambda\mu)^{1/4}}\right)\delta(\lambda-\mu) + \frac{D^*_\lambda C_\mu\sqrt{\lambda} - C^*_\lambda D_\mu\sqrt{\mu}}{\lambda-\mu}. \tag{5.111}$$

In our case, set $C_\lambda = N_{\lambda,k}$ and $D_\lambda = N_{\lambda,k}b_{\lambda,k}$. Then, normalization requires that

$$\pi N^*_{\lambda,k}N_{\mu,k}\left((\lambda\mu)^{1/4} + \frac{b^*_{\lambda,k}b_{\mu,k}}{(\lambda\mu)^{1/4}}\right)\delta(\lambda-\mu) = \delta(\lambda-\mu). \tag{5.112}$$

Setting $\lambda = \mu$ and choosing $N_{\lambda,k}$ to be real, we conclude that

$$N_{\lambda,k} = \left(\pi\left[\sqrt{\lambda} + \frac{|b_{\lambda,k}|^2}{\sqrt{\lambda}}\right]\right)^{-1/2}. \tag{5.113}$$

5.3.6 Numerical Implementation of the Cutoff: Results and Further Work

Having carefully put in place each piece of the numerical solution in the previous subsections, all that is left is to reap the fruits of numerics. The calculations are extremely long and computationally taxing, however, so the results shown here are preliminary. What is most important is that the solution can be carried all the way to its end. All that is left is some tuning of the numerics and heavier computation.

To begin, note that the numerical solution presented here uses a scale factor with power $\alpha = 4$, which is slightly different than the value $\alpha = 10$. The lower power greatly reduces the computation time required to

achieve a given numerical precision. This new parameter value produce a qualitatively identical spacetime, however. We will still use a cutoff at $\Omega = 5$. The tolerances are set to $\tau_1 = 3$ and $\tau_2 = 1$.

Recall that the first step of the algorithm is to minimize $\overline{\mathscr{C}}(A_k, B_k, C_k, b_{\lambda,k}; \lambda)$. Here, for each fixed $k \in \{0.25, 0.5, 0.75, , \ldots, 10\}$, this has been done for $\lambda = 0.5, 1, 1.5, \ldots, 50$. As an illustration, a plot of the values obtained by this optimization for A_k, B_k, C_k, and $b_{\lambda,k}$ as a function of λ for the value $k = 5$ is shown in figure 5.11. Reassuringly, $b_{\lambda,k}$ seems to vary rather continuously as a function of λ. The jitter in the other parameters, however, is a clear sign of numerical error (recall that A_k, B_k, and C_k should be independent of λ). In the rest of this calculation, A_k, B_k, and C_k are taken to be the average of the values returned throughout the optimization.

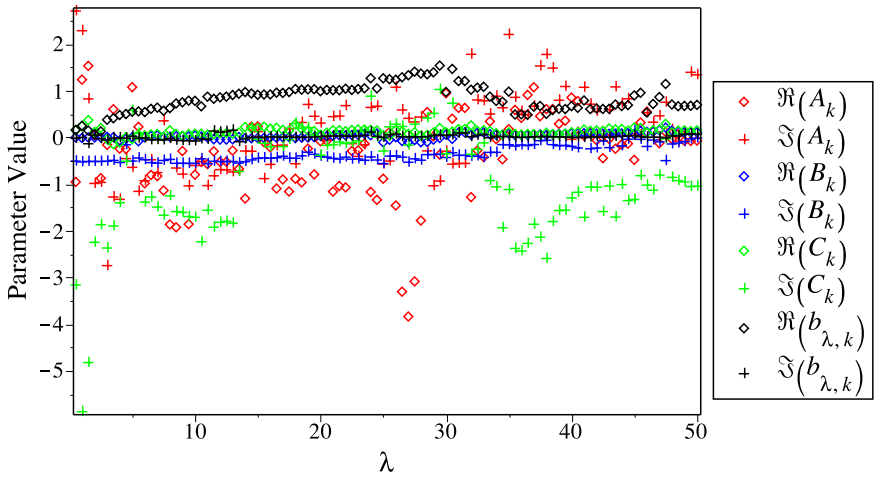

Figure 5.11: Propagator parameters obtained by minimizing $\overline{\mathscr{C}}(A_k, B_k, C_k, b_{\lambda,k}; \lambda)$ for the fixed value $k = 5$.

Once the $b_{\lambda,k}$ are known, one can compute the covariantly bandlimited propagator. This computation is slightly modified from the algorithm that was suggested earlier. Instead of computing $\mathcal{K}_F^c(t, s, k) = (P_{B_k(\Omega)}\mathcal{K}P_{B_k(\Omega)})(t, s, k)$, we compute $\mathcal{K}_F^c(t, s, k) = \mathcal{K}_F(t, s, k) - (\bar{P}_{B_k(\Omega)}\mathcal{K}_F\bar{P}_{B_k(\Omega)})(t, s, k)$, where $\hat{\bar{P}}_{B_k(\Omega)} := \hat{\mathbb{1}} - \hat{P}_{B_k(\Omega)}$. In other words, the large-eigenvalue components of $\mathcal{K}_F$ are discarded to compute $\mathcal{K}_F^c$, instead of keeping the small-eigenvalue components as in the original algorithm. The reason for this change is that in computing $P_{B_k(\Omega)}\mathcal{K}_F P_{B_k(\Omega)}$, one encounters integrals of the form

$$\int_0^\infty dt\, f_0^W(t) \int_0^t ds\, f_0^{W'}(s)\psi_{\lambda,k}^X(s). \tag{5.114}$$

The approximation machinery that we developed thus far is not apt to handle such integrals and would require significant modification in order to be able to do so. Futhermore, we would find ourselves performing integrals over λ which would begin at $\lambda = 0$. Therefore, we would need to account for the terms that contain derivatives of the Dirac delta function, $\delta^{(n)}(\sqrt{\lambda})$, which appear in the identities (5.98) and (5.99).

As such, here $\mathcal{K}_F^c(t,s,k)$ is computed as follows:

$$\begin{aligned}\mathcal{K}_F^c(t,s,k) &= \mathcal{K}_F(t,s,k) - (\bar{P}_{B_k(\Omega)}\mathcal{K}_F\bar{P}_{B_k(\Omega)})(t,s,k)\\ &= \mathcal{K}_F(t,s,k) - \frac{i}{(2\pi)^{3/2}}\int_{\Omega^2}\frac{1}{\lambda}\psi_{\lambda,k}(t)\psi^*_{\lambda,k}(s)\,d\lambda\\ &\quad - A_k(\bar{P}_{B_k(\Omega)}f_0^J)(t)(\bar{P}_{B_k(\Omega)}f_0^J)^*(s) - B_k(\bar{P}_{B_k(\Omega)}f_0^Y)(t)(\bar{P}_{B_k(\Omega)}f_0^Y)^*(s)\\ &\quad - C_k\left[(\bar{P}_{B_k(\Omega)}f_0^J)(t)(\bar{P}_{B_k(\Omega)}f_0^Y)^*(s) + (\bar{P}_{B_k(\Omega)}f_0^Y)(t)(\bar{P}_{B_k(\Omega)}f_0^J)^*(s)\right]\end{aligned} \tag{5.115}$$

where

$$(\bar{P}_{B_k(\Omega)}f_0^J)(t) = \int_{\Omega^2}\psi_{\lambda,k}(t)N_{\lambda,k}\left[\mathcal{I}_{Jc}(\infty) + b^*_{\lambda,k}\mathcal{I}_{Js}(\infty)\right]\,d\lambda$$

and

$$(\bar{P}_{B_k(\Omega)}f_0^Y)(t) = \int_{\Omega^2}\psi_{\lambda,k}(t)N_{\lambda,k}\left[\mathcal{I}_{Yc}(\infty) + b^*_{\lambda,k}\mathcal{I}_{Ys}(\infty)\right]\,d\lambda$$

The integrals over λ are simply computed as Riemann sums, and the infinite upper bound on these integrals is approximated by integrating out to $\lambda = 50$. As a concrete illustration, a plot of $|(\bar{P}_{B_k(\Omega)}\mathcal{K}_F\bar{P}_{B_k(\Omega)})(t = s, k_0)|$ for $k_0 = 5$ is shown in figure 5.12. This is what the covariant cutoff removes from the propagator $\mathcal{K}_F$. In particular, notice that the curve tapers off to a constant correction for large t, as is to be expected. The small oscillations are likely due to the fact that we are only using finitely many eigenfunctions to approximate the spectral integrals.

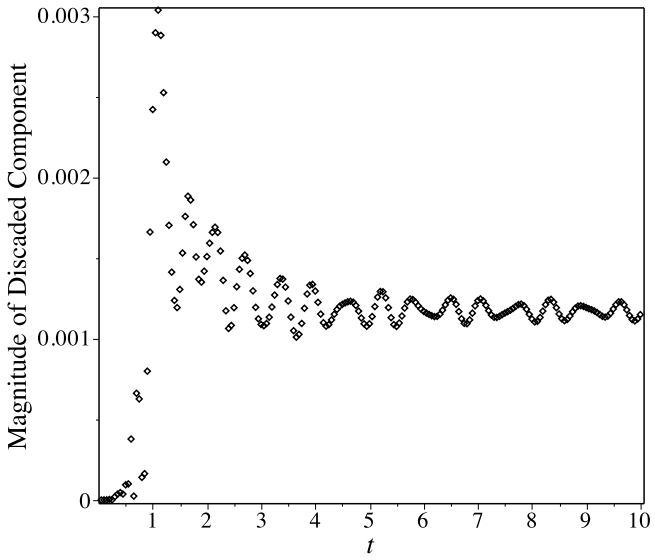

Figure 5.12: Plot of $|(\bar{P}_{B_k(\Omega)}\mathcal{K}_F\bar{P}_{B_k(\Omega)})(t = s, k_0)|$ for $k_0 = 5$. This is the large-eigenvalue component of $\mathcal{K}_F$ that is removed by the covariant cutoff. Other parameter values are $\alpha = 4$, $c = 1$, and $\Omega = 5$.

We immediately see that what is discarded from $\mathcal{K}_F$ is tiny compared to the magnitude of $\mathcal{K}_F$ for

almost all times. This is reflected in the plot of $|\mathcal{K}_F(t = s, 5)|$ and $|\mathcal{K}^c_F(t = s, 5)|$ shown below in figure 5.13. The two curves are essentially indistinguishable.

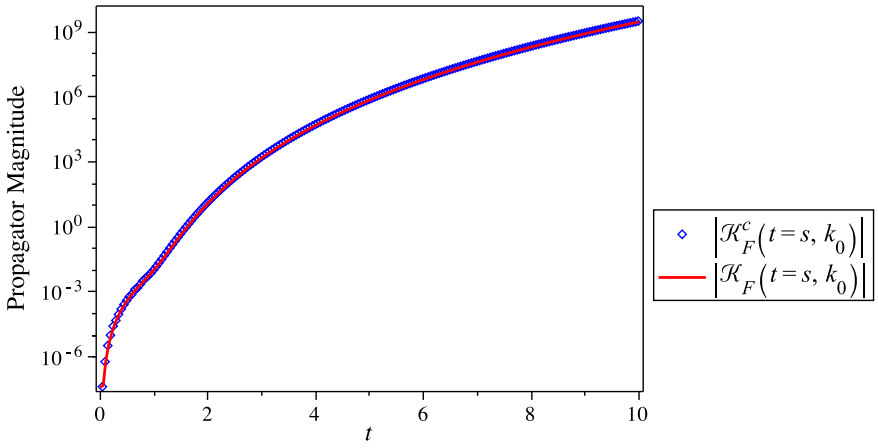

Figure 5.13: Plot of $|\mathcal{K}_F(t = s, k_0)|$ and the numerically-determined $|\mathcal{K}^c_F(t = s, k_0)|$ for $k_0 = 5$. Other parameter values are $\alpha = 4$, $c = 1$, and $\Omega = 5$.

A plot of $|\mathcal{K}_F|$ and $|\mathcal{K}^c_F|$ as a function of the comoving wavenumber k is shown in figure 5.14. Here, the propagators are evaluated at the equal time $t_0 = s_0 = 5t_{cross\ max}$, where $t_{cross\ max}$ is the mode crossing time of the $k = 10$ mode (*i.e.*, the largest crossing time of the modes plotted). For the parameter values that are in use, one has that $t_0 \doteq 6.11$. A plot of the fluctuation spectra $\delta\phi_k(t_0)$ and $\delta\phi^c_k(t_0)$ is shown in figure 5.15.

Here as well we see that the effect of the covariant cutoff on the fluctuations of a scalar field in a power-law FLRW spacetime is tiny. At this point in time, it is not clear how this effect could be experimentally measured. Indeed, from figure 5.16, we see that the relative difference between the full fluctuation spectrum and the covariantly-bandlimited fluctuation spectrum is at the 10^{-12} level at most. This suggests that the strength of the covariant cutoff's effect scales like σ^β, with $\beta \approx 2$. For a concrete comparison, the Planck satellite has errors of $5 - 9\,\mu K^2$ on measured values from about $1000\,\mu K^2$ to $2500\,\mu K^2$ over a large part of its measurement range [15]. Therefore, Planck offers at best about 0.2 % resolution on fluctuations at the 10^{-5} to 10^{-6} level, which is still several orders of magnitude away from the level at which the covariant cutoff operates. This still brings us closer to the Planck scale than what may be achieved with the Large Hadron Collider, however, which probes energies that are 15 orders of magnitude below the Planck energy!

Figure 5.16 also shows that the strength of the covariant cutoff's effect (relative to the base strength of fluctuations) continues to grow for comoving wavenumbers past the cutoff Ω. This behaviour contrasts with the case of flat spacetime, but is also seen in the late-time analytic approximation from section 5.3.3. Despite the considerable numerical jitter, it is reassuring that the numerical computation produces this same global trend that is seen in the results obtained from the late-time analytic approximation. The small oscillations that are superimposed on the global trend in the numerics are again most likely due to the fact that continuous spectral integrals were approximated with only a finite number of terms. This

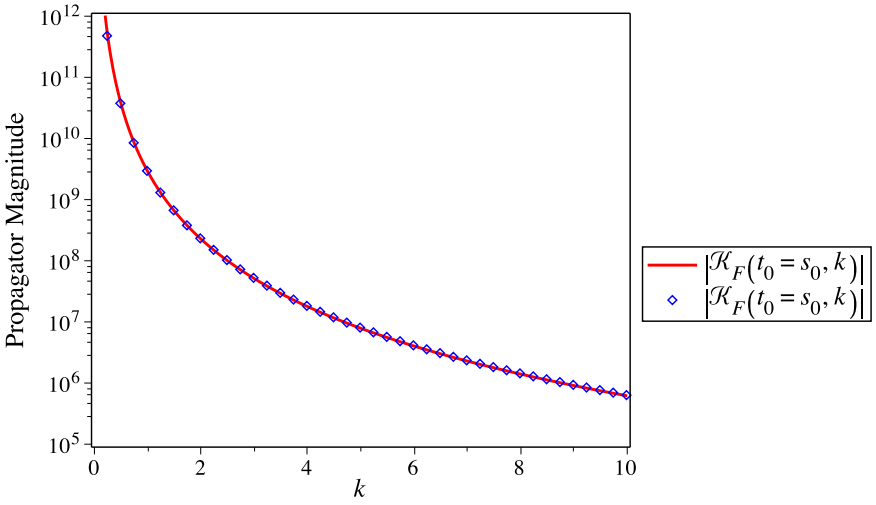

Figure 5.14: Plot of $|\mathcal{K}_F(t_0 = s_0, k)|$ and the numerically-determined $|\mathcal{K}_F^c(t_0 = s_0, k)|$ for $t_0 = s_0 = 5t_{cross\ max}$. For $\alpha = 4$, $c = 1$, and $k \in \{0.25, 0.5, 0.75, 1, \ldots, 10\}$, we have that $t_{cross\ max} \doteq 1.22$.

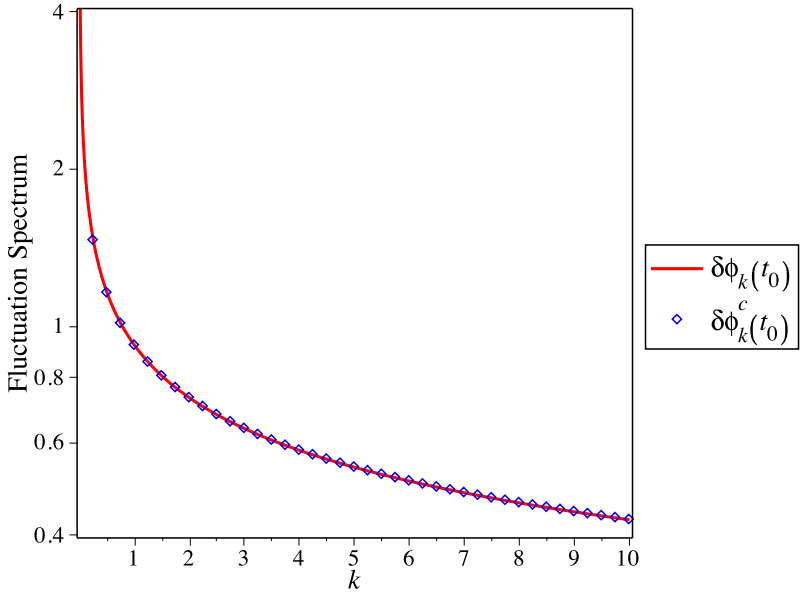

Figure 5.15: Plot of $\delta\phi_k(t_0)$ and the numerically-determined $\delta\phi_k^c(t_0)$ for $t_0 = 5t_{cross\ max}$. Other parameter values are $\alpha = 4$, $c = 1$, and $\Omega = 5$.

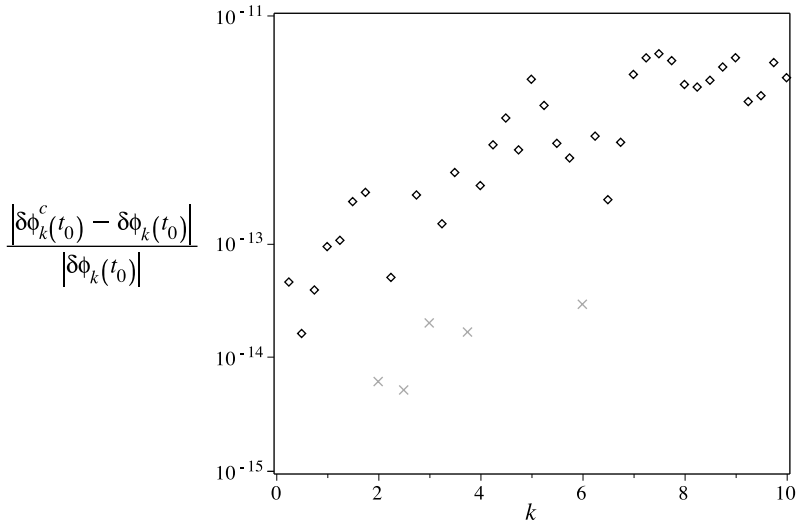

Figure 5.16: Relative difference between usual and covariantly bandlimited fluctuation spectra. Other parameter values are $\alpha = 4$, $c = 1$, and $\Omega = 5$. Crossed out points are points where the computer could not optimize the consistency condition (5.110).

assertion could be checked by seeing how these oscillations are affected when more or fewer eigenfunctions are used to compute the fluctuation spectrum.

As was mentioned at the beginning of this section, the numerical results presented here are preliminary results. Of course, it would be desirable to fill in the k dependence curves by computing data for more values of k. It would also be sensible to devise a way to estimate the error in the computed quantities. Additionally, the numerics could be improved by increasing the computation precision (here, quantities were computed to 6 digits of precision) and performing higher-resolution Riemann sums over λ.

Earlier, we noted that the parameters A_k, B_k, and C_k should be constant for all values of λ. Therefore, a possible improvement would be to modify the minimization algorithm to take this constraint into account. It may also be that significant numerical improvements could be obtained by improving the analytic approximations that are made thoughout the algorithm. In particular, it should be possible to improve the late-time approximations of $\psi^c_{\lambda,k}(t)$ and $\psi^s_{\lambda,k}(t)$. These eigenfunctions are only exactly cosine and sine functions respectively as $t \to \infty$. Before that, they each have a time-varying phase. A better approximation would estimate this phase.

Another option is to completely bypass any late-time approximations. Recall that these late-time approximations are necessary so that one may evaluate the integrals $\mathcal{I}_{WX}(\infty)$. Notice that these integrals appear in the constraint equation $\mathscr{C}(A_k, B_k, C_k, b_{\lambda,k}; \lambda, t) = 0$. By demanding that this constraint equation hold at a sufficiently large number of times, it should be possible to *also* determine the values of the integrals $\mathcal{I}_{WX}(\infty)$ via the optimization routine in addition to the other parameters.

Finally, it may be best to compute $\mathcal{K}_F^c$ by subtracting from $\mathcal{K}_F$ the projection $\bar{P}_{B_k(\Omega)}\mathcal{K}_F\bar{P}_{B_k(\Omega)}$, where

this projection is computed explicitly as

$$(\bar{P}_{B_k(\Omega)}\mathcal{K}_F\bar{P}_{B_k(\Omega)})(t,s,k) = \int_0^\infty d\zeta \int_0^\infty d\xi\, \bar{P}_{B_k(\Omega)}(t,\zeta)\mathcal{K}_F(\zeta,\xi,k)\bar{P}_{B_k(\Omega)}(\xi,s), \tag{5.116}$$

using expression (5.59) for $\mathcal{K}_F(t,s,k)$. For this, one would need to find a way to compute the integrals (5.114). This approach has the advantage, however, that the constants A_k, B_k, and C_k do not appear in the final calculation of the bandlimited propagator. As such, any error in these constants in not further compounded.

Chapter 6

Conclusion

In this thesis, we explored the effect that a new, fully-covariant, natural UV cutoff has on the Feynman propagator of a scalar quantum field. We did this because the Feynman propagator is a measure of the strength of the field's quantum fluctuations. In particular, we could then assess the effect of this covariant cutoff on the fluctuations of the scalar inflaton field. The fluctuations of the inflaton field are the seeds of the temperature and polarization fluctuations in the CMB. Therefore, a modification of the inflaton field's fluctuations due to this covariant cutoff is tantamount to an observational signature of the cutoff in the CMB.

Unfortunately, it seems that the signature of this covariant UV cutoff in the CMB is so small that it is likely undetectable. On the other hand, there is very little room to modify the inflaton field's fluctuation spectrum while remaining consistent with observed CMB statistics. As such, it is good that this covariant cutoff does not significantly modify the fluctuation spectrum of a scalar field. The existence of this covariant cutoff in nature is certainly not ruled out.

The studies in this thesis were concerned exclusively with the effect of this covariant UV cutoff in cosmology. However, this natural cutoff is applicable anywhere that there is a trans-Planckian problem [56]. For instance, it would be interesting to study this covariant cutoff in the context of black hole physics and of Hawking radiation. In a similar vein, it would also be interesting to apply this covariant cutoff to a recent proposal for computing entanglement entropy using two-point functions [57]. In this way, it might be possible to calculate the effect of this covariant cutoff on black hole entropy.

On the purely theoretical side, it would be interesting to study this covariant cutoff's effect on causality. Explicitly, this would mean studying the effect of the covariant cutoff on the canonical commutation relations. There is also the question of the origin of this covariant cutoff. As was discussed, assuming the existence of the covariant cutoff means assuming that fields in nature are covariantly bandlimited. In a path integral formulation of quantum field theory, one therefore only integrates over the space of covariantly bandlimited fields. In this sense, the covariant cutoff is somewhat sharp. Another approach to implementing this cutoff would be to modify the field's action instead of modifying the integration domain. Such a modification would consist of fully covariant terms that cause increasingly off-shell field configurations to be smoothly suppressed in the path integral up to the cutoff. One could presumably then show that modifying the integration domain is an effective limiting case of such covariant modifications of the action.

In closing, we see that while this covariant cutoff is likely not observable in cosmological measurements, its existence is not ruled out. As such, it would be interesting to study it in other physical settings. The question of whether this covariant cutoff is truly fundamental, or whether it is some effective approximation to much higher-energy quantum gravity effects is another question entirely. This covariant cutoff is very nice as-is, however, since it plainly lies at the collision point of quantum field theory and of general relativity. These are two physical theories that are very well understood and in which much confidence lies. As such, it remains that this covariant UV cutoff is a very transparent and natural way to study quantum gravity effects.

References

[1] L.J. Garay. Quantum gravity and minimum length. *International Journal of Modern Physics A*, 10:23, 1995.

[2] C. Rovelli and S. Speziale. Reconcile Planck-scale discreteness and the Lorentz-Fitzgerald contraction. *Physical Review D*, 67(6):064019, 2003.

[3] S. Doplicher, K. Fredenhagen, and J.E. Roberts. The quantum structure of spacetime at the Planck scale and quantum fields. *Communications in Mathematical Physics*, 172:187–220, 1995.

[4] S. Doplicher. Spacetime and fields, a quantum texture. *Proceedings of the 37th Karpacz Winter School of Theoretical Physics*, pages 204–213, 2001.

[5] G. Piacitelli. Quantum spacetime: a disambiguation. *Symmetry, Integrability and Geometry: Methods and Applications*, 6(073), 2010.

[6] T. Padmanabhan. Duality and zero-point length of spacetime. *Physical Review Letters*, 78(10):1854–1857, 1997.

[7] T. Padmanabhan. Hypothesis of path integral duality. I. Quantum gravitational corrections to the propagator. *Physical Review D*, 57(10):6206–6215, 1998.

[8] P. Martinetti, F. Mercati, and L. Tomassini. Minimal length in quantum space and integrations of the line element in noncommutative geometry. *Reviews in Mathematical Physics*, 24:1250010, 2012.

[9] A. Kempf. Fields over unsharp coordinates. *Physical review letters*, 85(14):2873–6, 2000.

[10] A. Kempf. Covariant information-density cutoff in curved space-time. *Physical Review Letters*, 92(22):221301, 2004.

[11] G. Shiu. Inflation as a probe of trans-Planckian physics: a brief review and progress report. *Journal of Physics: Conference Series*, 18:188–223, 2005.

[12] S. Bachmann and A. Kempf. The transplanckian question and the Casimir effect. *arXiv:gr-qc/0504076v1*, 2005.

[13] E. Calabrese, R.A. Hlozek, N. Battaglia, E.S. Battistelli, J.R. Bond, J. Chluba, D. Crichton, S. Das, M.J. Devlin, J. Dunkley, R. Dünner, M. Farhang, M.B. Gralla, A. Hajian, M. Halpern, M. Hasselfield, A.D. Hincks, K.D. Irwin, A. Kosowsky, T. Louis, T.A. Marriage, K. Moodley, L. Newburgh, M.D.

Niemack, M.R. Nolta, L.A. Page, N. Sehgal, B.D. Sherwin, J.L. Sievers, C. Sifón, D.N. Spergel, S.T. Staggs, E.R. Switzer, and E.J. Wollack. Cosmological parameters from pre-planck cosmic microwave background measurements. *Physical Review D*, 87(10):103012, 2013.

[14] Planck Collaboration. Planck 2013 results. I. Overview of products and scientific results. *arXiv:1303.5062v1*, 2013.

[15] Planck Collaboration. Planck 2013 results. XV. CMB power spectra and likelihood. *arXiv:1303.5075v2*, 2013.

[16] D. Hanson, S. Hoover, A. Crites, P.A.R. Ade, K.A. Aird, J.E. Austermann, J.A. Beall, A.N. Bender, B.A. Benson, L.E. Bleem, J.J. Bock, J.E. Carlstrom, C.L. Chang, H.C. Chiang, H-M. Cho, A. Conley, T.M. Crawford, T. de Haan, M.A. Dobbs, W. Everett, J. Gallicchio, J. Gao, E.M. George, N.W. Halverson, N. Harrington, J.W. Henning, G.C. Hilton, G.P. Holder, W.L. Holzapfel, J.D. Hrubes, N. Huang, J. Hubmayr, K.D. Irwin, R. Keisler, L. Knox, A.T. Lee, E. Leitch, D. Li, C. Liang, D. Luong-Van, G. Marsden, J.J. McMahon, J. Mehl, S.S. Meyer, L. Mocanu, T.E. Montroy, T. Natoli, J.P. Nibarger, V. Novosad, S. Padin, C. Pryke, C.L. Reichardt, J.E. Ruhl, B.R. Saliwanchik, J.T. Sayre, K.K. Schaffer, B. Schulz, G. Smecher, A.A. Stark, K. Story, C. Tucker, K. Vanderlinde, J.D. Vieira, M.P. Viero, G. Wang, V. Yefremenko, O. Zahn, and M. Zemcov. Detection of B-mode polarization in the cosmic microwave background with data from the South Pole Telescope. *arXiv:1307.5830v1*, 2013.

[17] S.W. Hawking and G.F.R. Ellis. *The Large Scale Structure of Space-Time*. Cambridge University Press, Cambridge, 1973.

[18] A. Kempf. General Relativity for Cosmology: AMath 875 Course Notes. (University of Waterloo), 2011.

[19] A.R. Liddle and D.H. Lyth. *Cosmological Inflation and Large-Scale Structure*. Cambridge University Press, Cambridge, 2000.

[20] A. Kempf. Quantum Field Theory for Cosmology: AMath 872 Course Notes. (University of Waterloo), 2012.

[21] W.H. Kinney. Cosmology, inflation and the physics of nothing. *Techniques and Concepts of High-Energy Physics XII*, pages 1–60, 2003.

[22] C.L. Bennett, A.J. Banday, K.M. Górski, G. Hinshaw, P. Jackson, P. Keegstra, A. Kogut, G.F. Smoot, D.T. Wilkinson, and E.L. Wright. Four-year COBE DMR cosmic microwave background observations: maps and basic results. *The Astrophysical Journal*, 464(1):L1–L4, 1996.

[23] N. Jarosik, C.L. Bennett, J. Dunkley, B. Gold, M.R. Greason, M. Halpern, R.S. Hill, G. Hinshaw, A. Kogut, E. Komatsu, D. Larson, M. Limon, S.S. Meyer, M.R. Nolta, N. Odegard, L. Page, K.M. Smith, D.N. Spergel, G.S. Tucker, J.L. Weiland, E. Wollack, and E.L. Wright. Seven-year Wilkinson Microwave Anisotropy Probe (WMAP) observations: sky maps, systematic errors, and basic results. *The Astrophysical Journal Supplement Series*, 192(2):14, 2011.

[24] V.F. Mukhanov. *Physical Foundations of Cosmology*. Cambridge University Press, Cambridge, 2005.

[25] M.E. Peskin and D.V. Schroeder. *An Introduction to Quantum Field Theory*. Westview Press, Boulder, CO, 1995.

[26] V.F. Mukhanov and S. Winitzki. *Introduction to Quantum Effects in Gravity*. Cambridge University Press, Cambridge, 2007.

[27] N.D. Birrell and P.C.W. Davies. *Quantum Fields in Curved Space*. Cambridge University Press, Cambridge, 1982.

[28] F. Lucchin and S. Matarrese. Power-law inflation. *Physical Review D*, 32(6):1316–1322, 1985.

[29] V.F. Mukhanov, H.A. Feldman, and R.H. Brandenberger. Theory of cosmological perturbations. *Physics Reports*, 215(5-6):203–333, 1992.

[30] D. Larson, J. Dunkley, G. Hinshaw, E. Komatsu, M.R. Nolta, C.L. Bennett, B. Gold, M. Halpern, R.S. Hill, N. Jarosik, A. Kogut, M. Limon, S.S. Meyer, N. Odegard, L. Page, K.M. Smith, D.N. Spergel, G.S. Tucker, J.L. Weiland, E. Wollack, and E.L. Wright. Seven-Year Wilkinson Microwave Anisotropy Probe (WMAP) observations: power spectra and WMAP-derived parameters. *The Astrophysical Journal Supplement Series*, 192(2):16, 2011.

[31] J. Weidmann. *Linear Operators in Hilbert Spaces*. Springer-Verlag, New York, NY, 1980.

[32] N.I. Akhiezer and I.M. Glazman. *Theory of Linear Operators in Hilbert Space: Two Volumes Bound as One*. Dover, Mineola, NY, 1993.

[33] J. Weidmann. Spectral theory of Sturm-Liouville operators: approximation by regular problems. *Sturm-Liouville Theory*, pages 75–98, 2005.

[34] A.W. Naylor and G.R. Sell. *Linear Operator Theory in Engineering and Science*. Springer-Verlag, New York, NY, 1982.

[35] S.A. Fulling. *Aspects of Quantum Field Theory in Curved Space-Time*. Cambridge University Press, Cambridge, 1989.

[36] M.A. Naimark. *Linear Differential Operators*. Frederick Ungar, New York, NY, 1968.

[37] R.T.W. Martin. *Bandlimited functions, curved manifolds, and self-adjoint extensions of symmetric operators*. Doctoral, University of Waterloo, 2008.

[38] A. Kempf, A. Chatwin-Davies, and R.T.W. Martin. A fully covariant information-theoretic ultraviolet cutoff for scalar fields in expanding Friedmann Robertson Walker spacetimes. *Journal of Mathematical Physics*, 54(2):022301, 2013.

[39] C.E. Shannon. *The Mathematical Theory of Communication*. University of Illinois Press, Chicago, IL, 1949.

[40] H.J. Landau. Necessary density conditions for sampling and interpolation of certain entire functions. *Acta Mathematica*, 117:37–52, 1967.

[41] I. Pesenson. A sampling theorem on homogeneous manifolds. *Transactions of the American Mathematical Society*, 352(9):4257–4269, 2000.

[42] Planck Collaboration. Planck 2013 results. XXII. Constraints on inflation. *arXiv:1303.5082v1*, 2013.

[43] A.D. Linde. Chaotic inflation. *Physics Letters B*, 129(3):177–181, 1983.

[44] A.A. Starobinsky. A new type of isotropic cosmological models without singularity. *Physics Letters B*, 91(1):99–102, 1980.

[45] V.F. Mukhanov and G.V. Chibisov. Quantum fluctuations and a nonsingular universe. *JETP Letters*, 33(10):532–535, 1981.

[46] A. Ashoorioon and R.B. Mann. On the tensor/scalar ratio in inflation with UV cutoff. *Nuclear Physics B*, 716(1-2):261–279, 2005.

[47] W.N. Everitt. A catalogue of Sturm-Liouville differential equations. In *Sturm-Liouville Theory*, pages 271–331. Birkhäuser Basel, Basel, 2005.

[48] R.L. Liboff. *Introductory Quantum Mechanics*. Addison Wesley, San Francisco, CA, 2003.

[49] D.G. Zill. *A First Course in Differential Equations with Applications*. PWS Publishers, Boston, MA, 1986.

[50] J. Wainwright. *Differential Equations 2: Course Notes for AM 351*. University of Waterloo, Waterloo, ON, 2002.

[51] R.T.W. Martin. Personal communication, 2012.

[52] W.N. Everitt, I.W. Knowles, and T.T. Read. Limit-point and limit-circle criteria for Sturm-Liouville equations with intermittently negative principal coefficients. *Proceedings of the Royal Society of Edinburgh: Section A Mathematics*, 103A(3-4):215–228, 1986.

[53] E.C. Titchmarsh. *Eigenfunction Expansions Associated with Second-order Differential Equations*. Oxford University Press, London, 1962.

[54] I.S. Gradshteyn and I.M. Ryzhik. *Table of Integrals, Series, and Products*. Elsevier Academic Press, Burlington, MA, 7 edition, 2007.

[55] *Methods Used by the Optimization Package*. (Maple 17 Online Help), http://www.maplesoft.com/support/help (Accessed 7 Jul, 2013).

[56] T. Jacobson. Trans-Planckian redshifts and the substance of the space-time river. *Progress of Theoretical Physics Supplement*, 136:1–17, 1999.

[57] R.D. Sorkin. Expressing entropy globally in terms of (4D) field-correlations. *arXiv:1205.2953v1*, 2012.

[58] H. Cheng. *18.305 Advanced Analytic Methods in Science and Engineering, Fall 2004*. (Massachusetts Institute of Technology: MIT OpenCourseWare), http://ocw.mit.edu (Accessed 22 Jul, 2013). License: Creative Commons BY-NC-SA.

APPENDICES

Appendix A

Massive Power Law Mode Functions

In this appendix, we will develop a method for calculating a divergent series representation of the eigenfunctions of H_k. In other words, we will find a divergent series solution of the ordinary differential equation (ODE) (5.38). Alternatively, one could replace the eigenvalue λ by a mass m^2. In this case, one obtains a divergent series representation for the mode functions $v_k(t) = a^{-3/2}(t)w(t)$ of a massive scalar field in a power-law FLRW spacetime.

The original method is explained in a practical lecture by Cheng [58]. Here, we will formalize the method and extend it so that we may compute massive power-law mode functions.

A.1 A Method for Calculating a Series Solution About an Irregular Singular Point

As a prototypical problem, let us consider the ODE

$$y''(x) + c(x)y'(x) + d(x)y(x) = 0, \tag{A.1}$$

for $x \in \mathcal{I} \subseteq \mathbb{R}$. Suppose that $x_0 \in \mathcal{I}$ is an irregular singular point, about which $c(x)$ and $d(x)$ have the following Laurent series:

$$c(x) = \frac{c_{-k_1-1}}{(x-x_0)^{k_1+1}} + \frac{c_{-k_1}}{(x-x_0)^{k_1}} + \cdots + c_0 + c_1(x-x_0) + \ldots \tag{A.2}$$

$$d(x) = \frac{d_{-2k_2-2}}{(x-x_0)^{2k_2+2}} + \frac{d_{-2k_2-1}}{(x-x_0)^{2k_2-1}} + \cdots + d_0 + d_1(x-x_0) + \ldots \tag{A.3}$$

Since x_0 is an irregular singular point, at least one of $k_1, k_2 \in \mathbb{Z}$ must be greater than zero. Let $k := \max\{k_1, k_2\}$. We will call k the *rank* of the singular point x_0.

Next, we introduce the following transformation:

$$y(x) = e^{F(x)}Y(x) \tag{A.4}$$

Under this transformation, the ODE (A.1) becomes

$$Y''(x) + [2F'(x) + c(x)]\,Y'(x) + [F''(x) + F'(x)(F'(x) + c(x)) + d(x)]\,Y(x) = 0. \tag{A.5}$$

We also assume the following ansatz for $F(x)$:

$$F(x) = \frac{A_k}{(x - x_0)^k} + \cdots + \frac{A_1}{x - x_0} \tag{A.6}$$

If the $A_j \in \mathbb{C}$, $j = 1, ..., k$, are systematically chosen so as to eliminate the k most divergent terms in the coefficient $[F'' + F'(F' + c) + d]$ (where we make use of the Laurent series expansions (A.2) and (A.3) for c and d), then the ODE (A.5) admits a Frobenius series solution,

$$Y(x) = \sum_{n=0}^{\infty} a_n (x - x_0)^{n+r} \qquad r \in \mathbb{R},\ a_0 \neq 0 \tag{A.7}$$

To illustrate the basic technique, let us consider a simple example.

Example A.1.1

Consider the ODE

$$y''(x) + \frac{1}{x^6} y(x) = 0, \tag{A.8}$$

which has an irregular singular point of rank $k = 2$ at $x = 0$. As such, let

$$F(x) = \frac{A_2}{x^2} + \frac{A_1}{x}. \tag{A.9}$$

Inserting this definition into the ODE (A.5) gives

$$Y'' - 2\left(\frac{2A_2}{x^3} + \frac{A_1}{x^2}\right) Y' + \left(\frac{4A_2^2 + 1}{x^6} + \frac{4A_2 A_1}{x^5} + \frac{A_1^2 + 6A_2}{x^4} + \frac{2A_1}{x^3}\right) Y = 0. \tag{A.10}$$

Continuing with the method, let us choose $A_2 = i/2$ and $A_1 = 0$ to eliminate the x^{-6} and x^{-5} terms:

$$Y'' - \frac{2i}{x^3} Y' + \frac{6i}{x^4} Y = 0 \tag{A.11}$$

(Note that we could just as well have chosen $A_2 = -i/2$). Finally, we insert the Frobenius series solution (A.7) into the ODE for Y:

$$\begin{aligned} 0 &= \sum_{n=0}^{\infty} \left[(n + r)(n + r + 1) a_n x^{n+r-2} - 2ix^{-3}(n + r) a_n x^{n+r-1} + 6ix^{-4} a_n x^{n+r}\right] \\ &= \sum_{n=0}^{\infty} \left[(n + r)(n + r + 1) a_n x^{n-2} - 2i(n + r - 3) a_n x^{n-4}\right] \\ &= -2i(r - 3) a_0 x^{-4} - 2i(r - 2) a_1 x^{-3} + \sum_{n=0}^{\infty} \left[(n + r)(n + r + 1) a_n - 2i(n + r - 1) a_{n+2}\right] x^{n-2} \end{aligned} \tag{A.12}$$

Proceeding as usual and demanding that the coefficients of x^n all vanish (with $a_0 \neq 0$), we find that

$$r = 3, \quad a_1 = 0, \quad \text{and} \quad a_{n+2} = \frac{n+3}{2i} a_n \ \text{ for } n > 0. \tag{A.13}$$

Therefore, a solution of ODE (A.8) is

$$y_1(x) = \exp\left(\frac{i}{2x^2}\right) x^3 \left[1 + \frac{3}{2i}x^2 - \frac{15}{16}x^4 + \dots\right]. \tag{A.14}$$

A second linearly independent solution is simply $y_2(x) = y_1^*(x)$. ▷

Intuitively, the method works for the following reason. When x_0 is an irregular singular point, solutions of the ODE (A.1) can be very ill-behaved. The prefactor $e^{F(x)}$, where $F(x)$ itself is singular at x_0, is a way of peeling the irregularly singular behaviour off of the solutions. For instance, this prefactor can cause solutions to oscillate infinitely quickly, to diverge exponentially, or to decay exponentially as $x \to x_0$.

Mathematically, the method works because the ansatz for $F(x)$ given by equation (A.6) ensures that the zero coefficient a_0 in the series solution (A.7) can be chosen to be nonvanishing. Suppose for a moment that $c(x) = c_{-1}x^{-1} + c_0 + c_1 x + \dots$ and $d(x) = d_{-2}x^{-2} + d_{-1}x^{-1} + d_0 + \dots$ in equation (A.1). The point $x = 0$ is then a regular singular point. We can thus assume a series solution of the form $y(x) = \sum_{n=0}^{\infty} a_n x^{n+r}$:

$$\begin{aligned}
0 &= \sum_{n=0}^{\infty} \left[(n+r)(n+r-1)a_n x^{n+r-2} + c(x)(n+r)a_n x^{n+r-1} + d(x)a_n x^{n+r}\right] \\
&= \sum_{n=0}^{\infty} \Bigg[(n+r)(n+r-1)a_n x^{n-2} + c_{-1}(n+r)a_n x^{n-2} + d_{-2}a_n x^{n-2} \\
&\qquad\qquad + \sum_{j=0}^{\infty} c_j (n+r) a_n x^{n-1+j} + \sum_{\ell=-1}^{\infty} d_\ell a_n x^{n+\ell}\Bigg] \\
&= \left[r(r-1+c_{-1}) + d_{-2}\right] a_0 x^{-2} + \sum_{n=1}^{\infty} f\left(n, r, \{c_j\}, \{d_\ell\}, \{a_m\}_{m=0}^{n}\right) x^{n-2}
\end{aligned} \tag{A.15}$$

For a Frobenius series solution, one keeps $a_0 \neq 0$ and sets $r = \frac{1}{2}[(1 - c_{-1} \pm \sqrt{(1-c_{-1})^2 - 4d_{-2}}]$. The sum in the last line of equation (A.15) then recursively defines each a_n for $n \geq 1$ through the requirement that the coefficient of x^{n-2} vanish.

Now, let us return to the case where $c(x)$ and $d(x)$ are described by the Laurent series (A.2) and (A.3). For simplicity, let $x_0 = 0$. We could again directly try a Frobenius series solution for $y(x)$, but we would find the following:

$$\begin{aligned}
0 = \sum_{n=0}^{\infty} \Bigg[&(n+r)(n+r-1)a_n x^{n-2} + c_{-k_1-1}(n+r)a_n x^{n-2-k_1} + d_{-2k_2-2}a_n x^{n-2-2k_2} \\
&+ \sum_{j=-k_1}^{\infty} c_j (n+r) a_n x^{n-1+j} + \sum_{\ell=-2k_2-1}^{\infty} d_\ell a_n x^{n+\ell}\Bigg]
\end{aligned} \tag{A.16}$$

In order to make the coefficient of x^{-2-k_1} or x^{-2-2k_2} (whichever has the larger negative power) vanish, we would need to set $a_0 = 0$. We would then recursively find that $0 = a_1 = a_2 = \dots$ (Even though we can get way with choosing $r = 0$ if x^{-2-k_1} has the largest negative power, this choice of r would force us to set $a_0 = 0$ later in the recursion.)

The problem here is that there is no second term in the sum in equation (A.16) to counterbalance the largest negative power of x, to which the coefficient a_0 is attached. This is precisely what the ansatz $y(x) = e^{F(x)}Y(x)$ achieves. Consider, for $F(x) \sim x^{-k}$ as $x \to 0$ and $k = \max\{k_1, k_2\}$, one has the following:

$$Y'' + [\underbrace{2F'}_{\sim \frac{1}{x^{k+1}}} + \underbrace{c}_{\sim \frac{1}{x^{k_1+1}}}]Y' + [\underbrace{F''}_{\sim \frac{1}{x^{k+2}}} + \underbrace{F'^2}_{\sim \frac{1}{x^{2k+2}}} + \underbrace{cF'}_{\sim \frac{1}{x^{k_1+k+2}}} + \underbrace{d}_{\sim \frac{1}{x^{2k_2+2}}}]Y = 0 \tag{A.17}$$

Noting that the derivative Y' contributes an extra negative power of x in the Frobenius series ansatz, we see that there are now terms to counterbalance both $c(x)$ (the $2F'$ term, with the F'^2 and cF' terms counterbalancing each other if $k_1 > k_2$) and $d(x)$ (the F'^2 term, with the $2F'$ and F'' terms counterbalancing each other if $k_2 > k_1$). Therefore, a Frobenius series solution (A.7) for Y with $a_0 \neq 0$ succeeds.

Note that the method as outlined above is subject to a cumbersome restriction: one must be able to expand $c(x)$ and $d(x)$ as the Laurent series given by equations (A.2) and (A.3) respectively. In particular, both k_1 and k_2 must be integers, and the pole of $d(x)$ at x_0 must be a pole of even order. Thus, the method is not directly applicable to ODEs such as $y'' + x^{-5/2}y = 0$ or $y'' + x^{-3}y = 0$. Note that the method still works if one of either $c(x)$ or $d(x)$ is analytic at x_0.

In particular, the case of equation (5.38), which describes the eigenfunctions of a power-law FLRW spacetime, is problematic. This is because in principle, α can be any positive real number. Below is a remedy for when $\alpha \in \mathbb{Q}^+$. This should be satisfactory in general, since one can approximate any real number with a rational number arbitrarily well.

Instead of constructing a cumbersome, rigorous proof, let us instead consider a more practical "proof by example."

Example A.1.2

Consider the ODE

$$y''(x) + \left(\frac{1}{x^{p/q}} + \frac{1}{x^{r/s}}\right) y(x) = 0, \tag{A.18}$$

where $p, q, r, s \in \mathbb{Z}^+$ and $p/q, r/s > 2$. So that we can apply the method outlined above, we make a change of variables $x = u^\gamma$, where γ is to be determined. Under this change of variables, the ODE (A.18) becomes

$$y''(u) + \frac{(1-\gamma)}{u} y'(u) + \gamma^2 \left(\frac{1}{u^{\gamma p/q}} + \frac{1}{u^{\gamma r/s}}\right) y(u) = 0, \tag{A.19}$$

where $'$ now denotes differentiation with respect to u. If we choose $\gamma = 2qs$, we obtain

$$y''(u) + \frac{(1-2qs)}{u} y'(u) + (2qs)^2 \left(\frac{1}{u^{2(s(p-2q)+1)}} + \frac{1}{u^{2(q(r-2s)+1)}}\right) y(u) = 0. \tag{A.20}$$

The solution method outlined above now applies to this ODE. ▷

A.2 Computation of the Mode Functions

The ODE (5.38) is of the form

$$y''(x) + \left(Ax^{-2\beta} - Bx^{-2} + C\right) y(x) = 0, \tag{A.21}$$

with $A, B, C > 0$ and $\beta > 1$. Let us solve this ODE. It is straightforward to show that the series solutions that one obtains are divergent series.

A.2.1 The Case of $\beta \in \mathbb{Q} \setminus \mathbb{Z}$

Assume that $\beta \in \mathbb{Q}$ and write $\beta = p/q$, with $p, q \in \mathbb{Z}^+$, $p > q$. Under the change of variables $x = u^q$, the ODE (A.21) becomes

$$y''(u) - \frac{(q-1)}{u} y'(u) + \frac{1}{q^2}\left(\frac{A}{u^{2(p-q)+2}} - \frac{B}{u^2} + Cu^{2(q-1)}\right) y(u) = 0. \tag{A.22}$$

Writing $y(u) = e^{F(u)}Y(u)$ and letting $\tilde{A} = q^{-2}A$, $\tilde{B} = q^{-2}B$, and $\tilde{C} = q^{-2}C$, we obtain

$$\begin{aligned} &Y'' + \left[2F' - (q-1)u^{-1}\right] Y' \\ &\quad + \left[F'' + F'^2 - (q-1)u^{-1}F' + \tilde{A}u^{-2(p-q)-2} - \tilde{B}u^{-2} + \tilde{C}u^{2(q-1)}\right] Y = 0. \end{aligned} \tag{A.23}$$

The point $u = 0$ is an irregular singular point of rank $k = p - q$, so let

$$F(u) = \sum_{j=1}^{p-q} \frac{F_j}{u^j}. \tag{A.24}$$

Consequently, we also have

$$F'(u) = -\sum_{j=1}^{p-q} \frac{jF_j}{u^{j+1}}, \qquad F''(u) = \sum_{j=1}^{p-q} \frac{j(j+1)F_j}{u^{j+2}}, \quad \text{and}$$

$$F'(u)^2 = \frac{1}{u^2}\left[\sum_{j=1}^{p-q} \frac{jF_j}{u^j}\right]^2 = \frac{1}{u^2} \sum_{m=2}^{2(p-q)} \frac{\left(\sum_{j=\max\{1,m-(p-q)\}}^{\min\{m-1,p-q\}} j(m-j)F_jF_{m-j}\right)}{u^m}.$$

Making these substitutions in equation (A.23) and grouping terms of the same power of u gives

$$\begin{aligned} Y'' - \left[2\sum_{j=1}^{p-q} \frac{jF_j}{u^{j+1}} + \frac{(q-1)}{u}\right] Y' + \Bigg[&\frac{\tilde{A} + (p-q)^2F_{p-q}^2}{u^{2(p-q)+2}} + \sum_{m=p-q+1}^{2(p-q)-1} \frac{\left(\sum_{j=m-(p-q)}^{p-q} j(m-j)F_jF_{m-j}\right)}{u^{m+2}} \\ &+ \sum_{m=2}^{p-q} \frac{\left(\sum_{j=1}^{m-1} j(m-j)F_jF_{m-j}\right) + m(m+q)F_m}{u^{m+2}} + \frac{(q+1)F_1}{u^3} - \frac{\tilde{B}}{u^2} + \tilde{C}u^{2(q-1)}\Bigg] Y = 0. \end{aligned} \tag{A.25}$$

Next, we systematically choose the F_j so as to eliminate the $p-q$ largest negative powers of u. Beginning with $u^{-2(p-q)-2}$, we have that $\tilde{A} + (p-q)^2 F_{p-q}^2 = 0$. Choosing the positive root, set

$$F_{p-q} = \frac{i\sqrt{\tilde{A}}}{p-q}. \tag{A.26}$$

The other $(p-q)-1$ coefficients are determined by the second sum, which covers the powers $u^{-2(p-q)-1}$ down to $u^{-(p-q)-3}$. The structure of this sum is such that the only possible choice of F coefficients is

$$F_{p-q-1} = \cdots = F_2 = F_1 = 0. \tag{A.27}$$

Therefore, equation (A.25) reduces to

$$Y'' - \left[\frac{2i\sqrt{\tilde{A}}}{u^{p-q+1}} + \frac{(q-1)}{u}\right] Y' + \left[\frac{ip\sqrt{\tilde{A}}}{u^{p-q+2}} - \frac{\tilde{B}}{u^2} + \tilde{C}u^{2(q-1)}\right] Y = 0. \tag{A.28}$$

Next, we write Y as the Frobenius series

$$Y(u) = \sum_{n=0}^{\infty} a_n u^{n+r}, \qquad a_0 \neq 0. \tag{A.29}$$

Substituting this expression into equation (A.28) gives

$$0 = \sum_{n=0}^{\infty} \left\{ [(n+r)(n+r-q) - \tilde{B}] a_n u^{n-2} + i\sqrt{\tilde{A}}[p - 2(n+r)] a_n u^{n-(p-q)-2} + \tilde{C} a_n u^{n+2(q-1)} \right\}. \tag{A.30}$$

Grouping powers of u, we obtain

$$\begin{aligned} 0 = {} & i\sqrt{\tilde{A}}\,[p-2r]\,a_0 u^{-(p-q)-2} + \sum_{n=1}^{(p-q)-1} i\sqrt{\tilde{A}}\,[p-2(n+r)]\,a_n u^{n-(p-q)-2} \\ & + \sum_{n=0}^{2q-1} \left\{ \left[(n+r)(n+r-q) - \tilde{B}\right] a_n + i\sqrt{\tilde{A}}\,[p - 2(n+(p-q)+r)]\,a_{n+(p-q)} \right\} u^{n-2} \\ & + \sum_{n=0}^{\infty} \left\{ \left[(n+r+2q)(n+r+q) - \tilde{B}\right] a_{n+2q} + i\sqrt{\tilde{A}}\,[2(r-n-q)-p]\,a_{n+p+q} + \tilde{C} a_n \right\} u^{n+2(q-1)}. \end{aligned} \tag{A.31}$$

For $a_0 \neq 0$, we see that we must choose $r = p/2$, whence

$$\begin{aligned} 0 = {} & -2i\sqrt{\tilde{A}} \sum_{n=1}^{(p-q)-1} n\, a_n u^{n-(p-q)-2} \\ & + \sum_{n=0}^{2q-1} \left\{ \left[\left(n+\frac{p}{2}\right)\left(n+\frac{p}{2}-q\right) - \tilde{B}\right] a_n - 2i\sqrt{\tilde{A}}(n+p-q) a_{n+p-q} \right\} u^{n-2} \\ & + \sum_{n=0}^{\infty} \left\{ \left[\left(n+\frac{p}{2}+2q\right)\left(n+\frac{p}{2}+q\right) - \tilde{B}\right] a_{n+2q} - 2i\sqrt{\tilde{A}}(n+q) a_{n+p+q} + \tilde{C} a_n \right\} u^{n+2(q-1)}. \end{aligned} \tag{A.32}$$

From the first line of equation (A.32), we can read off that

$$a_1 = \cdots = a_{(p-q)-1} = 0. \tag{A.33}$$

From the second line, we have that for $n \in \{p-q, \ldots, p+q-1\}$,

$$a_n = \begin{cases} \dfrac{(j(p-q)+p/2)\,(j(p-q)+p/2-q)-\tilde{B}}{2i\sqrt{\tilde{A}}(j+1)(p-q)}\, a_{j(p-q)} & n = (j+1)(p-q) \\ 0 & \text{otherwise} \end{cases} \tag{A.34}$$

for $j = 0, 1, \ldots, J$ and where $J := \max\{j \ : \ (j+1)(p-q) \leq p+q-1\}$. Finally, the last line gives the recursion for the rest of the coefficients:

$$a_{m+p+q} = \frac{(m+p/2+2q)\,(m+p/2+q)-\tilde{B}}{2i\sqrt{\tilde{A}}(m+q)}\, a_{m+2q} + \frac{\tilde{C}}{2i\sqrt{\tilde{A}}(m+q)}\, a_m \qquad m = 0, 1, 2, \ldots \tag{A.35}$$

It is rather complicated to write down for which m the coefficients a_{m+p+q} vanish. Therefore, a good numerical algorithm is to keep track of which n give nonzero a_n as they are computed, so as to economize memory as more and more a_n are computed.

A solution to the original ODE (A.21) is thus

$$y_1(x) = \exp\left(\frac{i\sqrt{A}}{q(p-q)} x^{-(p-q)/q}\right) x^{p/2} \left(1 + \frac{\frac{p}{2}(\frac{p}{2}-q) - B/q^2}{2i\sqrt{A}(p-q)/q}\, x^{(p-q)/q} + \cdots\right), \tag{A.36}$$

and a second linearly independent solution is $y_2(x) = y_1^*(x)$.

A.2.2 The Case of $\beta \in \mathbb{Z}$

For completeness, let us also write down the solution for the simpler case when $\beta \in \mathbb{Z}$. In this case, under the transformation $y(x) = e^{F(x)}Y(x)$, the ODE (A.21) becomes

$$Y'' + 2F'Y' + \left[F'' + F'^2 + Ax^{-2\beta} - Bx^{-2} + C\right] Y = 0. \tag{A.37}$$

This ODE has an irregular singularity of rank $k = \beta - 1$ at $x = 0$, so we let $F(x) = \sum_{j=1}^{\beta-1} F_j x^{-j}$. If we repeated the same analysis as in the previous subsection, we would again find that $F_1 = \cdots = F_{\beta-2} = 0$ and that

$$F_{\beta-1} = \frac{i\sqrt{A}}{\beta-1}. \tag{A.38}$$

Equation (A.37) thus becomes

$$Y'' - \frac{2i\sqrt{A}}{x^\beta} Y' + \left[\frac{i\beta\sqrt{A}}{x^{\beta+1}} - \frac{B}{x^2} + C\right] Y = 0. \tag{A.39}$$

Writing $Y(x) = \sum_{n=0}^{\infty} a_n x^{n+r}$ with $a_0 \neq 0$, we have

$$\begin{aligned}
0 &= \sum_{n=0}^{\infty} \left\{ [(n+r)(n+r-1) - B] a_n x^{n-2} + i\sqrt{A}[\beta - 2(n+r)] a_n x^{n-\beta-1} + C a_n x^n \right\} \\
&= i\sqrt{A}[\beta - 2r] a_0 x^{-\beta-1} + \sum_{n=1}^{\beta-2} \left\{ i\sqrt{A}[\beta - 2(n+r)] a_n x^{n-\beta-1} \right\} \\
&\quad + \left([r(r-1) - B] a_0 + i\sqrt{A}[2 - \beta - 2r] a_{\beta-1} \right) x^{-2} + \left([(r+1)r - B] a_1 - i\sqrt{A}[\beta + 2r] a_\beta \right) x^{-1} \\
&\quad + \sum_{n=0}^{\infty} \left\{ [(n+r+2)(n+r+1) - B] a_{n+2} - i\sqrt{A}[\beta + 2(n+1+r)] a_{n+\beta+1} + C a_n \right\} x^n . \qquad \text{(A.40)}
\end{aligned}$$

Setting the coefficients of x^n to zero in the previous equation, we conclude that $r = \beta/2$, $a_1 = \cdots = a_{\beta-2} = 0$,

$$a_{\beta-1} = \frac{\frac{\beta}{2}\left(\frac{\beta}{2} - 1\right) - B}{2i\sqrt{A}(\beta - 1)} a_0, \qquad \text{(A.41)}$$

$a_\beta = 0$, and then recursively

$$a_{n+\beta+1} = \frac{\left[\left(n + \frac{\beta}{2} + 2\right)\left(n + \frac{\beta}{2} + 1\right) - B\right] a_{n+2} + C a_n}{2i\sqrt{A}(n + \beta + 1)} ; \qquad n = 0, 1, 2, \ldots \qquad \text{(A.42)}$$

A solution to the original ODE (A.21) is thus

$$y_1(x) = \exp\left(\frac{i\sqrt{A}}{\beta - 1} x^{-(\beta-1)} \right) x^{\beta/2} \left(1 + \frac{\frac{\beta}{2}\left(\frac{\beta}{2} - 1\right) - B}{2i\sqrt{A}(\beta - 1)} x^{\beta-1} + \frac{C}{2i\sqrt{A}(\beta + 1)} x^{\beta+1} + \cdots \right) \qquad \text{(A.43)}$$

and a second linearly independent solution is $y_2(x) = y_1^*(x)$.

Appendix B

Characterizing Self-Adjoint Extensions in Power Law Spacetime

In this appendix, let us explicitly calculate the self-adjoint extension constraint

$$-i(2\pi)^{3/2}\lim_{s\to 0^+}\left[\mathcal{K}_F(t,s,k)g'_\mu(s)-(\partial_s\mathcal{K}_F(t,s,k))g_\mu(s)\right]=0 \tag{B.1}$$

for $g_\mu(t)\equiv g(t)=\sqrt{t}J_q(k\eta(t))+b\sqrt{t}Y_q(k\eta(t))$ and $\mathcal{K}_F$ as given by equation (5.59). While the calculation itself is not very illuminating, it is a nice and explicit application of the general theory from [33].

Since we are calculating a limit as $s\to 0^+$, we may assume that $s<t$ so that

$$\mathcal{K}_F(t>s,k)=\frac{1}{\sqrt{2\pi}}\frac{1}{8(\alpha-1)}(ts)^{1/2}H_n^{(2)}(k\eta(t))H_n^{(1)}(k\eta(s)) \tag{B.2}$$

and

$$\begin{aligned}\partial_s\mathcal{K}_F(t>s,k)=&\frac{1}{\sqrt{2\pi}}\frac{1}{8(\alpha-1)}t^{1/2}H_n^{(2)}(k\eta(t))\\&\times\left[\frac{1}{2}s^{-1/2}H_n^{(1)}(k\eta(s))+s^{1/2}\left[\frac{n}{k\eta(s)}H_n^{(1)}(k\eta(s))-H_{n+1}^{(1)}(k\eta(s))\right]k\eta'(s)\right].\end{aligned} \tag{B.3}$$

Discarding any prefactors that depend only on t and using the early-time approximations (5.56) and (5.57) for $g(s)$ and $g'(s)$, equation (B.1) reads

$$\begin{aligned}0=&\lim_{s\to 0^+}s^{1/2}H_n^{(1)}(k\eta(s))\frac{k}{c}s^{-\alpha/2}\left[\sin\omega_q(s)-b\cos\omega_q(s)\right]\\&-\left[\frac{1}{2}s^{-1/2}H_n^{(1)}(k\eta(s))+s^{1/2}\left[\frac{n}{k\eta(s)}H_n^{(1)}(k\eta(s))-H_{n+1}^{(1)}(k\eta(s))\right]k\eta'(s)\right]\\&\times s^{\alpha/2}\left[\cos\omega_q(s)+b\sin\omega_q(s)\right]\end{aligned} \tag{B.4}$$

Recall that $\eta(t) = (c(\alpha-1)t^{\alpha-1})^{-1}$ and $n = (3\alpha-1)/(2(\alpha-1))$. We also have the small t (and so large $\eta(t)$) asymptotic

$$H_n^{(1)}(k\eta(t)) \sim \sqrt{\frac{2c(\alpha-1)t^{\alpha-1}}{\pi k}} e^{i\omega_n(t)}. \tag{B.5}$$

Therefore, simplifying and dividing through by constant prefactors, equation (B.4) reduces to

$$\begin{aligned} 0 = \lim_{s\to 0^+} e^{i\omega_n(s)} \Bigg[& \frac{k}{c}\left[\sin\omega_q(s) - b\cos\omega_q(s)\right] \\ & - \left(\frac{s^{\alpha-1}}{2} + s^\alpha\left[-\frac{n(\alpha-1)}{s} + \frac{ik}{cs^\alpha}\right]\right)\left[\sin\omega_q(s) - b\cos\omega_q(s)\right]\Bigg] \\ = \lim_{s\to 0} e^{i\omega_n(s)} & \frac{k}{c}\left[(1-ib)\sin\omega_q(s) - (i+b)\cos\omega_q(s)\right]. \end{aligned} \tag{B.6}$$